The dual role of gamma interferon during herpes simplex virus type 1 infection

by

Vilma Decman

M.Sc., University of Zagreb, Faculty of Natural Sciences and Mathematics, Croatia 1999

Submitted to the Graduate Faculty of

School of Medicine in partial fulfillment

of the requirements for the degree of

Doctor of Philosophy

University of Pittsburgh

2005

UNIVERSITY OF PITTSBURGH

FACULTY OF SCHOOL OF MEDICINE

This dissertation was presented

by

Vilma Decman

It was defended on

July 18th, 2005

and approved by

William H. Chambers, PhD
Associate Professor, Department of Pathology

Yuan Chang, MD
Professor, Department of Pathology

JoAnne L. Flynn, PhD
Associate Professor, Department of Molecular Genetics and Biochemistry

Paul R. Kinchington, PhD
Associate Professor, Department of Ophthalmology

Robert L. Hendricks, PhD
Dissertation Director
Professor, Departments of Ophthalmology, Immunology and Molecular Genetics and Biochemistry

Copyright permission was granted for:

1. Decman V, Kinchington PR, Harvey SAK, Hendricks RL: **Gamma interferon can block herpes simplex virus type 1 reactivation from latency, even in the presence of late gene expression.** *J. Virol.* 2005, **79:**10339-47

Copyright permission letter is on file with Vilma Decman.

The dual role of gamma interferon during herpes simplex virus type 1 infection

Vilma Decman, PhD

University of Pittsburgh, 2005

Herpes simplex virus type 1 (HSV-1)-specific $CD8^+$ T cells and the cytokine gamma interferon (IFN-γ) are persistently present in trigeminal ganglia (TG) harboring latent HSV-1. We define "latency" as the retention of functional viral genomes in sensory neurons without the production of infectious virions and "reactivation" as a multistep process leading from latency to virion assembly. $CD8^+$ T cells can block HSV-1 reactivation in *ex vivo* mouse TG cultures and appear to be the sole source of IFN-γ in these cultures. Here we demonstrate that IFN-γ alone can block HSV-1 reactivation in some latently infected neurons, and we identify points of intervention in the life cycle of the reactivating virus.

Cell suspensions of TG that were latently infected with recombinant RE HSV-1 expressing enhanced green fluorescent protein (EGFP) from the promoter for infected cell protein 0 (ICP0) or glycoprotein C (gC) were depleted of endogenous $CD8^+$ or $CD45^+$ cells and cultured in the presence or absence of IFN-γ. Our results demonstrate that IFN-γ acts on latently infected neurons to reduce: (i) the incidence of HSV-1 reactivation; (ii) the number of neurons that express the ICP0 promoter; and (iii) the number of neurons that express the gC promoter in *ex vivo* TG cultures. Moreover, those neurons that expressed the ICP0 or gC promoters in the presence of IFN-γ showed a reduced incidence of progression to full reactivation and virion formation. Interestingly, we detected transcripts for ICP0, ICP4, and gH in neurons that expressed the ICP0 promoter in the presence of IFN-γ, but were prevented from fully reactivating and producing virions. Thus, the IFN-γ blockade of HSV-1 reactivation from latency

in neurons occurs at a point prior to expression of the ICP0 gene (required for reactivation) as well as at a very late point in reactivation following expression of at least some structural genes (e.g., gC and gH).

A second project tested the hypothesis that IFN-γ regulates the observed expansion (6-8 days post infection [p.i.]), contraction (8-30 days p.i.), and homeostasis/memory (>30 days p.i.) phases of the HSV-1-specific $CD8^+$ T cell response within the latently infected TG. We addressed this hypothesis by observing the effect of *in vivo* IFN-γ neutralization during the three phases of the response. IFN-γ neutralization significantly reduced the expansion phase through a 50% reduction in proliferation of HSV-1-specific $CD8^+$ T cells. IFN-γ neutralization also significantly accelerated the contraction phase through an as yet undefined mechanism. In contrast, IFN-γ neutralization did not affect the homeostasis/memory phase as no change in the number of HSV-1-specific $CD8^+$ T cells was observed when IFN-γ was neutralized between 30 and 38 days p.i..

A novel finding of these studies was that an HSV-1-specific $CD8^+$ memory precursor population ($CD8_{mp}$, defined by expression of CD127) that was present as a minor subpopulation of the $CD8^+$ effector population ($CD8_{eff}$) at 8 days p.i. exhibited a delayed expansion and contraction relative to the overall $CD8_{eff}$ population in the TG. $CD8_{mp}$ expansion was observed between 8-14 days p.i., and contraction occurred between 14-30 days p.i.. IFN-γ neutralization dramatically reduced the $CD8_{mp}$ expansion, though ultimately the number of $CD127^+CD8^+$ memory ($CD8_{mem}$) in the TG was not affected. The significance of this expansion and contraction of the $CD8_{mp}$ cells during the contraction phase of the $CD8_{eff}$ is not clear. We are currently determining if the disruption of the expansion and contraction of $CD8_{mp}$ through IFN-γ neutralization will influence the shift to a lower functional avidity in the $CD8_{mem}$ population that

ultimately develops. Since HSV-1-specific $CD8_{mem}$ appear to play an important role in regulating HSV-1 latency, optimizing this population could have important implications for controlling recurrent herpetic disease. Thus, defining the events that influence the generation of a functionally optimized $CD8_{mem}$ population will be an important goal of future research in our laboratory.

Acknowledgments

First and foremost, I would like to thank my mentor Dr. Robert L. Hendricks for his guidance, support and optimism in my work. His scientific expertise is unparalleled and I was honored to be his student.

I want to thank my parents, my sister and my husband for all their love and unwavering support.

I would also like to thank all the past and present members of the Hendricks lab, especially to Teresa W. Lee for excellent technical assistance and design of Figure 4, Andrew J. Lepisto for design of Figure 5 and Michael L. Freeman for reading of this manuscript and assistance in design of some of the figures.

TABLE OF CONTENTS

LIST OF FIGURES

1. Introduction

1.1. Herpes simplex virus type 1 (HSV-1) epidemiology

Herpes simplex virus type 1 (HSV-1) is one of the most ubiquitous human infectious agents worldwide [1]. The prevalence of HSV-1 infection increases consistently with age and a US population-based study showed an increase of HSV-1 prevalence from 44% in young adults (12–19 years) to 90% among those > 70 years old [2]. HSV-1 seroprevalence also varies with sex, socio-economic status and geographic location [1;3;4]. In the US, a higher HSV-1 seropositivity is observed in females (70.9%) compared to males (64.2%), and in Mexican Americans (85.1%) compared to African Americans (74.1%) and Caucasians (64.7%) [4].

Humans are considered to be the only natural reservoir of HSV-1 [5]. In most humans, primary HSV-1 infection occurs early in life (during childhood and adolescence) [6] and is often asymptomatic [5;7]. Virus is transmitted following close contact with the salivary secretions, skin, or mucous membranes of a person shedding virus. Following initial replication at primary site of infection, virus establishes latency in the neurons of sensory ganglia [8;9]. Due to establishment of latency and inability of the host immune system to fully eliminate the virus, HSV-1 infection persist for life [8]. Humans tend to experience HSV-1 reactivation from latency when immunologically compromised or in response to a variety of stimuli (i.e., stress, fever, UV light) [10-13]. Reactivation is often asymptomatic and the majority of infected individuals never experience recurrent herpetic disease [6]. When reactivation of latent virus results in clinical disease, it is often characterized by oral or facial lesions (i.e., cold sores, fever blisters). On rare

occasions, HSV-1 reactivation leads to the transport of virus to the brain where the severe infection of the central nervous system could result in potentially lethal encephalitis [5]. Recurrent infections of the cornea are only observed in about 1% of exposed individuals, but can be accompanied by immunopathology causing corneal scarring and permanent loss of vision [14]. Despite the availability of effective antiviral treatment and relatively rare occurrence, ocular HSV-1 disease is still the most common infectious cause of blindness in industrialized nations [5]. It is also a leading indication for corneal transplantation [15].

HSV-1 is usually transmitted via nonsexual contact, but recent studies showed that HSV-1 infections account for a growing proportion of genital herpes infections [16-19]. Moreover, in some instances, HSV-1 has become the most common cause of genital herpes [16;19]. The observed shift to more HSV-1 caused genital herpes could be a consequence of changing patterns of sexual activity such as increased oral-genital contact. Presumably, the initial transmission of genital HSV-1 is a consequence of oral-genital contact, but subsequent transmissions could occur through genital-genital contact [16].

1.2. HSV-1 morphology and genome organization

HSV-1 is a double stranded DNA virus. It belongs to the family of *Herpesviridae* and its virions have a characteristic morphology. Viral DNA is wrapped around a protein core that is enclosed inside the icosadeltahedral capsid. The capsid is surrounded by tegument (an amorphous protein structure) and outer viral envelope (a phospholipoprotein membrane). The tegument contains viral proteins necessary for the initiation of viral transcription (i.e., VP16), while outer viral envelope contains glycoproteins involved in a binding and entry of virus into host cells [20].

HSV-1 152-kbp genome consists of two segments of unique DNA, called the unique long (U_L) and unique short (U_S) region, flanked by inverted repeats (Figure 1) [21]. The genome contains at least 84 open reading frames distributed on both DNA strands and the genes located in the inverted repeat regions are present in two copies [22].

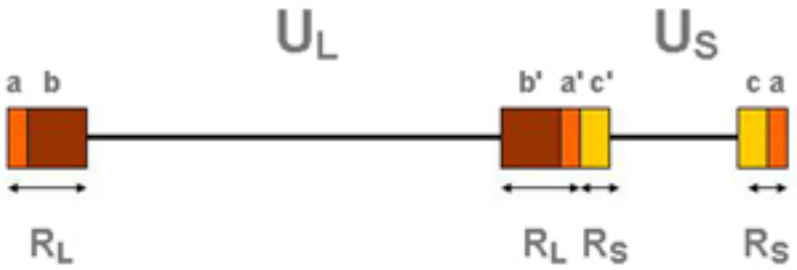

Figure 1: Schematic representation of the HSV-1 genome.

HSV-1 genome is divided into a unique long (U_L) and unique short (U_S) region. U_L and U_S regions are separated by inverted repeats (R_L and R_S, shown as boxes). Adapted from [21].

1.3. Lytic (productive) infection

A lytic (productive) infection is initiated by the binding of HSV-1 virions to the extracellular matrix, primarily through an interaction of two viral membrane glycoproteins, gB and gC, with specific proteoglycans [23]. This is followed by the fusion of viral and plasma membranes (mediated by another set of viral membrane glycoproteins; gD, gB, and gH/gL) and release of tegument proteins and the capsid into the cytoplasm. Once in the cytoplasm, viral capsids attach to microtubules and are transported to the nuclear pore, where viral DNA is released into the nucleus [24]. Upon release, viral DNA circularizes and the transcription from viral genome is initiated by interaction with the viral tegument protein VP16 [21].

During lytic infection the expression of HSV-1 genes is tightly regulated in a temporal and sequential manner (Figure 2) [25;26]. First to appear are immediate–early (IE or α) gene

transcripts. Their expression does not require *de novo* protein synthesis and is necessary for the expression of early and late gene transcripts. In addition, α gene products play an important role in the immune evasion [27-31]. The expression from α genes is followed by expression of early (E or β) gene transcripts. β genes encode proteins functioning primarily in DNA replication and production of substrates for DNA synthesis. Last to be expressed are late (L or γ) gene products. γ genes are subdivided into γ1 (leaky-late, transcripts expressed at low levels in the absence of DNA replication, but require DNA synthesis for optimal expression) and γ2 (true late, transcripts only expressed after the initiation of DNA synthesis) genes [32]. The γ genes encode virion structural proteins and proteins needed for virus assembly and egress.

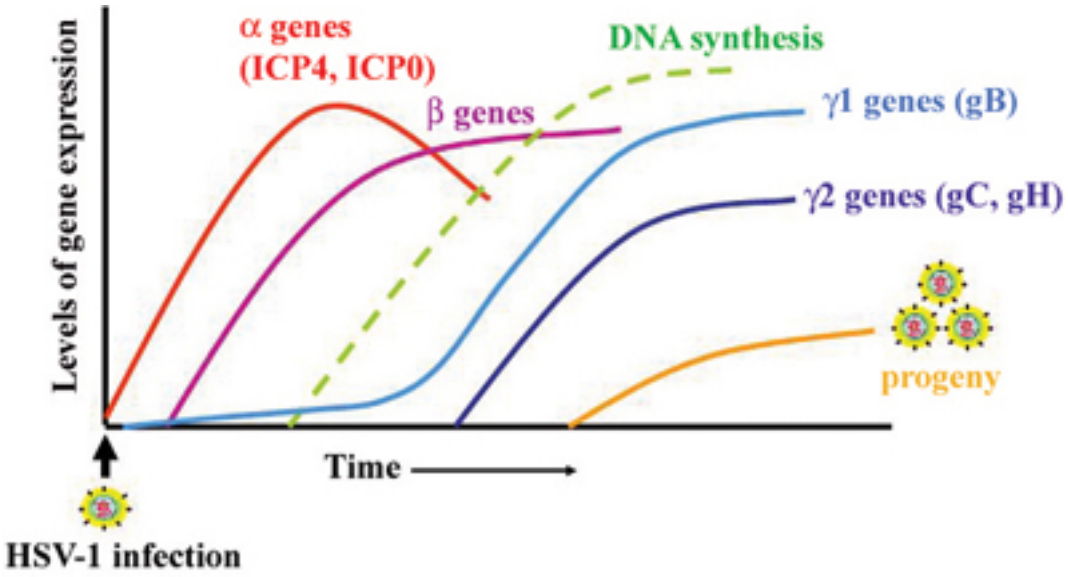

Figure 2: During lytic (productive) infection the expression of HSV-1 genes is tightly regulated in a temporal and sequential manner.

α gene transcripts are the earliest HSV-1 gene transcripts produced. They can be detected around 2-4 hours p.i.. Once α proteins are present in adequate amounts, the transcription of β genes occurs (around 5-7 hours p.i.), followed by viral DNA synthesis, γ gene transcripts expression and the production of progeny infectious virus. ICP4 (infected cell protein 4); ICP0 (infected cell protein 0); gB (glycoprotein B); gC (glycoprotein C); and gH (glycoprotein H).

Once α proteins are present in adequate amounts, the transcription of β genes occurs, followed by viral DNA replication, γ gene transcripts expression and the production of progeny infectious virus.

Detailed description of the HSV-1 genome and the function of viral proteins can be found at www.stdgen.lanl.gov [21].

1.4. HSV-1 promoters and viral gene expression

HSV-1 genes are transcribed by host cellular RNA polymerase II and each gene has its own promoter (Figure 3) [21;22]. The most complex are α gene promoters. They contain TATA element and upstream TAATGARAT motifs required for the initiation of transcription during lytic infection [33]. Briefly, viral tegument protein VP16 interacts with two cellular host proteins; octamer-binding protein 1 (Oct-1) and host cellular factor (HCF) and binding of this complex to the TAATGARAT motifs in α promoters leads to their activation [34-36]. Other *cis*-acting regulatory elements present in α promoters include binding sites for the transcription factor stimulatory protein 1 (Sp1) and in some cases, ICP4 binding site. In addition to ICP4 binding site, ICP0 promoter contains binding motifs for cAMP response element binding protein (CREBP) and F2 transcription factors [21;22].

β gene promoters contain binding sites for eukaryotic transcription factors (i.e., Sp1, CCAAT-binding protein [Cp1]) upstream from the TATA element. γ promoters have an initiator element (Inr) at the start site of transcription, and some of them, a downstream activation site. While some of γ1 gene promoters may contain upstream Sp1 binding sites, the composition of γ2 gene promoters is very simple. For example, a γ2 gene gC promoter contains a TATA-box and several ICP4 binding sites [22].

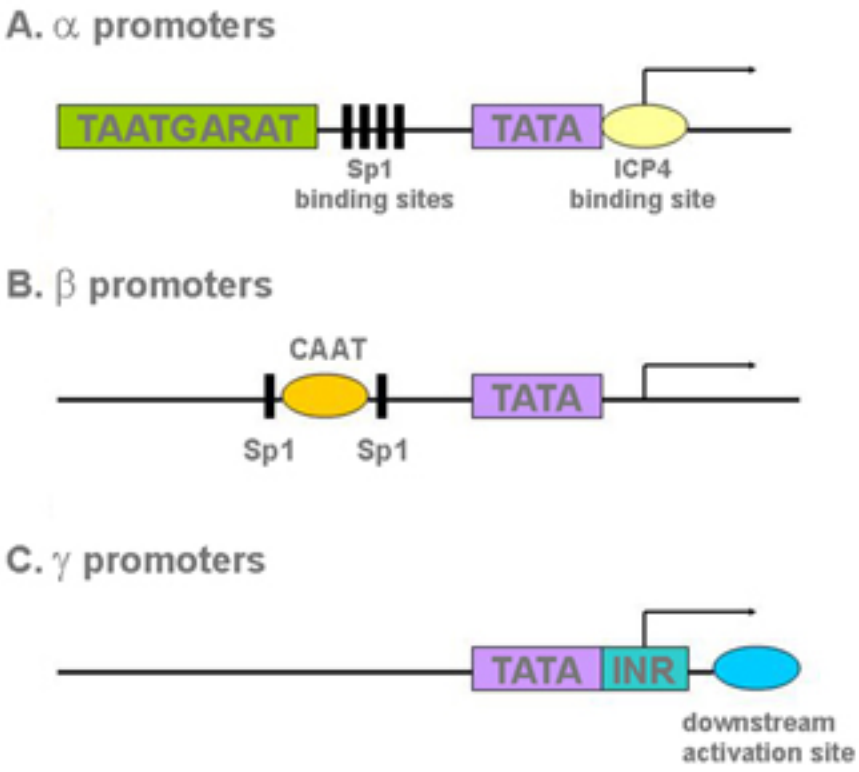

Figure 3: Schematic representation of the HSV-1 α, β and γ promoters.

General structure of α, β and γ promoters is shown. The number and arrangement of *cis*-acting regulatory elements varies among promoters of each class. α promoters contain TATA element and upstream TAATGARAT elements (may contain several of them). Other *cis*-acting regulatory elements present in α promoters are binding sites for transcription factors (i.e., Sp1), and at least in some α promoters, binding sites for ICP4 (A). β promoters have upstream binding sites for transcription factors (i.e., Sp1, Cp1) (B). γ promoters contain an initiator element (Inr) at the start of transcription, and at least some have a downstream activation site (C). Adapted from [21]

1.5. Murine HSV-1 infection model

Several animal models (mice, rats, guinea pigs and rabbits) proved to be a very useful in advancing our understanding of the different aspects of HSV-1 latency *in vivo* [8;37].

We use a mouse ocular model of HSV-1 infection to study the interaction between HSV-1 and the host immune response (Figure 4). In this model, upon initial infection of the epithelial surface of the cornea, viral replication in epithelial cells induces migration of Langerhans cells

(LC) into the cornea [38]. After acquiring viral antigens, LCs travel to the draining lymph nodes (DLNs, submandibular) where the viral antigens are presented to naïve T cells.

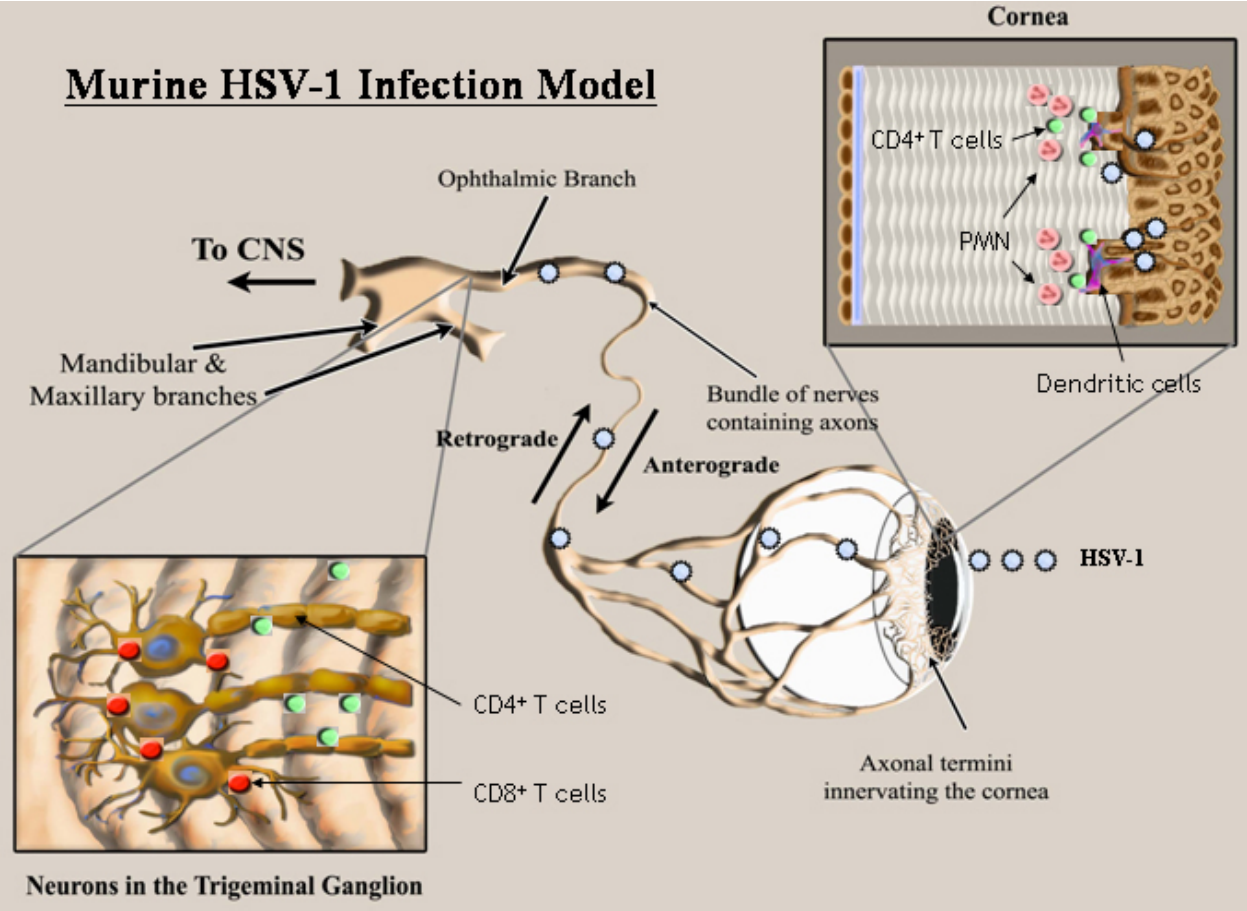

Figure 4: Murine HSV-1 infection model.

Following infection of the epithelial surface of the cornea, HSV-1 replicates in epithelial cells and gains access to the termini of sensory neurons. Virus is then transported by retrograde axonal transport to the neuron cell bodies in the trigeminal ganglion (TG). After a brief period of viral replication, a life-long latent infection is established in a portion of TG neurons. Although unique intrinsic properties of neurons contribute to the control of HSV-1 replication, but both innate and adaptive immune responses are required for the initial control of viral replication and establishment of latency. $CD8^+$ T and $CD4^+$ T cells start to infiltrate the TG early during infection (around day 5) and are retained in HSV-1 infected TG for the life of the host. The $CD8^+$ T cells are found in close apposition to the neuron cell bodies, whereas the $CD4^+$ T cells seem to be scattered throughout the ganglion, particularly in the axonal areas. Infectious virus is eliminated from cornea during the first few days p.i by infiltrating neutrophils (PMNs).

Although infiltrating neutrophils (PMNs) eliminate the infectious virus from cornea over the course of the first few days p.i. [39], during initial replication the virus gains access to local

nerve termini and is transported (by retrograde axonal transport) to the neuron cell bodies within the trigeminal ganglia (TG) [40]. Replicating virus is usually detected in the TG at 2 days p.i. [41]. After a brief period of viral replication, a life-long latent infection is established in a portion of sensory neurons [8].

Sensory neurons in the mouse TG represent a diverse population that can be classified according to their morphology, physiological response properties, neuropeptide content, synthesis of cytoplasmic enzymes, and expression of cell surface receptors [42]. The intrinsic properties of sensory neurons influence the outcome of HSV-1 infection. Although all neuronal populations in the TG are capable of supporting HSV-1 productive infection, some neurons are more permissive for productive infection, while in others, virus is more likely to establish latency [42;43]. In addition, both innate and adaptive immune responses are required for the establishment of uniform latency [44].

Macrophages, γδ T cells and NK T cells start to infiltrate TG during initial replication of virus in this tissue [44-48]. They control viral replication through production of the antiviral agents nitric oxide (NO), tumor necrosis factor alpha (TNF-α) and IFN-γ [44;45]. NO and TNF-α are mainly produced by macrophages [44] while γδ T cells and NK T cells produce IFN-γ [47;48]. The depletion of macrophages, neutralization of TNF-α or IFN-γ; or inhibition of NO production results in significantly increased viral titers and the number of infected neurons in the TG. This further strengthens the important role that innate immunity plays in limiting initial virus replication and lateral spread [44].

αβ T cells of the adaptive immune system are required for the elimination of replicating virus and establishment of latency in at least some neurons. In the absence of these cells, virus establishes latency in some neurons (as judged by LAT expression), but in a small number of

neurons the virus continues to replicate [49-52]. For example, during HSV-1 infection of severe combined immune deficiency (SCID) mice (which lack adaptive immunity, but have a strong innate response), persistent viral replication in some neurons ultimately leads to lethal encephalitis [50;51]. Adoptive transfer of αβ T cells restores the ability of SCID mice to establish uniform latency and survive HSV-1 infection [53]. It is not clear if the small numbers of neurons that require an adaptive immune response to establish a latent infection represent a functional subpopulation of neurons, or merely harbor higher viral loads.

During reactivation from latency, virus travels back along nerve fibers (anterograde axonal transport) to the periphery, at or near the site of primary infection [54;55]. Viral replication in epithelial cells at the site of reactivation causes new lesions [55]. Although reactivation can be induced in response to stimuli that are able to cause stress, either to the whole organism or directly to the neuron [56-58], many studies failed to detect spontaneous reactivation in the mouse model of latency [8;37]. Apparently, mice do not develop recurrent herpetic disease, although a recent study demonstrated that rare neurons in the latently infected TG express viral proteins and may represent the sites of spontaneous molecular reactivation *in vivo* [59]. HSV-1 latency seems to be more tightly regulated in mice compared to humans, which might reflect less reactivation, more efficient containment, or both. In addition, ICP47, an α gene product that blocks $CD8^+$ T cell recognition of infected cells by inhibiting the transporter associated with antigen presentation (TAP), was shown to inhibit the murine TAP relatively poorly compared to human TAP [27;60;61].

1.6. HSV-1 latency

HSV-1 latency is classically defined as the retention of complete viral genomes in the absence of the production of infectious virions. This definition accommodates the possible expression of a limited array of viral lytic genes while maintaining latency and is accepted for other members of the herpesvirus family [62;63]. During HSV-1 latency, the expression from the viral genome is silenced and for many years latency-associated transcripts (LAT), which are encoded in a single region of the HSV-1 genome and accumulate to high levels in the nucleus of some, but not all, latently infected neurons, were thought to be the only transcripts produced [64;65]. This popular concept of a complete lack of lytic gene expression during HSV-1 latency has been called into question by several recent studies [59;66;67]. Limited expression of HSV-1 lytic gene transcripts and proteins (the α gene, ICP4, and the β genes encoding ICP8 and thymidine kinase [TK]) has been detected in mouse sensory ganglia that lack detectable infectious virions. Thus, at any given time, a latent viral genome might be at different stages in the process of reactivation, but full reactivation does not occur until virion assembly is complete. The factors that determine whether the initiation of the reactivation process will lead to virion formation and emergence from latency are largely unknown.

Very little is known about the regulation of transcription from α promoters during reactivation from latency, but it appears that activation of α gene promoters occurs in the absence of VP16, most likely through the action of neuron-specific transcription factors [36]. It was demonstrated that neuronal transcription factors could activate the α gene promoters (ICP0, ICP4, and ICP27) *in vivo* in the absence of other viral proteins [68-70]. Furthermore, it seems that the sequence of HSV-1 gene expression during reactivation from latency may be quite different than during lytic infection [71-73]. One such study showed that the first gene product to

be expressed during reactivation from latency is ICP0 [73], while another study argued that during reactivation, the expression of early genes proceeds expression of immediate-early genes [71].

1.7. $CD8^+$ T cell involvement in the maintenance of HSV-1 latency

Several recent studies have suggested a role for host immunity in suppressing reactivation of the virus in latently infected neurons [45;57;67;74-82]. Leukocytes, including $CD8^+$ and $CD4^+$ T cells, infiltrate the TG during primary HSV-1 infection, and are retained in the ganglion apparently for the life of the animal. The $CD8^+$ T cells are found in close apposition to the neuron cell bodies, whereas the $CD4^+$ T cells seem to be scattered throughout the ganglion, particularly in the axonal areas [45;74;82]. Moreover, chemokines (essential for attracting T cells), including RANTES, MIP-1α, MIP-1β and MCP-1; and cytokines, including IFN-γ, TNF-α and IL-6, appear to be continuously present in latently infected mouse TG [45;74;76;83-85]. The tightly regulated production of these cytokines implies a persistent stimulation of the immune system in latently infected ganglia in the apparent absence of full reactivation.

The concept of persistent immunologic monitoring of latently infected neurons received further support from the recent observations that $CD8^+$ T cells specific for an epitope on the viral lytic gene product glycoprotein B (gB) (i) are retained in latently infected sensory ganglia, (ii) uniformly express an activation phenotype, (iii) form an apparent immunologic synapse with neurons, and (iv) can block full reactivation of HSV-1 from latency in *ex vivo* TG cultures [67;82]. These findings, combined with the detection of viral lytic gene transcripts and proteins in latently infected ganglia, suggest that certain viral lytic gene products (including gB) are consistently or intermittently expressed in latently infected mouse ganglia.

1.7.1. IFN-γ as a potential protective mechanism

The effector mechanisms employed by $CD8^+$ T cells to inhibit HSV-1 reactivation have not been fully defined, but our previous data identified IFN-γ as a potential contributing mechanism [81]. Although HSV-1-specific $CD8^+$ T cells could completely block HSV-1 reactivation from latency in single cell cultures of freshly excised latently infected TG (without eliminating the pool of latently infected neurons) [67], IFN-γ was not able to block reactivation in these cultures. However, IFN-γ did reduce the number of foci of reactivation (areas of cytopathic effect [CPE]) within these cultures, suggesting that IFN-γ can block the reactivation process in some, but not all, latently infected neurons and that IFN-γ is not the only effector molecule employed by $CD8^+$ T cells to inhibit HSV-1 reactivation from latency.

In vivo studies also suggested that IFN-γ plays an important role in the establishment and/or reactivation from latency [74;79;86-90]. Although HSV-1 does not reactivate spontaneously in IFN-γ deficient (GKO) or IFN-γ receptor deficient (RGKO) mice, the incidence of UV irradiation- and hyperthermia-induced reactivation in these mice was significantly higher than in wild type (WT) mice [79;87;89]. Moreover, HSV-1 antigens were detected in multiple neurons in the mutant mice but only in a single neuron in the control mice [79]. Unfortunately, in both studies, the alternative possibility that the increased reactivation rate results from a higher copy number of viral genomes in the sensory neurons of the IFN-γ deficient mice was not tested.

The studies detailed in the first part of this thesis (see Results, Figures 8-17) confirm the differential susceptibility of reactivating neurons to IFN-γ and define stages in HSV-1 reactivation from latency that are blocked by IFN-γ.

1.8. Cross-regulation between IFN-γ and ICP0

The elucidation of the effects of IFN-γ on viral gene expression could improve our understanding of complex virus-host interactions and define mechanisms employed by IFN-γ to inhibit HSV-1 reactivation. Emerging data support the theory that the net effect of cross-regulation between IFN-γ and the HSV-1 α gene product, ICP0, might influence the balance between HSV-1 latent and lytic infection.

1.8.1. ICP0

The ICP0 gene is located in the inverted repeat sequences (flanking U_L region) of HSV-1 genome and therefore present in two copies. One of the few spliced HSV-1 genes, ICP0 contains three exons (encoding amino acids 1-19, 20 to 241, and 242 to 775 of ICP0 protein) [91]. ICP0 is required for efficient reactivation from latency [92] and when provided *in trans*, ICP0 causes reactivation of latent HSV-1 genomes [90;93]. Experiments with transgenic mice demonstrated that neuronal transcription factors can activate expression from ICP0 promoter *in vivo* [68]. Moreover, the activity of this promoter was significantly increased by both UV irradiation and hyperthermia (stimuli that normally cause the reactivation of latent virus) [68]. Interestingly, a recent study demonstrated that the relative amount of circular genomes was higher in cells infected with mutant virus lacking ICP0 compared to cells infected with wild type virus. Thus, the authors argued that the establishment of circular genomes in latently infected neurons is the consequence of absence of ICP0 [94].

ICP0 acts as a promiscuous transactivator of gene expression, and activation of viral and cellular gene expression by ICP0 occurs at the level of mRNA synthesis [95]. Although ICP0 does not directly bind DNA, several studies have shown that a RING finger (zinc-binding)

domain of ICP0, encoded by exon 2, is required for transactivating activity of this protein. RING finger domains are almost exclusively found in the group of E3 ubiquitin ligases [96]. Accordingly, ICP0 interacts dynamically with proteasomes in infected cells and can act as an E3 ubiquitin ligase promoting ubiquitin-protein ligation [97]. ICP0 localizes to and subsequently disrupts discrete nuclear domains called ND10 bodies by promoting the degradation of ND10 components; PML and Sp100, in a proteasome-dependent manner [98]. HSV-1 genomes are deposited at the periphery of ND10 bodies. There is no direct evidence that ND10 disruption is required for viral replication [99], but a recent study demonstrated that destruction of PML abrogated the inhibitory effects of interferons on viral gene expression and replication [100]. Moreover, ICP0 plays an important role in the inhibition of antiviral gene production [30] by targeting interferon-induced antiviral proteins for destruction by proteasomes [100;101].

1.8.2. IFN-γ

IFN-γ counters the effects of ICP0 in several ways. During lytic infection, IFN-γ inhibits ICP0 expression (at low multiplicity of infection) [102;103] and strongly upregulates expression of the various components of ND10 bodies [104], including PML (mediate IFNγ inhibition of HSV-1 gene expression and replication). IFN-γ induced production of the cyclin-dependent kinase (cdk) inhibitors $p21^{WAF1/CIP1}$ and $p27^{Kip1}$ results in decreased cdk2 activity [105]. Work by Schaffer and colleagues [106;107] demonstrated that activity of this kinase is required for HSV-1 replication and α and β gene expression. Cdk2 expression is upregulated in neurons exhibiting HSV-1 reactivation from latency, and a cdk2 specific inhibitor can block HSV-1 reactivation [108]. Furthermore, cdks are required for the posttranslational modifications necessary for the transactivating activity of ICP0 [109], but not for the ability of ICP0 to degrade the components

of ND10 bodies [110]. In addition, IFN-γ regulates the expression of over 200 cellular genes, including many encoding transcription factors [111]. It is reasonable to propose that IFN-γ might influence the expression of host transcription factors or cell cycle proteins that could affect the expression of ICP0.

1.9. $CD8^+$ T cell response during viral infection

$CD8^+$ T cells play a major role in the clearance of most viral infections. A primary $CD8^+$ T cell response results in the control of initial infection and generation of memory $CD8^+$ T cells that can elicit protective immunity upon rechallenge with the same viral pathogen.

Following initial infection, the antigen-specific $CD8^+$ T cells expand within lymphoid organs and differentiate into effector cells ($CD8_{eff}$). Expansion involves rapid programmed cell division, resulting from an interaction of naïve $CD8^+$ T cells with antigen-bearing antigen presenting cells (APCs) within the lymphoid tissue. The $CD8_{eff}$ cells differ phenotypically from the naive precursors in that they down-regulate expression of molecules such as CD127 (IL-7Rα) and CD62L (L-selectin); while up-regulating expression of CD43, CD44, CD122 (IL-2Rβ) and LFA-1 [112;113]. The two main functions of $CD8_{eff}$ cells are targeted lysis of infected cells and cytokine secretion. The effector functions improve during the course of infection [114]. Early in infection, antigen-specific cells exhibit increased capacity to respond to antigen. This enhanced functional avidity seems to be a consequence of the optimization of signal transduction machinery. The maximal responsiveness is usually reached at the peak of antigen-specific $CD8^+$ T cell response and is maintained in memory T cells.

The majority of antigen-specific $CD8_{eff}$ cells (~90%) are eliminated during a contraction phase which correlates with pathogen clearance [115]. In the lymphoid organs contraction can

result from a combination of programmed cell death (apoptosis) and emigration [116]. The mechanisms of apoptosis during contraction are controversial and may depend on whether they are induced by activation or neglect. Two main pathways have been described: activation induced cell death (AICD, also called "active" apoptosis) that involves Fas/FasL interaction; and activated T cell autonomous death (ACAD, also called "passive" apoptosis) that does not depend on death cytokines or receptors. Both are thought to operate via caspases [117-119]. In some models contraction of the $CD8^+$ effector T cell pool in the spleen seems to be independent of caspase activation [120].

After the contraction phase, a small population of antigen-specific $CD8^+$ T cells (memory population, $CD8_{mem}$) survives and is maintained indefinitely [121]. Memory cells were detected for up to 2 years in mice [122] and 35-50 years in humans [123]. They have the ability to rapidly expand upon secondary rechallenge with the same pathogen and persist long term due to a self-renewal process (homeostatic proliferation) that is driven by IL-15, and to a lesser extent by IL-7 [124].

Identification of memory precursor cells ($CD8_{mp}$) within the $CD8_{eff}$ population has been the subject of many investigations. It was shown recently that the initial $CD8_{eff}$ population contains a small subpopulation (~5-15%) that expresses CD127 (IL-7Rα) and have a potential to develop into long-lived memory cells (Figure 5) [125]. The frequency of these $CD127^+$ $CD8_{mp}$ increases during the contraction phase, and they can represent as much as 90% of the $CD8^+$ memory pool during the homeostasis phase. It remains unclear if these $CD8_{mp}$ are directly generated during primary expansion or differentiate from $CD127^-$ effector cells.

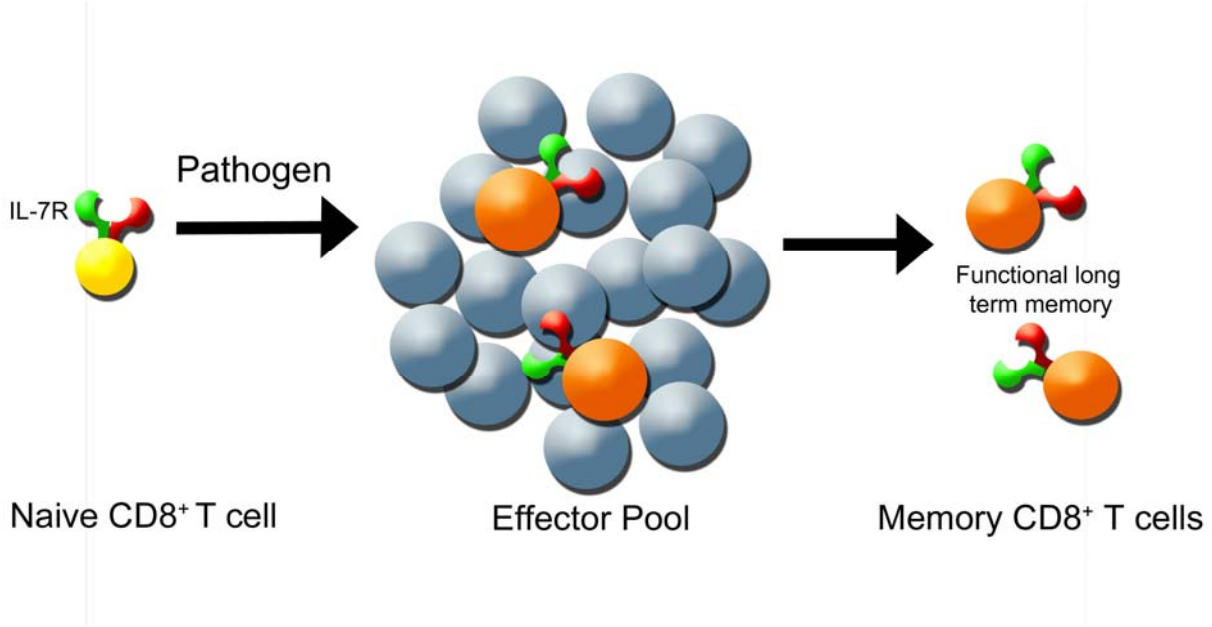

Figure 5: CD127 (IL-7Rα) expression identifies $CD8_{mp}$ cells within the $CD8_{eff}$ population.

Naïve and memory $CD8^+$ T cells express CD127. During the expansion phase, the initial $CD8_{eff}$ population contains a small subpopulation (~5-15% of cells) that expresses CD127 and has a potential to develop into long-lived memory population.

In some instances, $CD8^+$ T cell responses can be elicited toward more then one viral epitope, resulting in generation of different antigen-specific $CD8^+$ T cell subsets. Since the response to some epitopes is stronger (dominant) than the others (subdominant), a hierarchy of epitope-specific $CD8^+$ T cell responses can be observed. This phenomenon is called immunodominance and is regulated by many factors including T cell repertoire and antigen processing and presentation [126]. A recent study identified IFN-γ as another important mechanism [127]. The authors showed that the dominance hierarchy depended on the rate by which different epitope-specific $CD8^+$ T cells were able to initiate IFN-γ production in response to antigen. Namely, the fastest IFN-γ producers became the dominant subset.

1.10. $CD8^+$ T cell response in HSV-1 infected TGs

Several laboratories have demonstrated that $CD8^+$ T cells start to infiltrate the TG early during infection (around 5 days p.i.) [41]. At that time HSV-1 latency is already established in some of the neurons, but ongoing viral replication is detected in others. The initial response of $CD8^+$ T cells occurs in the submandibular lymph nodes which are the DLNs for the cornea [41;128]. Once in the TG, $CD8^+$ T cells go through the expansion and contraction phase. The initiation of the contraction phase correlates with virus clearance and the establishment of uniform latency (between 8 to 10 days p.i. viral replication ceases and replicating virus is no longer detected in the TG). Contraction extends until 30 days p.i.. Finally, a stable population of memory $CD8^+$ T cells is retained (in close apposition to neuron cell bodies) in the latently infected TGs for the life of the animal [67;82]. Thus, the $CD8^+$ T cell response observed in this non-lymphoid tissue during HSV-1 infection resembles the documented $CD8^+$ T cell response in the lymphoid tissues during viral infections [121]. As mentioned before, the timing of infiltration and the life-long retention of $CD8^+$ T cells in the infected TG suggest their possible involvement in both the initial establishment of latency in some neurons, and the maintenance of a latent state.

1.11. IFN-γ is an important determinant of the magnitude of $CD8^+$ T cell response

The abundance of $CD8^+$ T cells in an infected tissue is determined by the net effect of their infiltration, proliferation, death, and emigration, but how each of these processes is regulated is still a matter of extensive research. Previously published studies implicated the cytokine IFN-γ as an important determinant of the abundance of $CD8^+$ T cells.

IFN-γ is produced by activated $CD8^+$ T cells, Th1 $CD4^+$ T cells, NK and NK T cells [129]. It was shown that $CD8^+$ T cells initiate IFN-γ production rapidly upon antigen contact

[130]. IFN-γ binds to IFN-γ receptor (IFN-γR), which is ubiquitously expressed on all nucleated cells, and signals through Jak-Stat pathways (Figure 6) [129]. IFN-γR is composed of two chains; IFN-γR1 or α, a ligand-binding chain; and IFN-γR2 or β, a signal-transducing chain. Biologically active IFN-γ is a noncovalent homodimer of two mature polypeptides in an anti-parallel orientation [131]. IFN-γ homodimers bind to IFN-γR1 [132;133] and upon binding, the intracellular domains of the receptor chains go through the conformational changes that allow association of downstream signaling components with receptor. This results in Jak2 autophosphorylation and activation that leads to Jak1 transphosphorylation by Jak2. The Jak1 phosphorylation of functionally critical tyrosines of each IFN-γR1 chain results in formation of two adjacent docking sites for Stat1 [134-136]. Phosphorylation of the receptor-recruited Stat1 homodimer (probably by Jak2) induces its dissociation from the receptor and translocation to the nucleus [135;137]. In the nucleus, Stat1 homodimers bind to IFN-γ responsive promoter elements to initiate or suppress transcription of IFN-γ-regulated genes [111;138]. The first wave of transcription induced by IFN-γ occurs within 15–30 min of IFN-γ treatment [139] and many of genes induced are transcription factors that regulate the next wave of transcription [111].

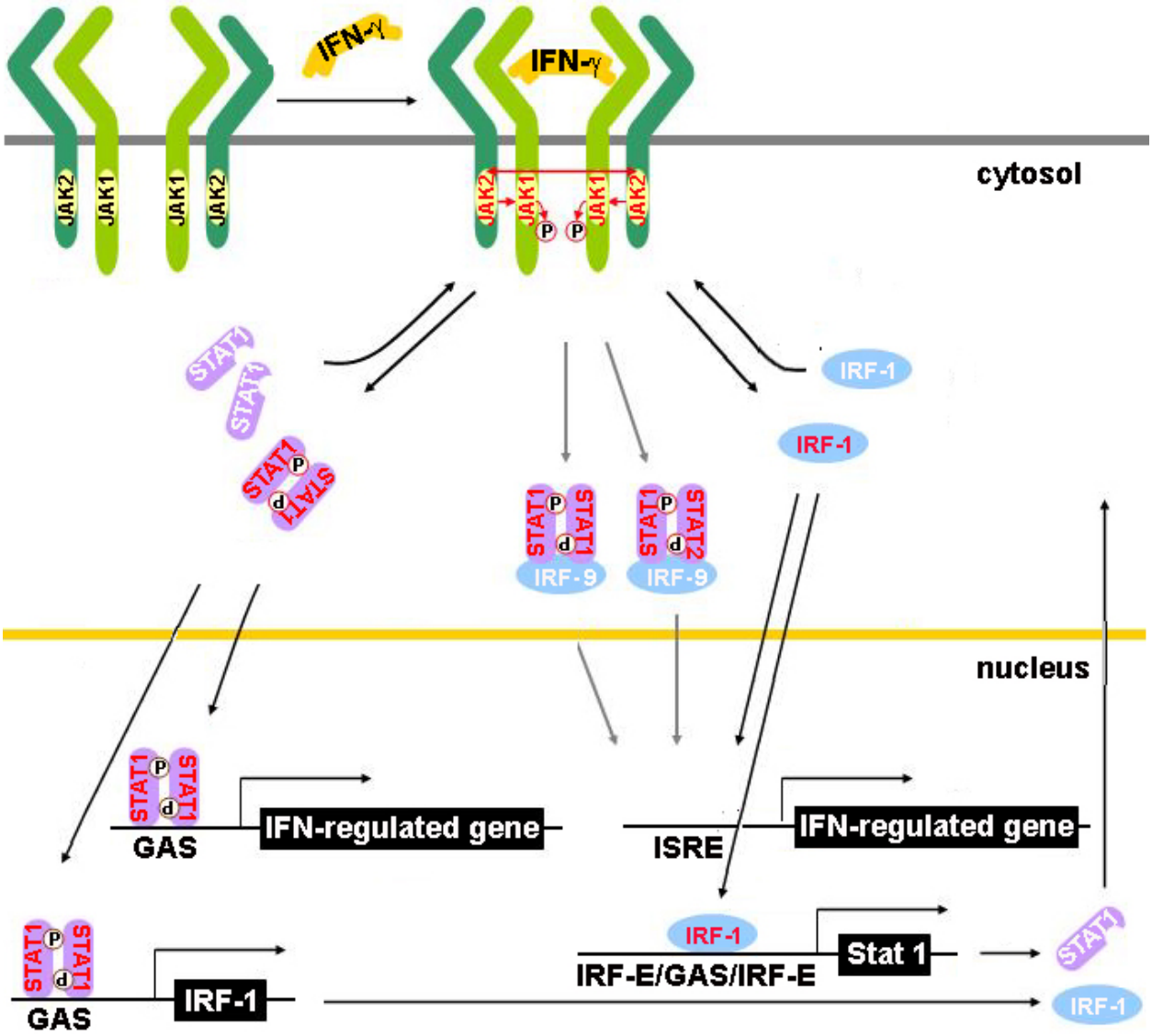

Figure 6: IFN-γ signaling.

The binding of IFN-γ homodimers to IFN-γR (IFN-γR1, light green; IFN-γR2, dark green) causes a conformational change in the IFN-γR which enables the Jak2 kinase to undergo autophosphorylation and activation. This results in Jak1 transphosphorylation by Jak2. The phosphorylation of tyrosines on each IFN-γR1 chain by activated Jak1 allows binding of Stat1 to the receptor. The phosphorylation of receptor-recruited Stat1 homodimer induces its dissociation and translocation to the nucleus. Stat1 homodimers then bind to promoter IFN-γ-activation site (GAS) elements to initiate or suppress transcription of IFN-γ-regulated genes. IFN-γ signaling also produces Stat1:Stat1:IFN regulatory factor (IRF)-9 and Stat1:Stat2:IRF-9 [IFN-stimulated gene factor 3 (ISGF3)] complexes. Stat1:Stat1:IRF9, ISGF3 and IRF-1 bind to IFN-stimulated response element (ISRE) promoter regions. IRF-1 promotes Stat1 transcription through an unusual ISRE site (IRF-E/GAS/IRF-E). Adapted from [129].

IFN-γ is best known for its direct antiviral actions mediated through the induction of double-stranded RNA activated protein kinase (PKR), 2'-5' oligoadenylate synthetase (2–5A

synthetase), and dsRNA specific adenosine deaminase (dsRAD). Many viral pathogens, including HSV-1, produce proteins that interfere with IFN-γ signaling at different stages and mitigate the anti-viral host response [140;141]. As mentioned previously, ICP0 protein inhibits antiviral gene production by targeting interferon-induced antiviral proteins for destruction by proteasomes [30].

IFN-γ upregulates both the class I and class II antigen presentation pathways, thus improving the host response to pathogens [142]. In humans, mutations of IFN-γ or its receptor result in recurrent bacterial and parasitic infections [143]. Similarly, GKO and RGKO mice also show deficiencies in natural resistance to infections with variety of pathogens such as HSV-1, vaccinia virus, *Leishmania major*, *Toxoplasma gondii*, and *Listeria monocytogenes* (LM) [89;144-148]. In addition, IFN-γ regulates the expression of over 200 cellular genes involved in transcriptional regulation, leukocyte-endothelial interactions, oxidative burst, tryptophan metabolism and apoptosis [111].

Due to the above mentioned properties it is not surprising that IFN-γ seems to modulate the magnitude of the adaptive immune response. IFN-γ also affects the immunodominance hierarchy of various epitope-specific $CD8^+$ T cells subsets [149;150]. The rapidity by which $CD8^+$ T cells initiate IFN-γ production influences their final abundance [127].

1.11.1. IFN-γ: stimulatory vs. suppressive role.

The exact nature of the contribution of IFN-γ to the three phases of the $CD8^+$ T cells response remains controversial. A study by the Harty and colleagues demonstrated elevated numbers and altered immunodominance of antigen-specific $CD8^+$ T cells in the absence of IFN-γ [149;151]. While in LM infected GKO mice the numbers of antigen-specific $CD8^+$ T cells stayed

elevated up to 150 days p.i., the majority of these cells was eliminated by day 10 p.i. in LM infected WT mice. Thus, the authors concluded that IFN-γ exerts the suppressive (pro-apoptotic) effects on the contraction of antigen-specific $CD8^+$ T cells. Since the clearance of pathogen is delayed in GKO mice, it still remains to be demonstrated if the observed IFN-γ effects were not influenced by potential contributing role of increased antigen loads on regulation of contraction. Studies in which the $CD4^+$ T cell response was monitored further supported the suppressive role of IFN-γ. One such study showed that IFN-γ enhanced apoptosis of activated $CD4^+$ T cells in mycobacteria infected hosts and at least *in vitro* this depended on the presence of activated macrophages and NO production. Again, the studies were done in GKO mice in which the pathogen grew in an uncontrolled manner [152].

The issue was further confounded by conflicting results from a recent study. That study demonstrated that IFN-γ exhibits stimulatory effects on the magnitude of antigen-specific $CD8^+$ T cell responses [153]. The number of antigen-specific cells was significantly reduced in LCMV infected RGKO mice compared to WT mice. After the dual adoptive transfer of IFN-γR^+ and IFN-γR^- $CD8^+$ T cells in LCMV infected host, the abundance of latter cells was markedly reduced. Although the absence of IFN-γR influenced the abundance of $CD8^+$ T cells; it did not affect their activation status or antigen-responsiveness.

We used a model of HSV-1 latency in the peripheral nervous system to investigate the involvement of IFN-γ in the initial expansion of HSV-1-specific $CD8_{eff}$ cells in a non-lymphoid tissue, as well as their subsequent contraction, the development of $CD8_{mp}$, and ultimately the establishment of a functionally optimized $CD8_{mem}$ population. The advantages of our system include: (i) the ability to trace virus-specific cells using dimers containing a very strongly immunodominant epitope, (ii) an accessible non-lymphoid tissue that retains memory cells for

the life of the animal, and (iii) a localized latent infection in which antigenic load is not dramatically altered by transient manipulation of the immune response. Results from our studies (Figures 18-30) support the stimulatory role of IFN-γ. The experiments detailed herein demonstrate an IFN-γ requirement for the optimal antigen-specific $CD8^+$ T cell response in HSV-1 infected TG. Furthermore, we defined the phases of antigen-specific $CD8^+$ T cell response affected by IFN-γ and revealed one of the possible mechanisms of IFN-γ actions.

2. Specific Aims

The specific goals that were set forth for my thesis project and the progress that was made in my studies are summarized below.

Specific aim 1: To investigate the effects of IFN-γ on viral gene expression in HSV-1 latently infected TG.

Hypothesis: IFN-γ inhibits HSV-1 reactivation from latency in some, but not all latently infected neurons by inhibiting multiple steps in the reactivation process.

In the first part of my thesis (see Results, Figures 8-17) I use TGs that are latently infected with recombinant viruses that express EGFP from different viral promoters to demonstrate that IFN-γ selectively blocks HSV-1 reactivation in a subgroup of latently infected neurons, and does so in part by inhibiting expression of an essential α gene, but also by inhibiting a very late step in reactivation following expression of viral structural proteins.

Specific aim 2: To investigate the effects of IFN-γ on the kinetics of antigen-specific $CD8^{\pm}$ T cell response in HSV-1 infected TG.

Hypothesis: IFN-γ regulates the magnitude of both the antigen-specific $CD8_{eff}$ and $CD8_{mp}$ response in HSV-1 infected TG.

In the second part of my thesis (see Results, Figures 18-30) I incorporate a useful model of HSV-1 latency in the peripheral nervous system to investigate the involvement of IFN-γ in the initial expansion of HSV-1-specific $CD8_{eff}$ cells in a non-lymphoid tissue, as well as their subsequent contraction, the development of $CD8_{mp}$, and ultimately the establishment of a functionally optimized $CD8_{mem}$ population. The advantages of our system include: (i) the ability to trace virus-specific cells using dimers containing a very strongly immunodominant epitope, (ii) an accessible non-lymphoid tissue that retains memory cells for the life of the animal, and (iii) a localized latent infection in which antigenic load is not dramatically altered by transient manipulation of the immune response. Using this model we demonstrated a dramatic effect of IFN-γ on the expansion and contraction of HSV-1-specific $CD8_{eff}$, and an IFN-γ regulated expansion phase of $CD8_{mp}$ that to our knowledge has not been previously shown.

3. Materials and Methods

3.1. Viruses

The wild-type (WT) HSV-1 RE and two recombinant HSV-1 strains expressing EGFP from viral promoters (HSV-1 RE-pICP0-EGFP and HSV-1 RE-pgC-EGFP) were used for these studies.

All viruses were grown in Vero cells. Intact virions were purified on OptiPrep gradients according to the manufacturer's instructions (Accurate Chemical & Scientific Corp., Westbury, NY) and quantified as plaque forming units (PFU) on Vero cell monolayers.

3.2. Construction of promoter-EGFP viruses

Two recombinant HSV-1 strains expressing EGFP from viral promoters (RE-pICP0-EGFP and RE-pgC-EGFP) were produced in collaboration with Dr. P. R. Kinchington, University of Pittsburgh. Both viruses were created on HSV-1 RE background and are null mutants at the gC locus (Figure 7). For the construction of RE-pgC-EGFP, a cloned PstI-EcoRI fragment (positions 95,811 to 96,789 in the WT HSV-1 genome, containing the gC promoter and the first part of the gC ORF) was used in the puc8 plasmid (a kind gift of N. DeLuca, University of Pittsburgh). The polylinker sites were removed by collapsing the sequences between the PstI and HindIII site. An NheI-XbaI fragment derived from pEGFP-N1 (Clontech, Palo Alto, CA) was then inserted into the unique NheI site located at the sequence encoding residue 6 of gC, resulting in an in-frame placement of the EGFP gene immediately following the sequence for the

first six gC residues. This plasmid was linearized and co-transfected with purified HSV-1 RE DNA into Vero cells using calcium phosphate co-precipitation, and progeny viruses with EGFP driven by the native gC promoter were identified by fluorescence and plaque purified.

To derive RE-pICP0-EGFP, a 707-bp StuI-NcoI ICP0 fragment containing the ICP0 promoter and introns (positions 1,553 to 2,259 in the WT genome) was ligated into the gC-EGFP vector cut with HindIII, blunt ended, and digested with NcoI. These sites were in the polylinker N terminal to the EGFP coding sequences and resulted in the placement of the ICP0 promoter downstream of the gC promoter driving EGFP. The virus was derived as described above, plaque purified and the insertion of the ICP0 promoter-EGFP coding sequence in the disrupted gC locus was confirmed by Southern blotting. The 707-bp ICP0 promoter contains all known promoter elements required for ICP0 transcription, including the six upstream TAATGARAT-like sequences [154].

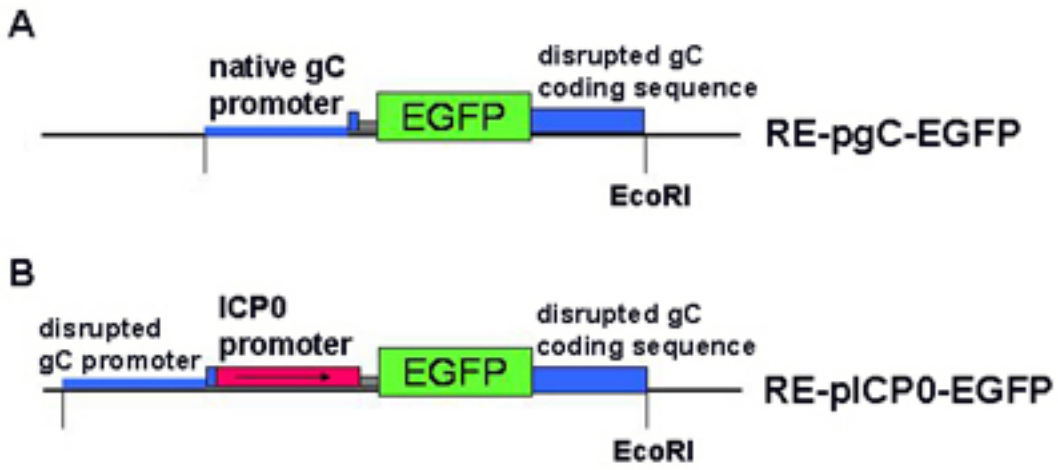

Figure 7: Schematic representation of RE-pgC-EGFP and RE-pICP0-EGFP.

3.3. Analysis of EGFP expression *in vitro*

Confluent monolayers of Vero cells were infected at an MOI of 10 PFU/cell for 1h with either RE-pICP0-EGFP or RE-pgC-EGFP. Infection was done in the presence of medium alone or medium containing either 150 μg/ml of cycloheximide (CHX) or 400 μg/ml of phosphonoacetic acid (PAA). Following 1 h incubation, virus-containing medium was removed and replaced with the same drug treatments.

For CHX reversal experiments, after 6 h of incubation with 150 μg/ml of CHX, the medium was removed, the monolayers were washed three times, and medium without CHX but containing 15 μg/ml of actinomycin D was added. Monolayers were incubated for two more hours in this actinomycin D containing medium. For PAA treatment, the drug was present during the entire 12-h incubation period.

CHX blocks protein synthesis by inhibiting the peptidyl transferase activity of the 60S ribosomal subunit.

PAA is a pyrophosphate analog. It inhibits HSV-1 DNA polymerase by interacting with the pyrophosphate binding site. This interaction results in the blockage of viral DNA synthesis.

Actinomycin D blocks *de novo* RNA transcription by binding to double-helical DNA and preventing it from being an effective template for RNA synthesis.

All samples were analyzed by SDS PAGE and transferred to Immobilon-P membranes. This was followed by immunoblotting with anti-EGFP antibodies (Affinity Bioreagents, Golden, CO) and secondary detection using West Dura reagents (Pierce Biotechnology, Inc., Rockford, IL). A parallel gel was fixed and stained with Coomassie brilliant blue to demonstrate equal loading of proteins in the various lanes.

3.4. *In vitro* replication kinetics

Slightly subconfluent monolayers of Vero cells were infected with WT HSV-1 RE, RE-pICP0-EGFP or RE-pgC-EGFP at a low multiplicity of infection (MOI) (0.01 PFU/cell) or a high MOI (10 PFU/cell). Cells and supernatants were harvested at 4, 8, 12, 24 and 48 h p.i. for the high MOI and at 4, 24 and 48 h p.i. for the low MOI and then subjected to three freeze-thaw cycles. The titers of each virus at given time points were quantified on Vero cell monolayers.

3.5. Mice

Six- to 8-week-old female BALB/c mice (Frederick Cancer Research Center, Frederick, MD) or 4- to 6-week-old female C57BL/6 mice (Jackson Laboratory, Bar Harbor, ME) were anesthetized by the intramuscular injection of 2.0 mg of ketamine hydrochloride and 0.04 mg of xylazine (Pheonix Scientific; St Joseph, MO) in 0.2 ml of HBSS (BioWhittaker, Walkersville, MD). The right eye corneas of BALB/c mice or both corneas of C57BL/6 mice were scarified 10 times in a crisscross fashion with a sterile 30-gauge needle and HSV-1 (10^5 PFU/3 μl of RPMI, BioWhittaker) was applied topically. All experimental procedures were reviewed and approved by the University of Pittsburgh Institutional Animal Care and Use Committee (IACUC).

3.6. Preparation of TG cultures

On day 35 after HSV-1 corneal infection of BALB/c mice, the ipsilateral TG were excised, treated with collagenase type I (40 U/TG; Sigma-Aldrich, St. Louis, MO) for 1.5 h at 37°C, and dissociated into a single-cell suspension by trituration. The cells from multiple TG were pooled and counted. We obtained an average yield of 20,096 ± 360 neurons per TG, which is similar to the yield reported previously [67;155]. TG cell suspensions were depleted of $CD8^+$

T lymphocytes alone or of all infiltrating bone marrow-derived ($CD45^+$) cells by immunomagnetic separation using magnetic beads (six beads/cell) coated with monoclonal antibodies to CD8α or CD45 (Dynal ASA, Oslo, Norway), as previously described [81]. The efficiency of depletion was > 98%, as determined by immunofluorescence staining for CD8α or CD45. Following immunomagnetic separation, an overall reduction in cell numbers in the TG cell suspensions was observed, and adjustments to the pre-separation neuron density were made. The equivalent number of cells from 1/10 of a TG was added to each well of a 96-well tissue culture plate and incubated with 200 μl of DMEM (BioWhittaker) containing 10% FBS (HyClone, Logan, UT) and 10 U/ml of recombinant murine IL-2 (R&D Systems, Inc., Minneapolis, MN). To half of the cultures recombinant mouse IFN-γ (rmIFN-γ, 1,000 WHO units/ml=1.2 μg/ml; R&D Systems) was added. Thus, each individual TG culture (1/10 of a TG) contained 200 WHO units (0.24 μg) of rmIFN-γ. Previous experiments showed this to be the optimal treatment. The IFN-γ preparation used for the studies was certified by the manufacturer to be below the level of detection for endotoxin.

The cultures were examined daily for 10 days by confocal microscopy for the expression of EGFP in neurons and surrounding fibroblasts. Preliminary studies demonstrated that nondepleted TG cultures and cultures that were mock depleted with magnetic beads coated with an irrelevant antibody exhibited identical reactivation frequencies and numbers of EGFP-positive neurons. After establishing this fact, only TG cells that were depleted of $CD8^+$ T cells or $CD45^+$ cells were used in the studies.

3.7. RNA extraction and cDNA preparation

TG were excised 35 days after corneal infection with HSV-1 RE-pICP0-EGFP, depleted of $CD8^+$ T cells, and cultured in the presence of rmIFN-γ as described above (1/10 TG/well in a 96 well plate). After 6 or 10 days in culture, the supernatants were removed and assayed for infectious virus by a standard virus plaque assay. Lysates from five TG cultures were pooled, and total RNA was extracted using RNeasy columns (QIAGEN, Valencia, CA) according to the manufacturer's instructions.

During purification on RNeasy columns, RNA samples were treated with DNase I to reduce contaminating viral DNA. The RNAs were then additionally digested with RNase-free DNaseI using a DNA-free™ kit (Ambion Inc., Austin, TX). cDNAs were generated from either 150 or 300 ng of total RNA using a High Capacity cDNA Archive Kit (Applied Biosystems Inc.; ABI, Foster City, CA) according to the manufacturer's instructions.

3.8. Real-time PCR analysis of viral transcripts

Quantitative real-time PCR assays were performed using reagents from Applied Biosystems Inc. (ABI). An ABI Prism 7700 Sequence Detector was used, running 96-well plates with 50 µl/well final volumes. For instrument control and data analysis, we used the default settings of ABI Primer Express v. 1.5a software. Each assay comprised triplicate measurements of both cDNA and a control (no reverse transcriptase [RT]) at 7.5 or 15 ng per well. Samples were mixed with the appropriate primer-probe set and TaqMan Universal PCR Master Mix (Roche, Branchburg, NJ).

Primer-probes sets for the mouse housekeeping gene encoding pyruvate carboxylase (Pcx, cat. number, Mm00500992_m1) and for the viral transcripts ICP4, ICP0 and gH were

designed and custom-synthesized by the ABI Assays-by-Design service. The sequences were as follows: for ICP4, forward primer (5'-GCAGCAGTACGCCCTGA-3'), reverse primer (5'-TTCTGGAGCCACCCCATG-3'), and probe [5'-(FAM)CACGCGGCTGCTGTACA(NFQ)-3']; for ICP0, forward primer (5'- CACCACGGACGAGGATGAC-3'), reverse primer (5'-CGGCGCCTCTGCGT-3') and probe [5'-(FAM)ACGACGCAGACTACG(NFQ)-3']; and for gH, forward primer (5'- CGACCACCAGAAAACCCTCTTT-3'), reverse primer (5'-ACGCTCTCGTCTAGATCAAAGC-3'), and probe [5'-(FAM)TCCGGACCACTTTTC(NFQ)-3'].

For assay validation of each primer-probe set, cDNA or a no-RT control from infected tissue (from HSV-1 RE-infected mouse TG on day 3) was used to generate a standard curve of the change in cycle threshold (ΔC_T) versus the log (ng cDNA/well) for the range of 0.1 to 100 ng/well. Three separate analyses gave correlation coefficients and PCR efficiencies (mean ± SD) as follows: for ICP4, R^2 = 0.989 ± 0.007 and efficiency = 97% ± 5%; for ICP0, R^2 = 0.991 ± 0.005 and efficiency = 99% ± 2%; for gH, R^2 = 0.992 ± 0.006 and efficiency = 98% ± 2%; and for Pcx, R^2 = 0.989 ± 0.006 and efficiency = 105% ± 3%.

Analysis panels comprising all four primer-probe sets were performed using material from 15 distinct biological samples (five TG preparations from group 1, group 2 and group 3 cultures [as defined in Results]). Some samples were subjected to multiple parallel processing to verify the reproducibility of the entire procedure. A strong correlation was observed between analysis panels from parallel extractions for samples with high levels of viral transcripts (group 3 cultures), with R^2 values of 0.997 and 0.987 when assayed in the same plate and 0.940 when assayed in different plates. For samples with low levels of viral transcripts (group 1 and 2 cultures) assayed in different plates, R^2 was 0.896 ± 0.017 (n=3). The Pcx data consistently

showed low no-RT control levels, which were undetectable (i.e., C_T = 40) in 59 of 61 measurements. The C_T values for Pcx successfully distinguished the 18 assays run at 15 ng/well (mean C_T = 25.4 [2.3 fold more material]) from the 5 assays run at 7.5 ng/well (mean C_T = 26.6). After Pcx correction, duplicate or triplicate analysis panels were averaged. We considered samples with a C_T of 40 to lack transcripts, and expressed the relative amount of transcripts in samples as 40 – C_T.

The ICP4 and gH genes are intronless, and their primer-probe sets cause a measurable amplification of contaminating viral DNA in no-RT controls, while the primer-probe set for ICP0 crosses an intron-exon boundary and results in no-RT control levels that are low or undetectable. For all three transcripts we elected to treat the no-RT controls as a separate group in statistical analysis.

3.9. Preparation of adenovirus vectors

Replication-defective adenovirus vectors (Ad.CMV-rtTA, Ad.TRE-ICP0 and Ad.TRE-n212) used in the studies were a kind gift of W. P. Halford, Tulane University Health Sciences Center. In Ad.CMV-rtTA, a reverse tetracycline-regulated transactivator (rtTA) is expressed from the CMV promoter. Ad.TRE-ICP0 and Ad.TRE-n212 express WT and mutant (expresses the first 211 of 775 amino acids of ICP0) form of ICP0, respectively, under the control of a tetracycline response element (TRE) promoter [93].

Adenovirus vectors were propagated in 293 cells as previously described [93]. Briefly, 293 cell suspensions (in DMEM containing 10% FBS) were mixed with each adenovirus vector at the final MOI of 0.05 PFU/cell. Infected cells were incubated at 37°C for 5-6 days until all cells showed CPE (i.e., were round-shaped) and then subjected to freeze/thaw cycle. After the

removal of cellular debris by low-speed centrifugation, the supernatants were aliquoted and stored at -80°C until further use. The titers of adenovirus vectors were determined on 293 cell monolayers following the protocol described in the Adeno-X Tet-Off Expression System User Manual (Clontech Laboratories, Inc.; Palo Alto, CA; catalog #: K1651-1, pages 36-37).

3.10. Infection of TG cultures with adenovirus vectors

TG were excised 35 days after corneal infection with HSV-1 RE-pICP0-EGFP, depleted of $CD8^+$ T cells and cultured in the presence or absence of rmIFN-γ as described above (1/10 TG/well in a 96 well plate). Doxycycline hyclate (DOX; Fluka, Buchs, Switzerland) was added to TG cell medium (DMEM containing 10% FBS and 10 U/ml of rmIL-2) at a final concentration of 3 μM. At day 1 post culturing, TG cell cultures were co-infected with Ad.CMV-rtTA (MOI = 10 PFU/cell) and either Ad.TRE-ICP0 or Ad.TRE-n212 at an MOI of 30 PFU/cell. Briefly, infections were performed by adding either 30 μl of Ad.CMV-rtTA + Ad.TRE-ICP0 or 30 μl of Ad.CMV-rtTA + Ad.TRE-n212 to each well. The cultures were examined daily for 10 days by confocal microscopy for the expression of EGFP in neurons and surrounding fibroblasts.

3.11. Neutralization of IFN-γ at various times after HSV-1 corneal infection

At various times after HSV-1 corneal infection, groups of C57BL/6 mice received a single or multiple intraperitoneal injections (i.p.) of 1 mg/mouse of purified rat anti-IFN-γ monoclonal antibody (mAb, clone R4-6A2). For the exact regiment of treatments see Results, section 4.2. The endotoxin content in each antibody preparation was determined using LAL (Limulus Amebocyte Lysate) test and showed to be below the level of detection (> 0.125 EU [Endotoxin Units]/ml).

Preliminary studies demonstrated no difference in relevant cell numbers in the TGs of untreated HSV-1 infected mice and TGs of HSV-1 infected mice treated with a control mAb (anti-HLA-DR, clone 2.83). After establishing this fact, only untreated mice were used in subsequent studies.

3.12. Preparation of TG single-cell suspensions

At various times after HSV-1 corneal infection, C57BL/6 mice were sacrificed and both TGs from the same animal were removed, placed in a single tube and treated with collagenase type I (40 U/TG, Sigma-Aldrich). After collagenase treatment (1 h at 37^{o}C), TGs were triturated until no apparent tissue fragments remained. One TG equivalent was then removed, filtered through a 40 μm cell strainer cap (BD Biosciences Discovery Labware, Bedford, MA), stained with appropriate antibodies and subjected to flow cytofluorometric (FCM) analysis. The remaining TG equivalent was used for DNA isolation and subsequent determination of a viral genome copy number.

3.13. Preparation of DLN single-cell suspensions

At various times after HSV-1 corneal infection, C57BL/6 mice were sacrificed and DLNs (submandibular LNs) were excised. Single-cell suspensions of DLNs from individual animals were prepared by running both DLNs through the 40 μm cell strainer cap (BD Biosciences Discovery Labware). The red blood cell lysis was done by incubation of pelleted cells with red blood cell lysis buffer (NH_4Cl/Tris buffer) for 5 min at RT. DLN suspensions were then pelleted by low-speed centrifugation, resuspended in 5 ml of RPMI containing 5% FBS and counted. Cells were stained with appropriate antibodies and subjected to FCM analysis.

3.14. TG and LN flow cytofluorometry (FCM)

For FCM analysis, single-cell suspensions of TGs (one TG equivalent per tube) or DLNs (3 x 10^6 cells/tube) were incubated with anti-mouse CD16/CD32 (FcγRIII/II; clone 2.4G2; BD Pharmingen; to prevent a non-specific binding of fluoresceinated mAbs) and then stained for cell surface markers and $gB_{498-505}$-specific $CD8^+$ T cells. Cell surface markers were detected using the following antibodies from BD Pharmingen: APC-Cy7-conjugated anti-CD8α (53-6.7), PE-Cy7-conjugated anti-CD4 (RM4-5), PerCP-conjugated anti-CD45 (30-F11), FITC-conjugated anti-CD69 (H1.2F3) and appropriate isotype controls. APC-conjugated anti-CD127 (A7R34) was purchased from eBioscience (San Diego, CA).

To visualize $gB_{498-505}$-specific $CD8^+$ T cells, PE-conjugated Dimer X (H-$2K^b$: Ig; BD Pharmingen) reagent was loaded with $gB_{498-505}$ peptide (SSIEFARL; Research Genetics, Carlsbad, CA) overnight prior to use. Briefly, $gB_{498-505}$ peptide (stock concentration, 2 mg/ml) and Dimer X reagent were mixed in ratio 0.3325 µl: 5 µl. 5 and 10 µl of gB peptide-loaded dimer were then added to each TG and DLN staining tube, respectively. All stains were done for 1 h at 4°C.

3.14.1. BrdU staining (identifies cells that divided during the BrdU pulse)

C57BL/6 mice received a single intraperitoneal injection (1 mg/mouse) of BrdU 14 h before they were sacrificed (see Results, Figures 22 and 23).

BrdU staining was carried out using a BrdU Flow Kit (BD Pharmingen) in accordance with the manufacturer's instructions. Briefly, cells were stained for cell surface molecules (1 h at 4°C), and then fixed and permeabilized. After second permeabilization, cells were treated with

DNase to expose incorporated BrdU. BrdU was then detected using FITC-conjugated anti-BrdU antibody.

3.14.2. Ki-67 staining (identifies cells that were dividing at the time of excision)

Ki-67 staining was carried out using a FITC-conjugated Ki-67 Kit (BD Pharmingen) in accordance with the manufacturer's instructions. Briefly, cells were stained for cell surface molecules (1 h at 4°C), and then fixed, permeabilized and stained with FITC-conjugated anti-Ki-67 antibody (clone B56).

3.14.3. Annexin V staining (identifies apoptotic cells)

Annexin V staining was carried out using an Annexin V-FITC Apoptosis Detection Kit I (BD Pharmingen) in accordance with the manufacturer's instructions. Briefly, cells were stained for cell surface molecules (1 h at 4°C), resuspended in binding buffer and then incubated with annexin V-FITC antibody (15 min at RT). Stained cells were analyzed within one hour.

After all above mentioned staining procedures (except after annexin V staining), cells were fixed in 1% paraformaldehyde (PFA, Electron Microscopy Sciences, Fort Washington, PA) and analyzed on a FACSAria (Becton Dickinson) using FACSDIVA data analysis software. The entire content of each individual TG was analyzed to provide an estimate of the absolute number of marker-positive cells per TG. The absolute number of marker-positive cells in the DLNs of individual animal was calculated based on the number of marker-positive cells per 500,000 collected events and total number of cells in DLNs of that animal.

3.15. DNA extraction and preparation

For DNA isolation, single-cell suspensions of one TG equivalents were centrifuged at low speed and resuspended in 200 µl of 1X PBS. DNA was extracted from the PBS-resuspended TG equivalents according to the manufacturer's instructions using DNeasy columns (QIAGEN). Total DNA was eluted from the column with 100 µl of DNase-free water. The DNA content in each TG sample was determined on a SPECTRAmax384 spectrophotometer (Sunnyvale, CA).

For the purpose of real-time PCR analysis each TG DNA sample was prepared at a final concentration of 1 ng/µl. The aliquots were stored at -80° C until use.

3.16. Real-time PCR for viral genome copy number

The gene encoding HSV-1 protein gH was selected for the quantification of viral genomes. The primer-probe set for the gH gene was designed and custom-synthesized by the ABI Assays-by-Design service (for primer-probe set sequence see Material and Methods, section 3.8). Samples were mixed with the gH primer-probe set and TaqMan Universal PCR Master Mix (Roche) and real-time PCR assays were performed using an ABI Prism 7700 Sequence Detector running 96-well plates (50 µl/well final volumes). For instrument control and data analysis, we used the default settings of ABI Primer Express v. 1.5a software.

Standard curves were created using serial 10-fold dilutions of gH plasmid for the range of 10^0 to 10^6 copies. Uninfected C57BL/6 mice TG DNA (500 ng) was added to all plasmid standards to compensate for the potential inhibition of amplification by added DNA. The analysis of serial 10-fold dilutions of gH plasmid standards showed that the threshold sensitivity of the assay was 10^0 copies; the C_T value for 10^0 copies of gH plasmid was 36.1 ± 0.8 (mean ± SD, n = 7); readily distinguishable from the blank control (C_T = 40). The plotted C_T shift for each

$\log_{10}$ change in the concentration of gH plasmid showed 100% efficiency for the range of 10^3 to 10^6 copies. For the range of 10^3 to 10^4 copies of gH plasmid, the mean efficiency was 105% (n = 7) and these two gH plasmid standards were chosen to run in parallel with TG DNA samples in each assay. The genome copy number in TG DNA samples was then calculated based on C_T values obtained for these two standards. Thus, each assay comprised duplicate measurements of TG DNA samples (25 ng/well), gH plasmid standards (10^3 and 10^4 copies, 25 ng/well) and a control (water).

3.17. Statistics

3.17.1. *In vitro* replication kinetics

The differences in replication rates between WT HSV-1 RE vs. RE-pICP0-EGFP; WT HSV-1 RE vs. RE-pgC-EGFP; and WT HSV-1 RE vs. RE-pgC-EGFP were determined by Student's *t* test.

3.17.2. Reactivation and EGFP expression in *ex vivo* TG cultures

The significance of differences in numbers of EGFP expressing neurons (that did and did not proceed to full reactivation) and in reactivation rates between rmIFN-γ- and medium only-treated TG cultures were determined using pooled data in Fisher's Exact Test.

3.17.3. Real-time PCR analysis of viral transcripts

For each viral transcript, Pcx-corrected data (cDNA and no-RT controls) were pooled from all experiments and analyzed using Student Newman-Keuls test (*t* tests among multiple sample groups). In this test, the cDNA and no-RT data for each viral transcript were treated as separate groups.

3.17.4. Analysis of cell numbers in the TGs and DLNs of untreated and anti-IFN-γ mAb treated animals

The differences in the numbers of relevant $gB_{498-505}$-specific $CD8^+$ T cell populations in the TGs and DLNs of untreated and anti-IFN-γ mAb treated mice were determined by Student's *t* test.

4. Results

4.1. IFN-γ inhibits HSV-1 reactivation from latency

Previous work published by our lab defined IFN-γ as a potential contributing mechanism employed by $CD8^+$ T cells in the inhibition of HSV-1 reactivation from latency in *ex vivo* TG cultures [67;81;82]. The present studies were undertaken to determine if IFN-γ is able to block HSV-1 reactivation in some, or all latently infected neurons; and at what step in the reactivation process inhibition occurs. To address these issues, we created two recombinant viruses that express EGFP driven by the promoters for the α gene, encoding ICP0 (RE-pICP0-EGFP), and the γ2 gene, encoding gC (RE-pgC-EGFP). By monitoring *ex vivo* cultures of TGs that were latently infected with these recombinant viruses, we directly observed the effect of IFN-γ on: i) HSV-1 reactivation from latency in neurons; and ii) the expression from these two promoters during the reactivation process.

4.1.1. Construction of promoter-EGFP viruses.

RE-pICP0-EGFP and RE-pgC-EGFP were created on HSV-1 RE background and are null mutants at the gC locus. The construction of both recombinant viruses is explained in detail in the Materials and Methods, section 3.2.. Briefly, in HSV-1 RE-pgC-EGFP, the EGFP gene is inserted immediately after the coding sequence for the first six gC residues, thus leaving the gC promoter in its natural context in the viral genome. In HSV-1 RE-pICP0-EGFP, an ICP0 promoter-EGFP coding sequence was placed in the disrupted gC locus.

For schematic representation of both recombinant viruses see Materials and Methods, Figure 7.

4.1.2. Analysis of EGFP expression *in vitro*.

The inserted 707-bp ICP0 promoter contains all known promoter elements required for ICP0 transcription, including the six upstream TAATGARAT-like sequences [154]. Accordingly, an analysis of EGFP protein expression from this promoter confirmed that EGFP is subject to IE gene regulation.

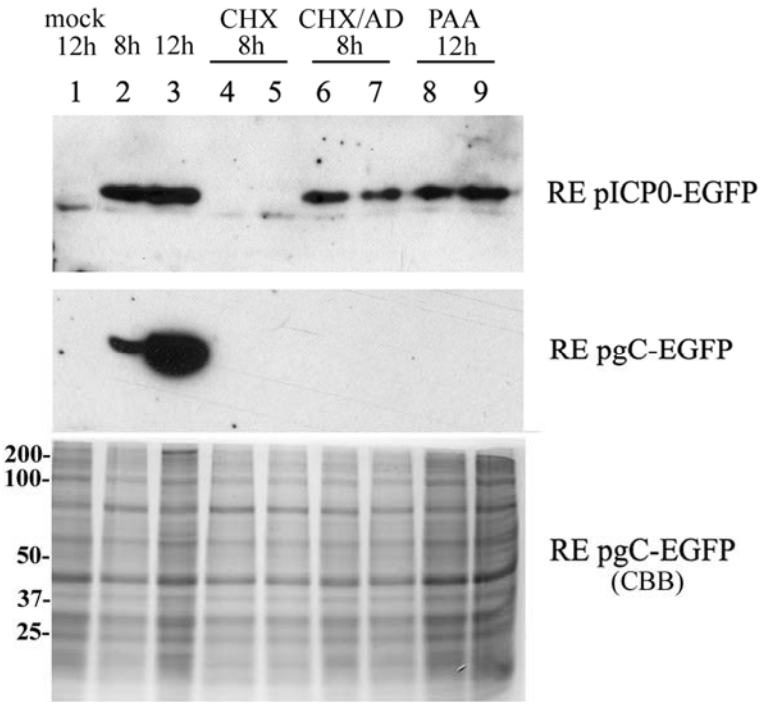

Figure 8: Analysis of viral promoter activity *in vitro*.

Vero cell monolayers were infected at an MOI of 10 PFU/cell with RE-pICP0-EGFP or RE-pgC-EGFP and analyzed by Western blotting for EGFP expression. The times of infection and drug treatments were as follows: lane 1, mock infected for 12 h; lane 2, 8 h; lane 3, 12 h; lanes 4 and 5, 8 h in medium containing 150 µg/ml of cycloheximide (CHX); lane 6 and 7, 8 h with prior incubation in cycloheximide for 6 h followed by washout and 2 h of incubation in the presence of 15 µg/ml of actinomycin D (AD); lanes 8 and 9, 12 h in medium containing 400 µg/ml of PAA. Coomassie brilliant blue (CBB) staining was done to demonstrate equal loading of proteins in the various lanes.

As shown in Figure 8 (top panel), EGFP was expressed in the presence of the viral DNA synthesis inhibitor PAA, but could not be detected when protein synthesis was blocked by cycloheximide (CHX). EGFP was detected after CHX removal and incubation in the presence of actinomycin D (which blocks *de novo* RNA transcription) as shown in lanes 6 and 7. Thus, the ICP0 promoter in RE-pICP0-EGFP is expressed as a true IE gene.

In RE-pgC-EGFP, EGFP is driven by the native gC promoter. As expected (Figure 8, middle panel), EGFP expression was not detected in the presence of either PAA or CHX or after CHX reversal. Thus, EGFP was expressed from the gC promoter as a true late (γ2) gene.

Coomassie brilliant blue (CBB) staining was done to demonstrate equal loading of proteins in the various lanes (Figure 8, bottom panel).

4.1.3. Replication kinetics *in vitro*.

gC deletion mutants replicate normally in cell cultures [154]. At both a low MOI (Figure 9A) and a high MOI (Figure 9B) RE-pICP0-EGFP and RE-pgC-EGFP replicated to similar degrees but were somewhat compromised relative to WT virus.

At low MOI, the difference in replication rates between WT virus and each recombinant virus was statistically significant at 24 h p.i., but not at other time points tested. At high MOI, at all time points tested (exception: RE-pICP0-EGFP vs. RE-pgC-EGFP at 8 and 48 h p.i.) the differences in replication rates between WT HSV-1 RE vs. RE-pICP0-EGFP; WT HSV-1 RE vs. RE-pgC-EGFP; and RE-pICP0-EGFP vs. RE-pgC-EGFP were statistically significant. Similar replication kinetics of all three viruses indicates that there were no additional defects in recombinant viruses, although both of them were compromised relative to WT virus.

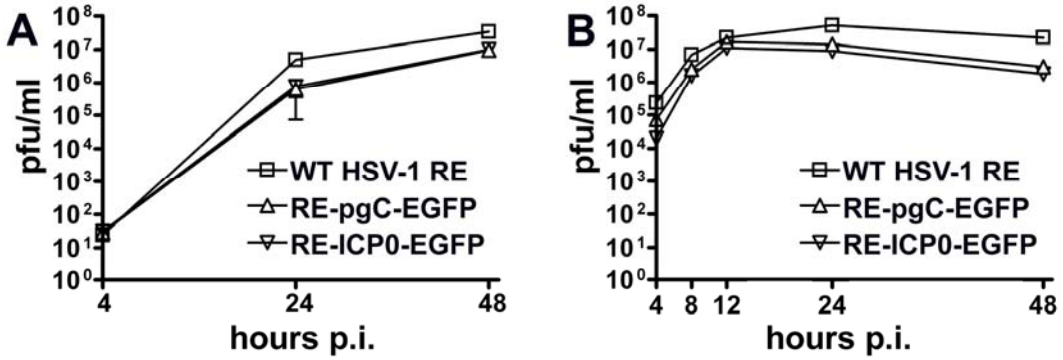

Figure 9: Viral replication kinetics in Vero cell monolayers

Slightly subconfluent monolayers of Vero cells were infected with WT HSV-1 RE, RE-pICP0-EGFP or RE-pgC-EGFP at an MOI of 0.01 PFU/cell (A) or at an MOI of 10 PFU/cell (B). At the indicated times p.i., cells and supernatants were harvested, and subjected to three freeze-thaw cycles and the viral titers were determined. The results are shown as the mean ± SEM and are representative of two experiments. For MOI of 0.01 PFU/cell, at 24 h p.i. the difference in replication rates between WT virus and each recombinant virus was statistically significant (Student's *t* test; $0.05 > P > 0.01$) (A). For MOI of 10 PFU/cell, at all time points tested (exception: RE-pICP0-EGFP vs. RE-pgC-EGFP at 8 and 48 h p.i.) the difference in replication rates between WT HSV-1 RE, RE-pICP0-EGFP and RE-pgC-EGFP virus was statistically significant (Student's *t* test; $0.05 > P > 0.001$) (B).

4.1.4. Analysis of the EGFP expression from the viral promoters in *ex vivo* TG cultures

TG were excised from mice 35 days after HSV-1 corneal infection with the recombinant HSV-1 viruses, RE-pICP0-EGFP or RE-pgC-EGFP. TG were dispersed into single cell suspensions, depleted of either $CD8^+$ T cells alone or of all infiltrating bone marrow-derived ($CD45^+$) cells, and cultured in the presence or absence of recombinant mouse IFN-γ (1,000 U/ml) in 96 well tissue culture plates. To evaluate the effect of IFN-γ on HSV-1 reactivation in individual neurons, it was important to prepare cultures that contain no more than one reactivating neuron. Our preliminary studies demonstrated that each latently infected mouse TG contains two to six neurons that proceed to full HSV-1 reactivation in ex vivo TG cultures. Accordingly, the cells from each TG were dispersed into 10 separate cultures. The TG cultures were examined daily by fluorescence microscopy for EGFP expression from the ICP0 or gC promoter.

Based on the outcome of daily observations over a 10 day period, the cultures could be divided into three groups.

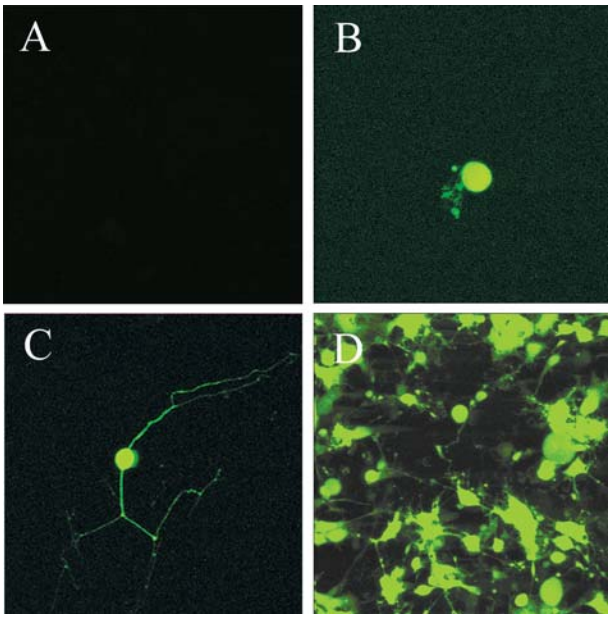

Figure 10: Analysis of the EGFP expression from the viral promoters in *ex vivo* TG cultures.

35 days after corneal infection with RE-pICP0-EGFP or RE-pgC-EGFP, TG were excised, the cells were dispersed with collagenase and depleted of $CD8^+$ T cells or $CD45^+$ cells, and the remaining cells from each TG were distributed evenly into 10 wells of a 96-well plate. The cultures were incubated with or without 1,000 U/ml of rmIFN-γ, and examined daily for 10 days by fluorescence microscopy for EGFP expression from the viral promoters. Three different outcomes are depicted: group 1 (A) no viral promoter activity (EGFP expression) detected; group 2 (B), stable or transient promoter activity detected in neurons, but no virus released to surrounding cells (note that EGFP was restricted to the somata, short neurites and growth cones); and group 3 (C and D), viral promoter activity detected as EGFP expression in neuronal somata and long axons (C) spread within 24 h to surrounding fibroblasts (D). Magnification, x20.

Group 1 cultures never exhibited EGFP-positive cells and were deemed to have no promoter activity (Figure 10A). When combined supernatants and cell homogenates of group 1 cultures were added to monolayers of Vero cells, no viral CPE was observed. The latter observation confirms that detectable EGFP expression from the ICP0 or gC promoter always precedes the production of infectious virions, that our recombinant virus is not contaminated with WT virus, and that reversion to the WT does not occur during the establishment of latency.

Group 2 cultures (Figure 10B) contained neurons that expressed the gC or ICP0 promoter, but HSV-1 did not fully reactivate. In group 2 cultures, neurons expressed EGFP for 1 to 9 days, but EGFP never spread to surrounding fibroblasts. No culture contained more than one EGFP-positive neuron, and in cultures containing neurons that transiently expressed EGFP, re-expression never occurred (i.e., the same neuron never re-expressed EGFP from the ICP0 promoter, nor did a second neuron within the same culture initiate ICP0 promoter activity). The EGFP in the non-reactivating neurons was restricted to the somata of the cell. The combined supernatants and cell homogenates from group 2 cultures failed to produce viral CPE on Vero cell monolayers.

Group 3 cultures (Figure 10C and D) contained neurons that exhibited ICP0 or gC promoter activity and progressed to full reactivation with virion formation and release. For the purpose of this thesis, the term "reactivation" refers to virion formation with spread to surrounding cells, as illustrated in group 3 cultures. In group 3 cultures, EGFP always spread from a neuron to surrounding fibroblasts within 24 h of initial detection (Figure 10C). It was of interest to note that EGFP filled the axons just prior to virus spread from a neuron to surrounding fibroblasts (Figure 10D).

Data are presented for EGFP expression and reactivation from latency in TG neurons during the first 10 days in culture. After 10 days, the cultures became overgrown with fibroblasts and the cells began to lift off the surface of the culture dish. Although we consider the data generated after 10 days in culture to be suspect, we did follow the cultures out to 20 days and never observed the initiation of virus production beyond day 10. Thus, we tentatively concluded that all reactivation-competent neurons reactivate within the first 10 days in culture. We also

found that observing the spread of EGFP from neurons to surrounding fibroblasts is a more sensitive means of monitoring reactivation than plaque assay (data not shown).

4.1.5. IFN-γ inhibits HSV-1 reactivation from latency in *ex vivo* TG cultures.

The TG cultures described above were used to assess the capacity of IFN-γ to inhibit HSV-1's process of reactivation from latency. The incidence of HSV-1 reactivation (group 3 cultures) when latently infected TG were cultured with medium alone was 23%, 35%, and 35%, respectively, for RE-pICP0-EGFP infected TG depleted of either $CD8^+$ T cells (Figure 11A) or $CD45^+$ cells (Figure 11B), and RE-pgC-EGFP infected TG depleted of $CD8^+$ T cells (Figure 11C). The addition of IFN-γ to the cultures reduced the frequency of full reactivation by 50% compared to medium only-treated cultures, confirming our hypothesis that IFN-γ can directly inhibit the process of HSV-1 reactivation from latency in some neurons, whereas HSV-1 reactivation in other neurons is refractory to IFN-γ.

The incidence of HSV-1 reactivation was lower in medium only-treated RE-pICP0-EGFP infected TG cultures depleted of $CD8^+$ T cells (23%, Figure 11A) than in those depleted of $CD45^+$ cells (35%, Figure 11B). This observation can be explained by additional protective mechanisms supplemented by bone marrow-derived cells present in $CD8^+$ T cell depleted cultures that are not present in $CD45^+$ cell depleted cultures. Alternatively, this could be a consequence of different numbers of cells being plated from different groups; since during $CD8^+$ T cell depletion we lose 20-25% of neurons and during $CD45^+$ cell depletion 44-50%. Although we adjusted cell numbers in cultures based on pre-depletion neuron density, the latter possibility cannot be completely excluded. In any case this does not influence the inhibitory potential of IFN-γ as treatment with IFNγ reduced reactivation by 2 fold in both cases.

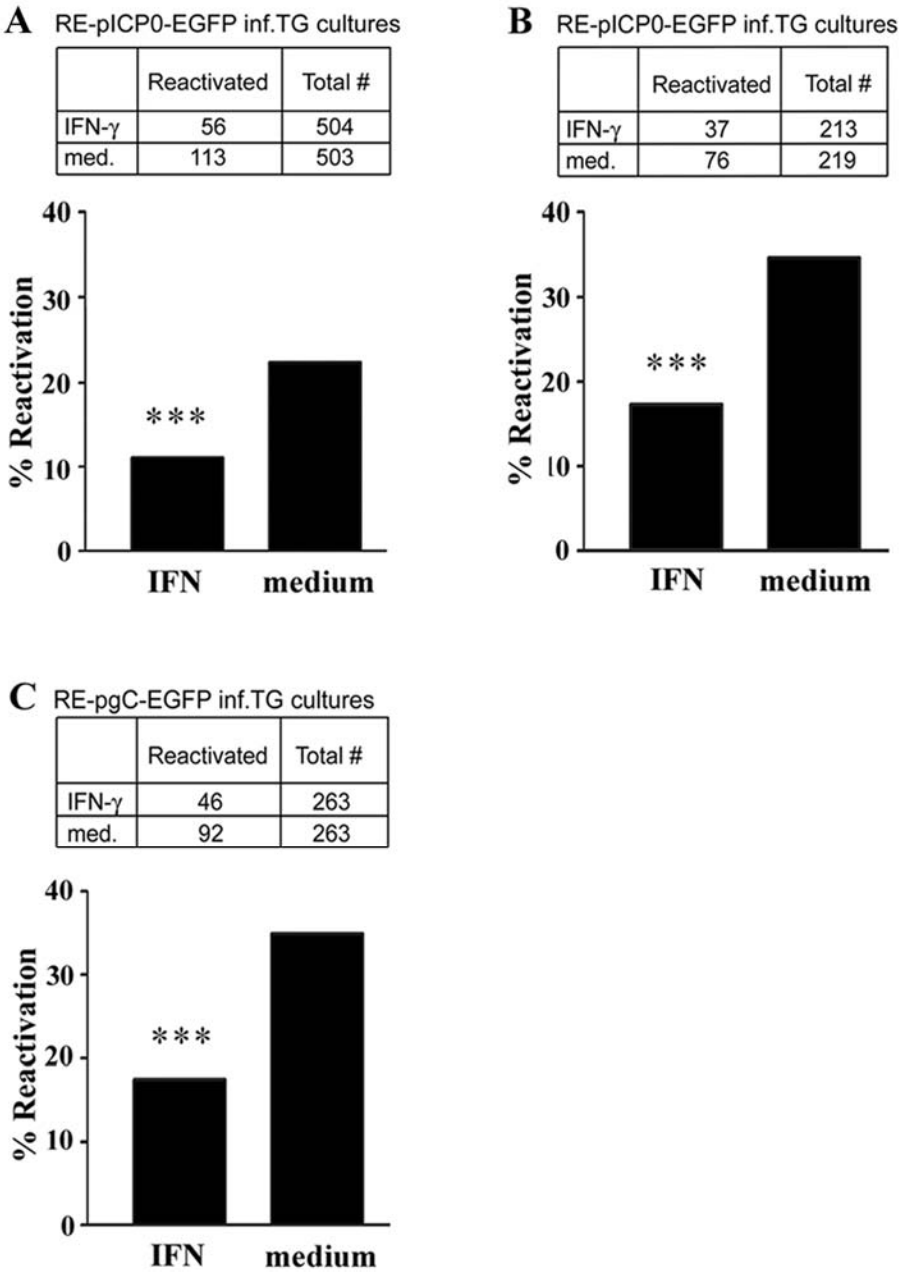

Figure 11: IFN-γ inhibits full reactivation of HSV-1 from latency in *ex vivo* TG cultures.

TG were excised 35 days after corneal infection with RE-pICP0-EGFP (A and B) or RE-pgC-EGFP (C), dissociated into single cell suspensions, depleted of $CD8^+$ T cells (A and C) or $CD45^+$ cells (B), incubated with or without 1,000 U/ml IFN-γ, and examined daily for 10 days for ICP0 or gC promoter activity (EGFP expression). The data are presented as the cumulative percentages of total cultures exhibiting HSV-1 reactivation from latency, as assessed by the spread of EGFP from neurons to surrounding fibroblasts (group 3 cultures). The significance of the difference in reactivation frequency for pooled data from six experiments (A), three experiments (B), or four experiments (C) was assessed by Fisher's Exact Test. ***, $P < 0.0001$.

4.1.6. IFN-γ inhibits reactivation in part by blocking ICP0 gene expression.

Since IFN-γ has been shown to inhibit the expression of ICP0 during a lytic infection of non-neuronal cells [102;103], we sought to determine if the inhibition of HSV-1 reactivation from latency in neurons is associated with reduced ICP0 promoter activity. TG were excised from mice 35 days after a corneal infection with RE-pICP0-EGFP, depleted of $CD8^+$ T cells or $CD45^+$ cells, and cultured in the presence or absence of IFN-γ. As illustrated in Figure 12, IFN-γ significantly reduced the number of neurons that initiated EGFP expression from the ICP0 promoter (i.e. fewer group 2 and 3 cultures). Again, the effect was independent of the presence of $CD8^+$ T cells (Figure 12A) or other inflammatory cells (Figure 12B).

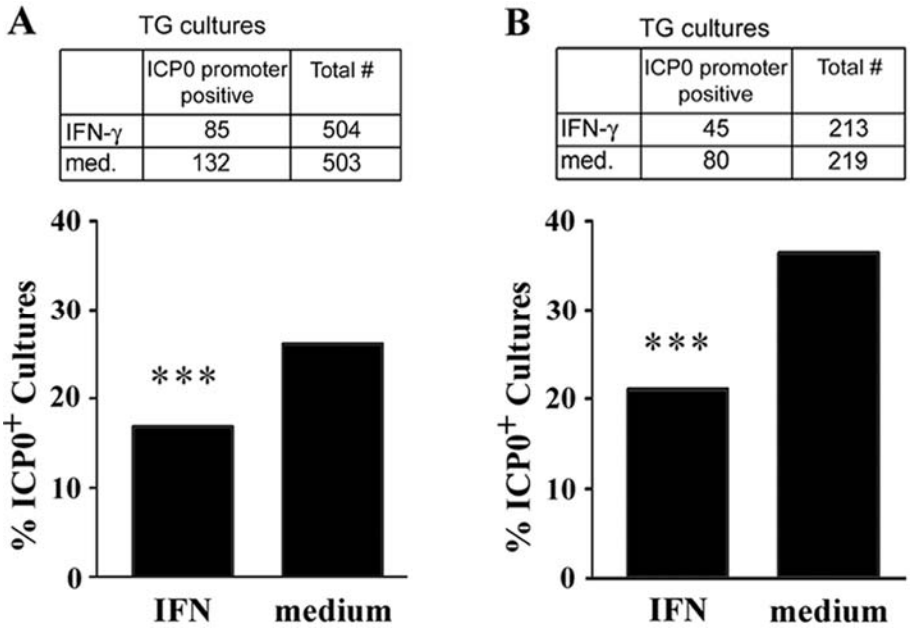

Figure 12: IFN-γ inhibits reactivation in part by blocking ICP0 gene expression.

TG were excised 35 days after corneal infection with RE-pICP0-EGFP, dissociated into single cell suspensions, depleted of $CD8^+$ T cells (A) or $CD45^+$ cells (B), incubated with or without 1,000 U/ml IFN-γ, and examined daily for 10 days for ICP0 promoter activity (EGFP expression). The data are presented as the cumulative percentages of cultures containing ICP0 promoter-positive ($ICP0^+$) neurons (group 2 and 3 cultures). The significance of the difference in promoter activity for pooled data from six experiments (A) or three experiments (B) was assessed by Fisher's Exact Test. ***, $P = 0.0003$ (A) or 0.0005 (B).

4.1.7. IFN-γ blocks an event downstream of ICP0 promoter expression.

As described above, IFN-γ reduced but did not completely eliminate ICP0-EGFP gene expression in latently infected neurons (Figure 12). Interestingly, in neurons that did express the ICP0 promoter, IFN-γ significantly inhibited the progression to full reactivation and virion formation (group 2 cultures) (Figure 13), suggesting an additional IFN-γ-mediated block of an event downstream of ICP0 expression.

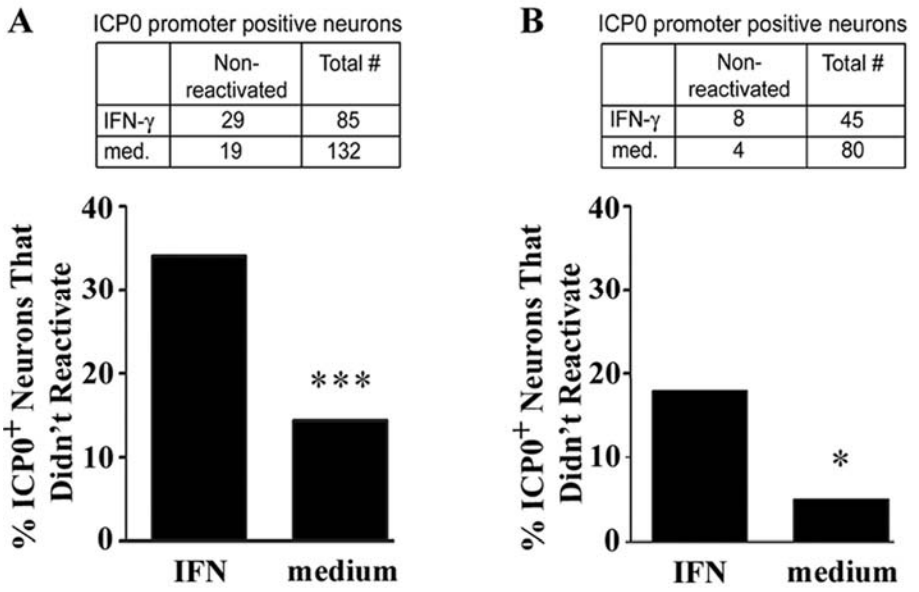

Figure 13: IFN-γ blocks an event downstream of ICP0 promoter expression.

TG were excised 35 days after corneal infection with RE-pICP0-EGFP, dissociated into single cell suspensions, depleted of $CD8^+$ T cells (A) or $CD45^+$ cells (B), incubated with or without 1,000 U/ml IFN-γ, and examined daily for 10 days for ICP0 promoter activity (EGFP expression). The data are presented as the cumulative percentages of ICP0 promoter-positive ($ICP0^+$) neurons that failed to reactivate (group 2 cultures). The significance of the difference in reactivation frequency among ICP0 promoter positive neurons for pooled data from six experiments (A) or three experiments (B) was assessed by Fisher's Exact Test. ***, $P = 0.0008$; *, $P = 0.0275$.

4.1.8. IFN-γ blocks gC promoter expression as well as a step in the reactivation process that occurs after gC promoter expression.

Although the capacity of ICP0 to directly regulate HSV-1 late gene expression during reactivation from latency in neurons is unproven, we hypothesized that the reduced ICP0 promoter activity in IFN-γ treated cultures would be associated with a similar reduction in gC promoter activity. Moreover, since IFN-γ blocked a step in reactivation after ICP0 expression, it was of interest to determine if the blocked event occurred before or after expression of the γ2 gene encoding gC. TG were excised from mice 35 days after a corneal infection with RE-pgC-EGFP, depleted of $CD8^+$ T cells, and cultured in the presence or absence of IFN-γ. As illustrated in Figure 14A, IFN-γ significantly reduced the number of neurons that expressed EGFP from the gC promoter. Again, the effect was independent of the presence of $CD8^+$ T cells.

A more surprising observation in these studies was that IFN-γ could block reactivation from latency and virus release from neurons in which the gC promoter was active (Figure 14B). IFN-γ treatment significantly increased the number of neurons exhibiting a persistent expression of EGFP from the gC promoter without virus spread to surrounding fibroblasts (group 2 cultures). This observation suggests that IFN-γ can inhibit a step in reactivation that occurs after the expression of viral γ2 structural genes. Again, EGFP expression persisted for 1 to 9 days without spread to surrounding fibroblasts and was restricted to the somata of the neurons.

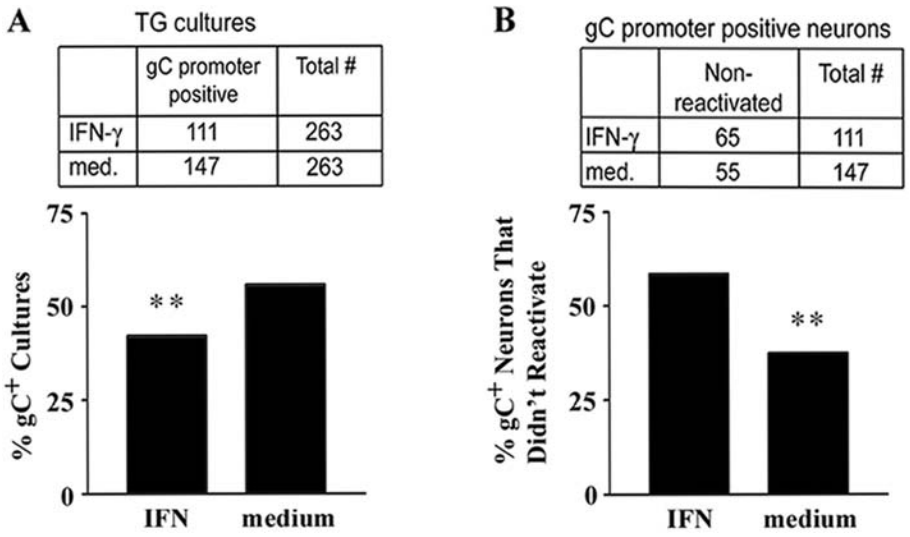

Figure 14: IFN-γ blocks gC promoter expression as well as a step in the reactivation process that occurs after gC promoter expression.

TG were excised 35 days after corneal infection with RE-pgC-EGFP, dissociated into single cell suspensions, depleted of $CD8^+$ T cells, incubated with or without 1,000 U/ml IFN-γ, and examined daily for 10 days for gC promoter activity (EGFP expression). (A) The cumulative percentages of cultures containing gC promoter-positive (gC^+) neurons (group 2 and 3 cultures). The significance of the difference in promoter activity for pooled data from four experiments was assessed by Fisher's Exact Test. **, $P = 0.0022$; (B) The cumulative percentages of gC promoter-positive (gC^+) neurons that failed to reactivate (group 2 cultures). The significance of the difference in reactivation frequency among gC promoter-positive neurons for pooled data from four experiments was assessed by Fisher's Exact Test. **, $P = 0.001$ (B).

4.1.9. Validation of real-time PCR primer-probe sets.

For assay validation of each primer-probe set, cDNA (Figure 15) or a no-RT control (not shown) from infected tissue (from HSV-1 RE-infected mouse TG on day 3) was used to generate a standard curve of the change in cycle threshold (ΔC_T) versus the log (ng cDNA/well) for the range of 0.1 to 100 ng/well. Three separate analyses gave correlation coefficients and PCR efficiencies (mean ± SD) as follows: for ICP4 (Figure 15A), $R^2 = 0.989 \pm 0.007$ and efficiency = 97% ± 5%; for ICP0 (Figure 15B), $R^2 = 0.991 \pm 0.005$ and efficiency = 99% ± 2%; for gH (Figure 15C), $R^2 = 0.992 \pm 0.006$ and efficiency = 98% ± 2%; and for Pcx (Figure 15D), $R^2 = 0.989 \pm 0.006$ and efficiency = 105% ± 3%.

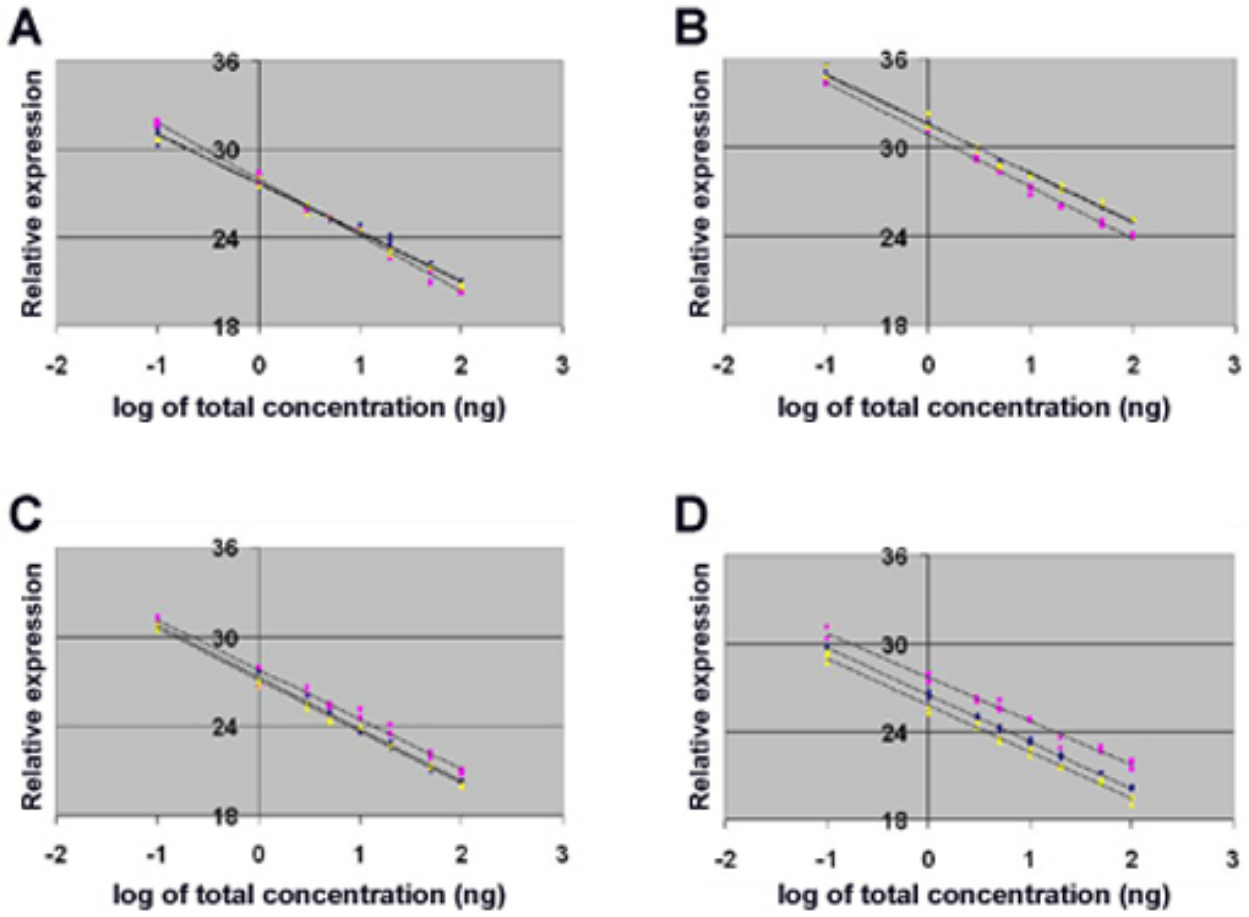

Figure 15: Standard curves generated by real-time PCR for each primer-probe set.

For assay validation of each primer-probe set, cDNA from infected tissue (HSV-1 RE-infected mouse TG on day 3) was used to generate a standard curve of the change in cycle threshold (ΔC_T) versus the log (ng cDNA/well) for the range of 0.1 to 100 ng of input cDNA. The relative amounts of transcripts in samples are shown as $40 - C_T$ (samples with a C_T value of 40 were considered to lack transcripts). Each primer-probe set was tested in three separate analyses. The standard curves are shown for ICP4 (A), ICP0 (B), gH (C) and Pcx (D) primer-probe sets.

4.1.10. HSV-1 α and γ2 gene transcripts could be detected in the absence of full reactivation.

The observation that the promoters for the α gene, ICP0 and the γ2 gene, gC are active in neurons that do not produce infectious virions suggested that an analysis of viral transcripts in Group 2 cultures was warranted. Accordingly, mouse TG were excised 35 days after a corneal infection with HSV-1 RE-pICP0-EGFP, the cells were dispersed with collagenase and depleted

of $CD8^+$ T cells, and cultures were prepared as described previously (see Results, section 4.1.4.) and supplemented with IFN-γ. All cultures were monitored and assigned to group 1 (no promoter activity), group 2 (promoter activity but no reactivation), or group 3 (reactivation) as described above. RNAs were extracted from pooled cells obtained from Group 1, Group 2, and Group 3 cultures, reverse transcribed or not, and then subjected to quantitative real-time PCR using primers and probes specific for ICP4 (sensitivity, 10^2 copies), ICP0 (sensitivity, 10^2 copies), gH (sensitivity, 10^0 copies) and the cellular control gene Pcx.

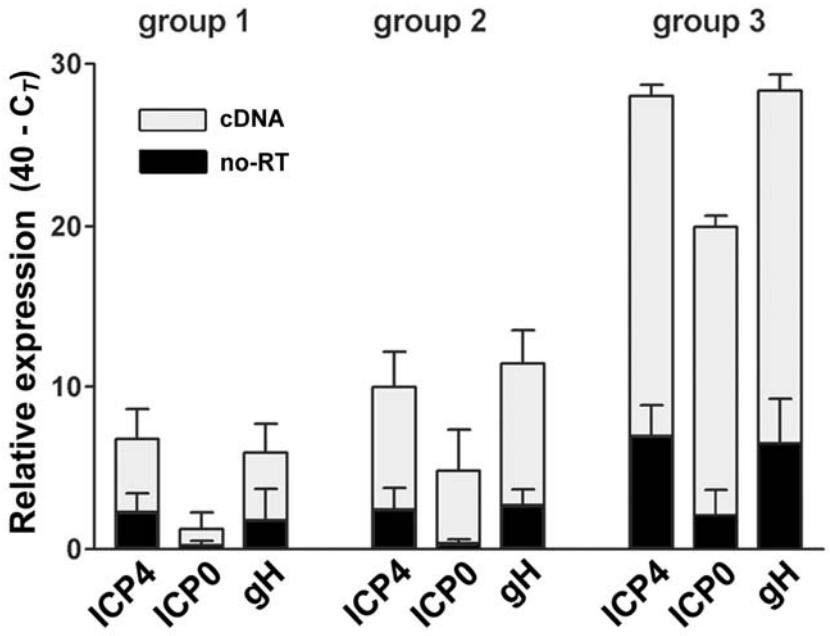

Figure 16: Quantitative real-time PCR analysis of IFN-γ treated cultures of TG obtained 35 days after RE-pICP0-EGFP HSV-1 corneal infection.

For each viral transcript, Pcx-corrected data (see Materials and Methods, section 3.8.) were pooled from all experiments and analyzed using Student Newman-Keuls test (*t* tests among multiple sample groups). Since samples with a C_T value of 40 were considered to lack transcripts, the relative amounts of transcripts in samples are shown as $40 - C_T$. The cDNA values among the group 1 (no ICP0 promoter activity), group 2 (ICP0 promoter activity, but no reactivation), or group 3 (reactivation) neurons are significantly different ($P < 0.01$) for all three transcripts. For the group 2 and group 3, the cDNA values are significantly different ($P < 0.01$) from those of the equivalent no-RT controls. For group 1, there is no significant difference between cDNA and the no-RT control, except for ICP4, which shows a small difference ($P < 0.05$). ICP4 and gH genes are intronless, and their primer-probe sets generate marginal measurements for no-RT controls, while the primer-probe set for ICP0 crosses an intron-exon boundary and the no-RT control levels were low or undetectable.

Two interesting observations emerged from the resulting data (Figure 16). First, EGFP expression from the ICP0 promoter was as sensitive as real-time PCR in detecting ICP0 gene expression. Thus, ICP0 transcripts were only detectable in group 2 and group 3 cultures containing EGFP-positive cells. Second, and most importantly, ICP0, ICP4, and gH transcripts were readily detectable in group 2 cultures containing ICP0 promoter-positive neurons that did not produce infectious virions. In contrast, ICP0 and gH transcript levels were below the sensitivity of our assay in group 1 cultures that lacked ICP0 promoter activity. A very low, but statistically significant, level of ICP4 transcripts was detected in the group 1 cultures ($P < 0.05$). These findings provide strong evidence that IFN-γ can maintain HSV-1 in a latent state in neurons (as defined by a lack of virion formation) in the presence of HSV-1 α and even γ2 gene expression and may inhibit virus production at a very late stage of the viral cycle in neurons. The very low level of ICP4 transcripts in neurons that lack ICP0 transcripts does not result in detectable γ2 (gH) gene transcription.

4.1.11. ICP0 overexpression reverses IFN-γ mediated inhibition of HSV-1 reactivation

Previous studies [93] demonstrated that replication-defective adenovirus vectors can efficiently deliver proteins to cultured TG neurons without inducing reactivation. We used this experimental system, to deliver WT or mutant forms of ICP0 to latently infected neurons and check the capacity of ICP0 to induce reactivation of latent viral genomes in the presence and absence of IFN-γ. In Ad.TRE-ICP0 and Ad.TRE-n212, the WT and mutant (expresses the first 211 of 775 amino acids of ICP0) form of ICP0, respectively, are under the control of a tetracycline response element (TRE) promoter. The expression from TRE promoter in TG

cultures was induced by co-infection of these cultures with an adenovirus vector that expresses the reverse tetracycline-regulated transactivator (rtTA) in the presence of doxycycline (DOX).

D34 $CD8^+$ T cell depleted TG cultures were treated with IFN-γ or medium only as previously described (see Results, section 4.1.4.). Adenovirus vectors expressing WT or mutant form of ICP0 were added to the cultures one day post culturing.

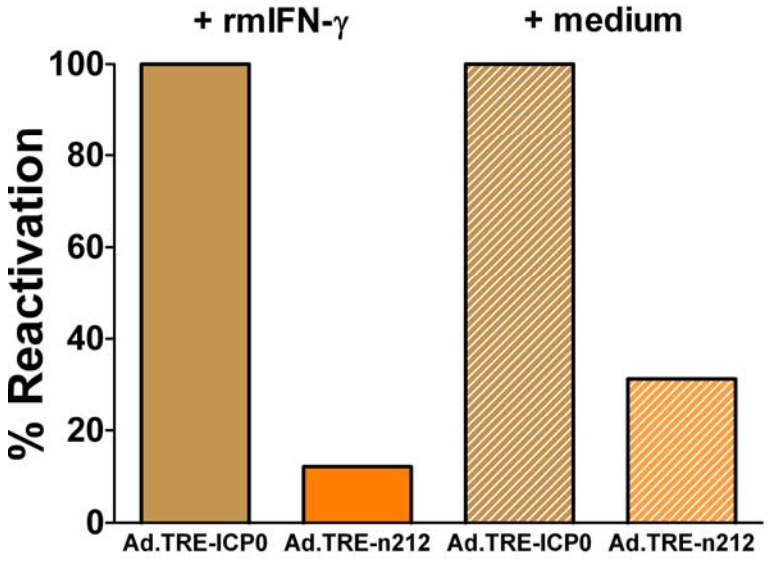

Figure 17: ICP0 over-expression reverses IFN-γ mediated inhibition of HSV-1 reactivation.

TG were excised 35 days after corneal infection with RE-pICP0-EGFP, dissociated into single cell suspensions, depleted of $CD8^+$ T cells and incubated with or without 1,000 U/ml IFN-γ. At day 1 post culturing, TG cell cultures were coinfected with Ad.CMV-rtTA (MOI = 10 PFU/cell) and either Ad.TRE-ICP0 or Ad.TRE-n212 (MOI = 30 PFU/cell). The cultures were examined daily for 10 days for ICP0 promoter activity (EGFP expression). The data are presented as the cumulative percentages of total cultures exhibiting HSV-1 reactivation from latency, as assessed by the spread of EGFP from neurons to surrounding fibroblasts.

As shown in Figure 17, ICP0 over-expression from Ad.TRE-ICP0 completely abrogated inhibitory effects of IFN-γ on HSV-1 reactivation from latency. Moreover, ICP0 over-expression caused reactivation of latent virus in all IFN-γ-treated cultures including those that do not reactivate normally *ex vivo*. Similarly, ICP0 over-expression caused reactivation of latent virus in

all medium only-treated cultures. The reactivation rates in vehicle (Ad.TRE-n212) treated cultures in the presence and absence of IFN-γ were similar to those previously observed.

4.2. IFN-γ regulates the magnitude of antigen-specific $CD8^+$ T cell response in the TG during HSV-1 infection

Previous studies have shown that IFN-γ affects the abundance of antigen-specific $CD8^+$ T cells in the lymphoid tissues during acute and chronic viral infections [149;153], but the contributions of IFN-γ to the three phases of $CD8^+$ T cell response were controversial and seemed to vary in different settings. Nothing is known about the actions of this cytokine in relevant non-lymphoid tissues. Thus, in the second part of our studies we used a murine HSV-1 infection model in the peripheral nervous system to investigate the involvement of IFN-γ in the initial expansion and contraction of HSV-1-specific $CD8_{eff}$ cells, as well as, IFN-γ role in the development of $CD8_{mp}$, and in the establishment of a functionally optimized $CD8_{mem}$ population. The murine HSV-1 infection model offers several advantages including: (i) the ability to trace virus-specific cells using dimers containing a strong immunodominant epitope, (ii) an easily accessible non-lymphoid tissue that retains memory cells for the life of the animal, and (iii) a localized latent infection in which antigenic load is not dramatically altered by transient manipulation of the immune response.

4.2.1. The kinetics of antigen-specific $CD8^+$ T cell response in HSV-1 infected TG

First, we determined the kinetics of the antigen-specific $CD8^+$ T cell response in HSV-1 infected TG. Accordingly, the TGs were excised from mice 5, 7, 8, 14, 22, 40 and 60 days after HSV-1 corneal infection and the frequency, absolute number and surface phenotype of $CD8^+$ T

cells specific for an epitope on the viral lytic gene product glycoprotein B ($gB_{498-505}$) were analyzed by flow cytofluorometry (FCM).

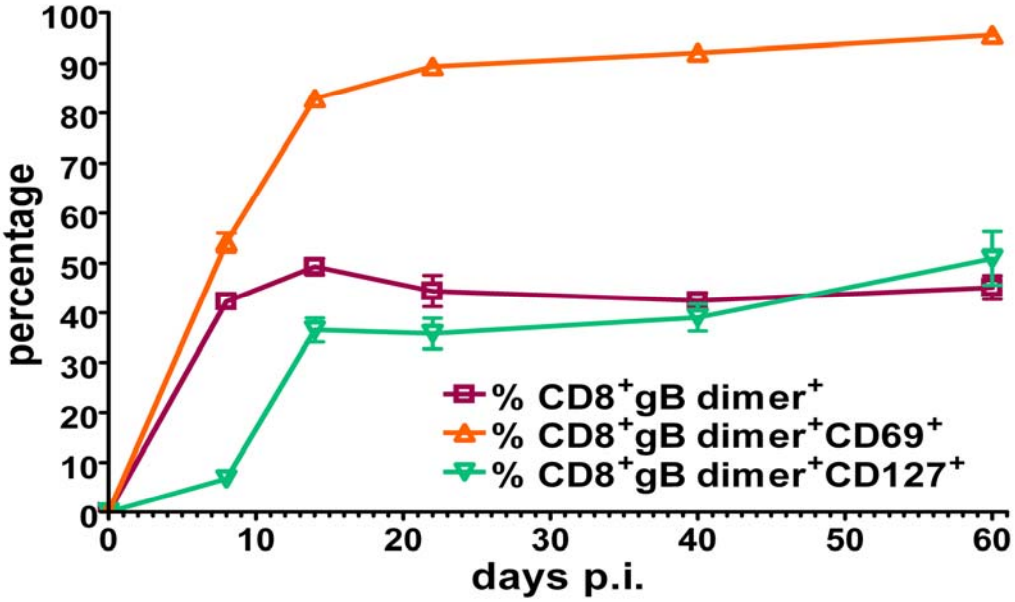

Figure 18: The percentage of $CD8^+$ T cell subsets in HSV-1 infected TG.

TG were removed 8 (n = 11), 14 (n = 18), 22 (n = 6), 40 (n = 23) and 60 days (n = 5) after bilateral HSV-1 corneal infection; stained, and analyzed by FCM. The cells were gated on CD8 and analyzed for the expression of gB dimer, CD69, and CD127. Percentages of individual $CD8^+$ T cell subsets per TG were determined, and pooled data are shown as means ± SEM.

Forty-50% of all $CD8^+$ T cells retained in the TG after day 8 are $gB_{498-505}$-specific $CD8^+$ T cells (Figure 18). Previous studies demonstrated that $CD8^+$ T cells play an important role in the reduction of viral replication during acute infection and suggested their possible role in the maintenance of latency [41;82;156]. $gB_{498-505}$-specific $CD8^+$ T cells show selective localization within the ophthalmic branch of the HSV-1 infected TGs and are found in close apposition to neuron cell bodies [45;82]. The potential protective role of these cells *in vivo* is further supported by the observation that the majority of $gB_{498-505}$-specific $CD8^+$ T cells that are retained in the TG

show an activation phenotype (CD69 expression) and 40%, after day 14, express a memory marker CD127 (IL-7Rα).

The kinetics of the gB-specific response in infected TGs closely resembles the observed kinetics of $CD8^+$ T cell response in the lymphoid tissues during viral infections (Figure 19) [121]. In the TG, gB-specific $CD8^+$ T cells were first detected 5 days p.i.. Their infiltration follows the transport of virus to the TG and initiation of viral replication in neurons (2-3 days p.i.). The numbers of $gB_{498\text{-}505}$-specific $CD8^+$ T cells then increase dramatically, reaching maximal levels at day 8 p.i. By that time, the virus uniformly entered a latent state within all sensory neurons, and replicating virus was no longer detectable in infected TGs [41].

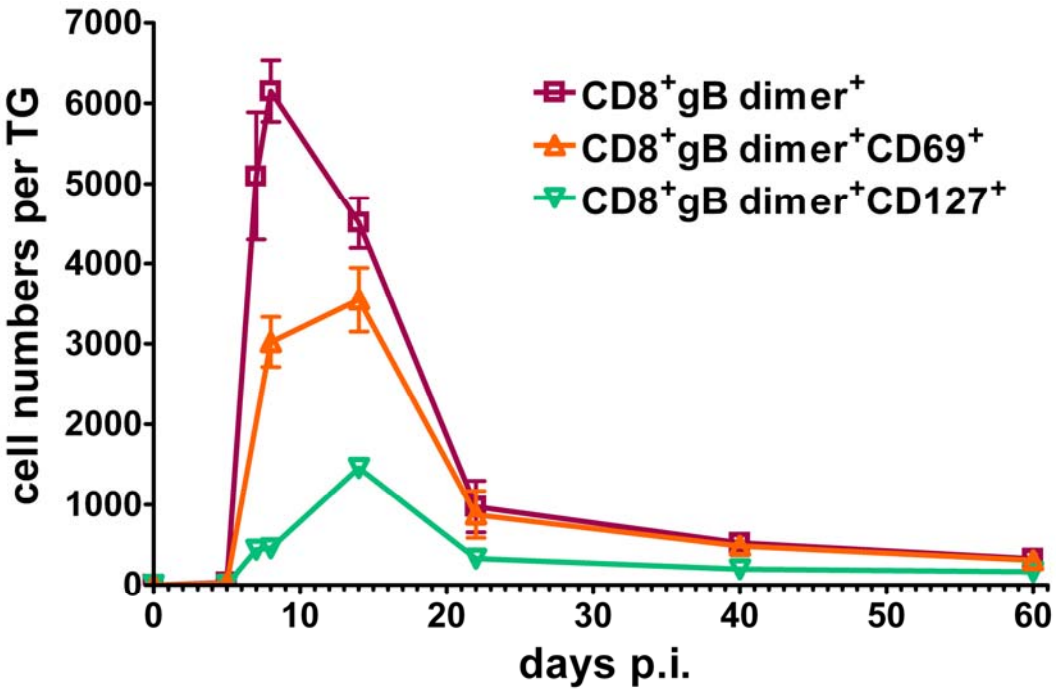

Figure 19: Kinetics of $gB_{498\text{-}505}$-specific $CD8^+$ T cell response in HSV-1 infected TG.

The TGs were excised from mice 5 (n = 4), 7 (n = 7), 8 (n = 22), 14 (n = 40), 22 (n = 6), 40 (n = 23) and 60 (n = 5) days after HSV-1 corneal infection and the absolute numbers and surface phenotype of $gB_{498\text{-}505}$-specific $CD8^+$ T cells were analyzed by FCM. The results are shown as means ± SEM of absolute numbers of cells per TG.

The establishment of latency is accompanied by a slow contraction of the $gB_{498-505}$-specific $CD8^+$ T cell population (from day 8 through day 30 p.i.), followed by the establishment of a stable memory population representing about 10% of their number at the peak of the effector response. The memory population persists seemingly for the life of the animal.

An interesting observation emerged from the above shown kinetics data. Although the size of the overall gB-specific $CD8_{eff}$ population peaked at 8 days p.i., cell populations expressing the activation marker CD69 and those expressing the $CD8_{mp}$ marker CD127 increased in numbers through 14 days p.i.. Although the number of $CD127^+$ $CD8_{mp}$ cells declined from 14-22 days p.i., the proportion they represented of the overall gB-specific $CD8_{eff}$ population steadily increased from approximately 7% at the peak of the $CD8_{eff}$ response (8 days p.i.) to approximately 50% of the stable $CD8_{mem}$ population (> 30days p.i.). To our knowledge this is the first demonstration that $CD127^+$ $CD8_{mp}$ cells undergo an expansion and contraction in tissue. We are currently investigating the functional significance, if any, of the expansion and contraction of the $CD127^+$ $CD8_{mp}$ cells, and why their expansion and contraction are delayed relative to the overall gB-specific $CD8_{eff}$ population. We propose that expansion and contraction might influence the functional avidity of the memory population, and are determining if the delay in the $CD127^+$ $CD8_{mp}$ cells reflects delayed infiltration, delayed proliferation within the TG, or delayed differentiation from effector cells.

4.2.2. IFN-γ neutralization early during infection diminishes primary expansion of antigen-specific $CD8_{eff}$ cells in the TG

The effects of IFN-γ on $CD8^+$ T cell response were assessed by *in vivo* IFN-γ neutralization during the three phases of the antigen-specific $CD8^+$ T cell response. Mice were

treated with neutralizing anti-IFN-γ monoclonal antibody (mAb, single or multiple i.p. injections) at different times after HSV-1 corneal infection and the absolute numbers and phenotype of $gB_{498-505}$-specific $CD8^+$ T cells were analyzed.

To determine if IFN-γ influenced the initial expansion of antigen-specific $CD8^+$ T cells, mice received a single i.p. injection of anti-IFNγ mAb (1mg/mouse) six days after HSV-1 corneal infection or were left untreated. Two days later, at the peak of gB-specific $CD8^+$ T cell response, the TGs and DLNs (submandibular) from both sides were removed and analyzed by FCM (Figure 20A).

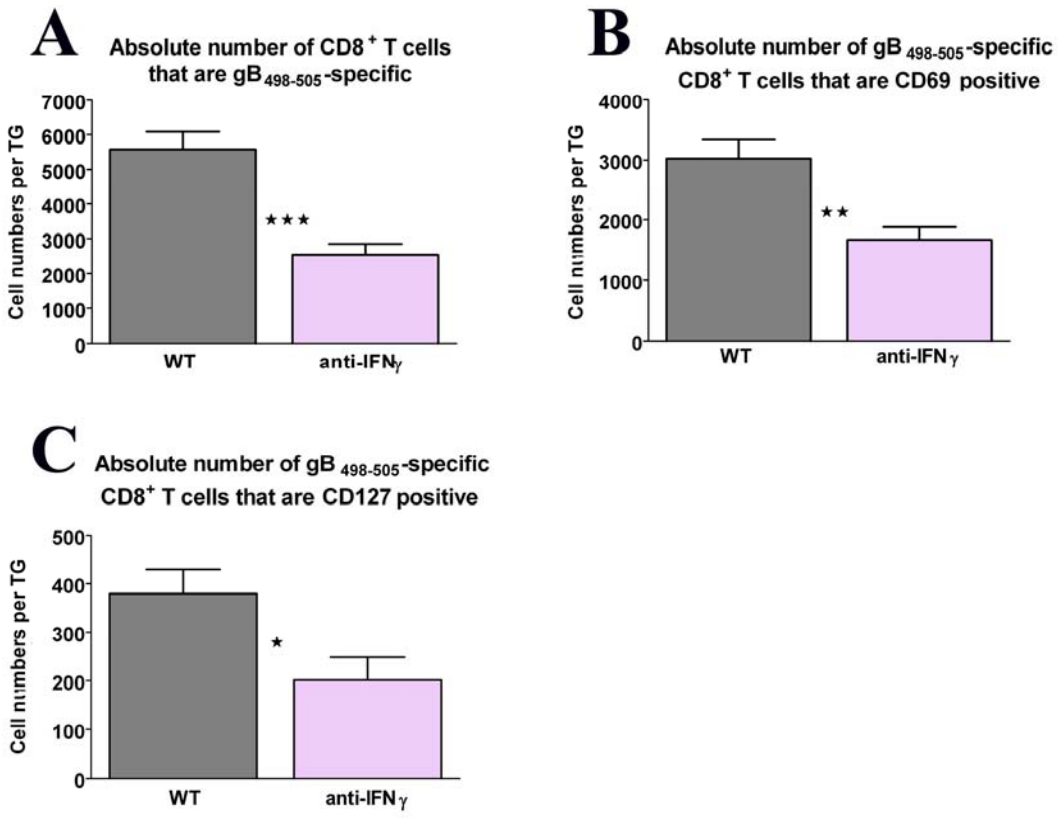

Figure 20: IFN-γ neutralization early during infection diminishes primary expansion of antigen-specific $CD8_{eff}$ cells in the TG.

Six days after HSV-1 corneal infection, mice received a single i.p. injection of anti-IFN-γ mAb (1mg/mouse, n = 11) or were left untreated (n = 11). At day 8 p.i. the TGs from both sides were removed, stained and analyzed by FCM. Cell numbers in the TG are represented as the absolute number of $CD8^+$ T cells that are $gB_{498-505}$-specific (A), and

the absolute number of $gB_{498-505}$-specific $CD8^+$ T cells that are either CD69 (B) or CD127 positive (C). Results are shown as the means ± SEM of the absolute numbers of cells per TG. ***, $P < 0.001$; **, $P = 0.0018$; *, $P = 0.0167$.

IFN-γ neutralization resulted in a marked decrease in the number of HSV-1-specific $CD8_{eff}$ in the TG, demonstrating a necessary role for IFN-γ in the expansion phase of the $CD8^+$ T cell response (Figure 20A). Although the absolute number of activated ($CD69^+$) $CD8_{eff}$ cells was reduced (Figure 20B), this reduction reflected the reduction in the overall population of gB-specific $CD8^+$ T cells in the anti-IFN-γ treated group. The frequency of gB-specific $CD8^+$ T cells in the anti-IFN-γ treated group was actually slightly higher than that of the untreated controls, suggesting that IFN-γ deprivation does not adversely influence the activation status of the remaining cells. Similarly, the absolute numbers of $CD8_{mp}$ ($CD127^+$) cells were reduced in the absence of IFN-γ (Figure 20C), but the generation of HSV-1-specific $CD8_{mp}$ did not require IFN-γ as $CD127^+$ HSV-1-specific $CD8^+$ T cells represented approximately 7% of the total HSV-1-specific $CD8^+$ T cells in anti-IFN-γ-treated and control mice. Furthermore, the neutralization of IFN-γ at day 6 p.i. did not alter viral replication in the TG, as shown in Results, section 4.2.11.

The reduced expansion of $CD8_{eff}$ cells in the TG following IFN-γ neutralization could reflect: i) the reduced infiltration into the TG (due to inadequate production or emigration of HSV-1-specific $CD8^+$ T cells in the lymphoid organs and/or reduced extravasation from the blood into the TG); ii) inadequate proliferation in the TG; iii) rapid death; or iv) rapid emigration from the TG.

4.2.3. IFN-γ neutralization early during infection does not influence the antigen-specific CD8$^+$ T cells response in day 8 DLNs

To determine if the reduced expansion of HSV-1-specific CD8$^+$ T cells in the TG was due to an effect of IFN-γ on their expansion in the DLNs, we analyzed the DLNs from the same animals. Interestingly, IFN-γ did not affect the initial expansion of gB-specific cells in DLNs (Figure 21), demonstrating a differential requirement for IFN-γ in the expansion phase of the HSV-1-specific CD8$^+$ T cell response in lymphoid and non-lymphoid tissues.

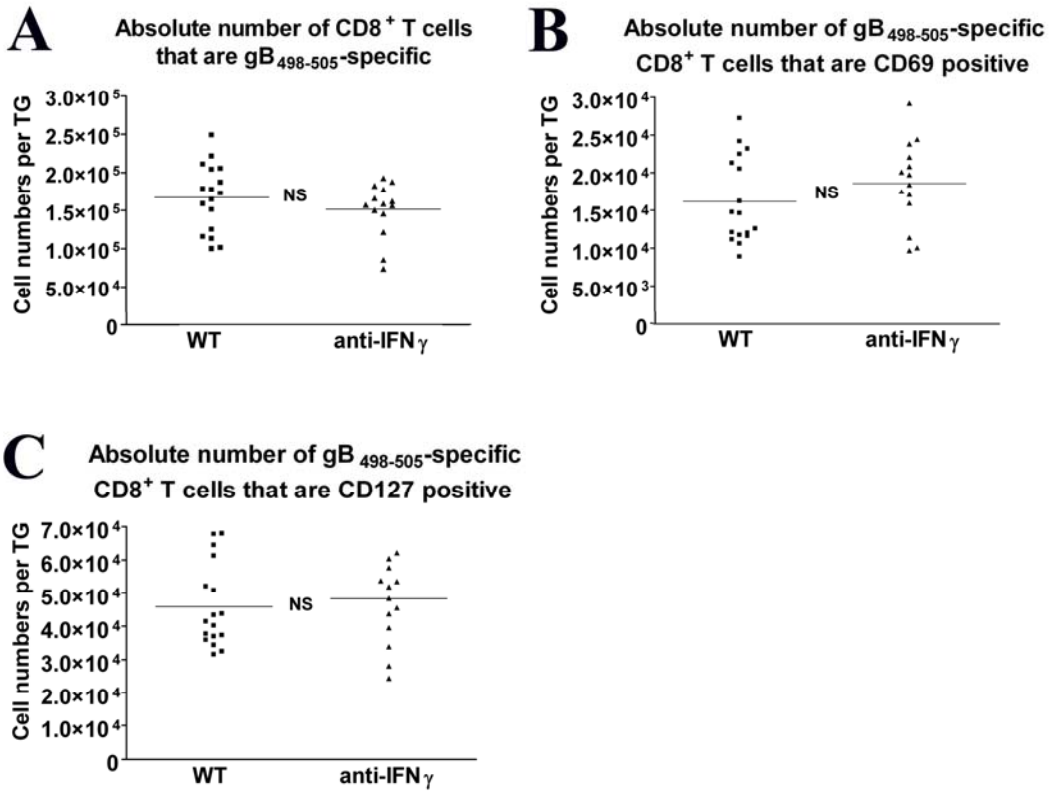

Figure 21: IFN-γ does not influence the initial expansion of gB$_{498-505}$-specific CD8$^+$ T cells in the DLNs.

Six days after HSV-1 corneal infection, mice received a single i.p. injection of anti-IFN-γ mAb (1mg/mouse, n = 14) or were left untreated (n = 17). Two days later the DLNs were removed, stained and analyzed by FCM. Cell numbers in the DLNs are represented as the absolute number of CD8$^+$ T cells that are gB$_{498-505}$-specific (A), and the absolute number of gB$_{498-505}$-specific CD8$^+$ T cells that are either CD69 (B) or CD127 positive (C). Results are shown as the means ± SEM of the absolute numbers of cells per both DLNs. NS = not significant.

4.2.4. IFN-γ stimulates the proliferation of HSV-1-specific $CD8_{eff}$ cells in the TG

The abundance of $CD8^+$ T cells in particular tissue reflects the net effect of their infiltration, proliferation, death and/or emigration. Thus, we hypothesized that the reduced numbers of antigen-specific cells in the TG at early time points could be a consequence of either reduced proliferation or infiltration of these cells in the absence of IFN-γ, and/or increased apoptosis. To test the hypothesis that reduced proliferation results in decreased numbers of gB-specific cells, mice treated with anti-IFN-γ mAb at day 6 p.i., were given BrdU at day 7 p.i. and sacrificed on day 8 p.i.. BrdU staining did not reveal any differences between untreated and treated mice. The same percentage of cells (~26%) in both groups showed BrdU incorporation (Figure 22A). The downside of this approach is that all of the cells that proliferate after BrdU injection will incorporate BrdU regardless of the actual site of their proliferation. By this scenario, the cells that proliferated in the DLNs and then infiltrated TGs would show BrdU incorporation. In addition, we do not know how fast BrdU is removed from the system.

To better assess the proliferation of cells in the TG and distinguish between cells that proliferated *in situ* in the TG from those that proliferated recently in the DLNs and subsequently infiltrated TG, we performed Ki-67 staining. Ki-67 is a nuclear cell proliferation associated antigen localized in the nucleus. Although its exact function is not known, Ki-67 is expressed in all active stages of the cell cycle and thus, widely used for the detection of proliferating cells [157].

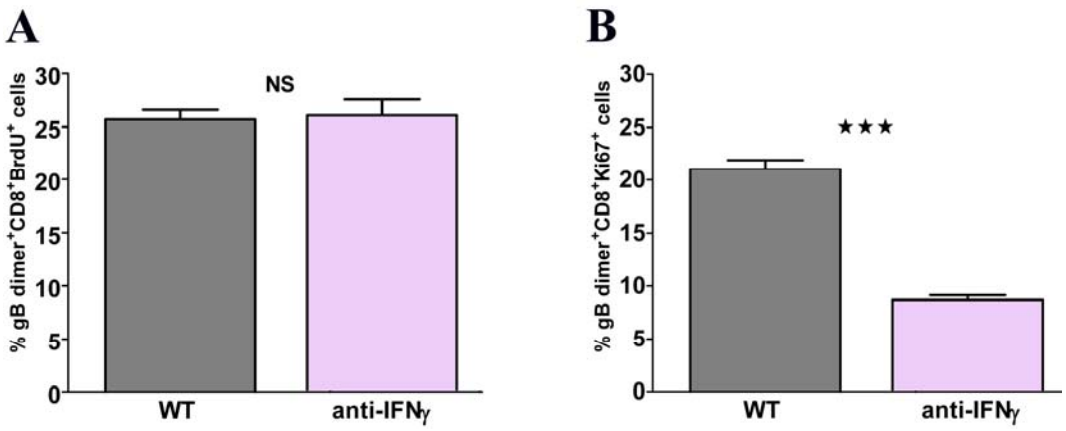

Figure 22: IFN-γ neutralization diminishes primary expansion of antigen-specific $CD8_{eff}$ cells in the TG by inhibiting their *in situ* proliferation.

Six days after HSV-1 corneal infection, mice received a single i.p. injection of anti-IFN-γ mAb (1mg/mouse; BrdU, n = 10; Ki-67, n = 7) or were left untreated (BrdU, n = 9; Ki-67, n = 7). At 7 (Ki67) or 8 (BrdU, injected at day 7 p.i.) days p.i,. the TGs from both sides were removed; stained and analyzed by FCM. Data are represented as the means ± SEM of the percentage of $gB_{498-505}$-specific $CD8^+$ T cells positive for BrdU (A) or Ki-67 (B) per TG. ***, $P < 0.001$.

Ki-67 staining revealed that the neutralization of IFN-γ resulted in the lower proliferative rate of gB-specific cells in the TG (Figure 22B). 21% of gB-specific cells proliferated in the TGs of untreated mice, but only 8.7% in the TGs of anti-IFN-γ mAb treated mice.

When Ki-67 staining was done in the DLNs of same animals, there was no difference between untreated and treated groups (Figure 23). About 38% of gB-specific cells in the DLNs stained positive for Ki-67. This is in an agreement with our previous observation that IFN-γ seems to be dispensable for the regulation of antigen-specific $CD8^+$ T cell response in DLNs (see Figure 21). Furthermore, when we repeated the same experiment using BrdU incorporation approach (BrdU was injected on day 7 p.i.), a similar percentage of gB-specific $CD8^+$ T cells in DLNs showed proliferation (~41%, data not shown).

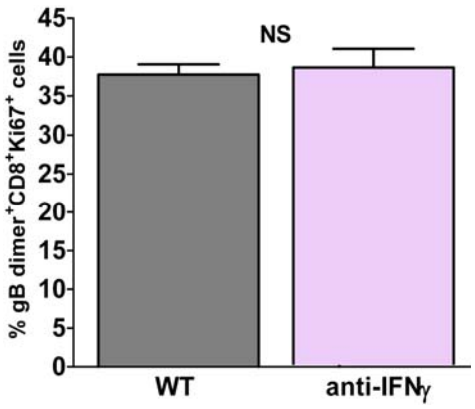

Figure 23: IFN-γ does not affect *in situ* proliferation of antigen-specific $CD8^+$ T cells in the DLNs.

Six days after HSV-1 corneal infection, mice received a single i.p. injection of anti-IFN-γ mAb (1mg/mouse, n = 8) or were left untreated (n = 7). One day later, the DLNs were removed; stained and analyzed by FCM. Data are represented as the means ± SEM of the percentage of $gB_{498-505}$-specific $CD8^+$ T cells positive for Ki-67 per DLN. NS = not significant.

4.2.5. IFNγ neutralization accelerates an early contraction of antigen-specific $CD8_{eff}$ cells

To assess the effects of IFN-γ on antigen-specific $CD8_{eff}$ cells during the early stages of contraction, mice were treated with anti-IFN-γ mAb on day 10 and 12 p.i. (after the expansion phase was complete). The mice were sacrificed two days later, and gB-specific $CD8_{eff}$ cells were quantified in the TGs. Contraction of the gB-specific $CD8^+$ T cells was observed in both the untreated and anti-IFN-γ-treated groups, but was significantly accelerated in the treated group (Figure 24). Thus, IFN-γ appears to delay the contraction phase of the response.

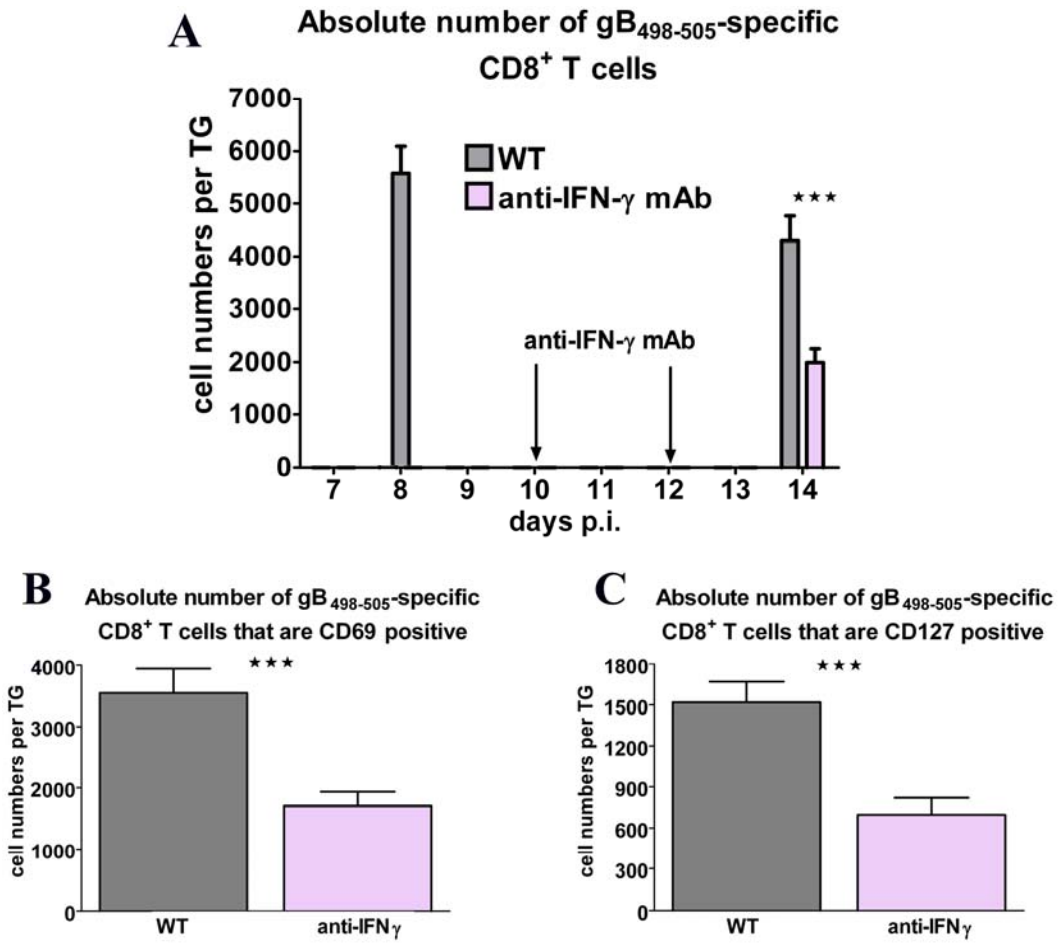

Figure 24: Neutralization of IFN-γ accelerates an early contraction of antigen-specific $CD8_{eff}$ cells.

Mice received an i.p. injection of anti-IFN-γ mAb (1mg/mouse, n = 19) at 10 and 12 days p.i. or were left untreated (n = 18). At day 14 p.i. the TGs were removed; stained and analyzed by FCM. Cell numbers in the TG are presented as the absolute number of $CD8^+$ T cells that are $gB_{498-505}$-specific at both day 8 and 14 p.i. (A), and the absolute number of $gB_{498-505}$-specific $CD8^+$ T cells that are either CD69 (B) or CD127 positive (C) at day 14 p.i.. Results are shown as the means ± SEM of the absolute numbers of cells per TG. ***, $P < 0.001$.

The numbers of gB-specific $CD8_{mp}$ and activated $CD8_{eff}$ cells were also reduced (Figure 24B and C). As noted previously (see Figure 19), at day 14 p.i., when total gB-specific $CD8_{eff}$ population is contracting, both $CD8_{mp}$ and activated $CD8_{eff}$ populations are still expanding. IFN-γ neutralization resulted in a statistically significant decrease in both populations suggesting that IFN-γ plays role in the delayed expansion of these cells.

4.2.6. BrdU and Ki-67 staining in the TG during contraction phase

BrdU and Ki-67 staining was repeated in mice in which the deprivation of IFN-γ early during contraction resulted in decreased numbers of gB-specific cells in the TG to investigate if observed reduction in cell numbers was a consequence of IFN-γ effects on proliferation of $CD8_{eff}$ cells during contraction phase (Figure 25).

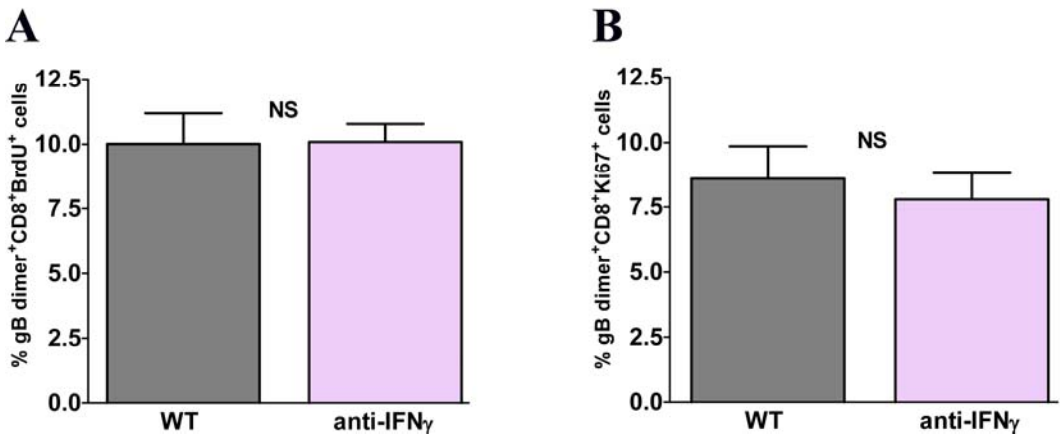

Figure 25: Neutralization of IFN-γ early during contraction does not affect *in situ* proliferation of antigen-specific $CD8_{eff}$ cells in the TG.

Mice received an i.p. injection of anti-IFN-γ mAb (1mg/mouse, BrdU, n = 9, Ki-67, n = 8) at day 10 and 12 p.i. or were left untreated (BrdU, n = 9, Ki-67, n = 7). At day 14 p.i. the TGs were removed; stained and analyzed by FCM. Data are represented as the means ± SEM of the percentage of $gB_{498-505}$-specific $CD8^+$ T cells positive for BrdU (injected at day 13 p.i., A) or Ki-67 (B) per TG. NS = not significant.

IFN-γ deprivation during the early contraction phase did not affect *in situ* proliferation of gB-specific $CD8_{eff}$ cells in the TG. The percentage of cells that were Ki-67 positive was undistinguishable between treated and untreated animals suggesting that IFN-γ regulation of early contraction involves some other mechanism(s). The BrdU (injected on day 13 p.i.) incorporation approach showed the similar percentage of proliferating cells as did Ki-67 staining.

4.2.7. Annexin V staining in the TG and DLN at day 14 p.i.

We next wanted to determine if the observed reduction in gB-specific $CD8_{eff}$ cell numbers was a consequence of the increased apoptosis of these cells in the absence of IFN-γ. Therefore, we assessed the rate of apoptosis of gB-specific $CD8_{eff}$ cells *in situ* by annexin V staining. We were not able to detect any statistically significant difference in the percentages of apoptotic cells between anti-IFN-γ mAb-treated and untreated animals (Figure 26).

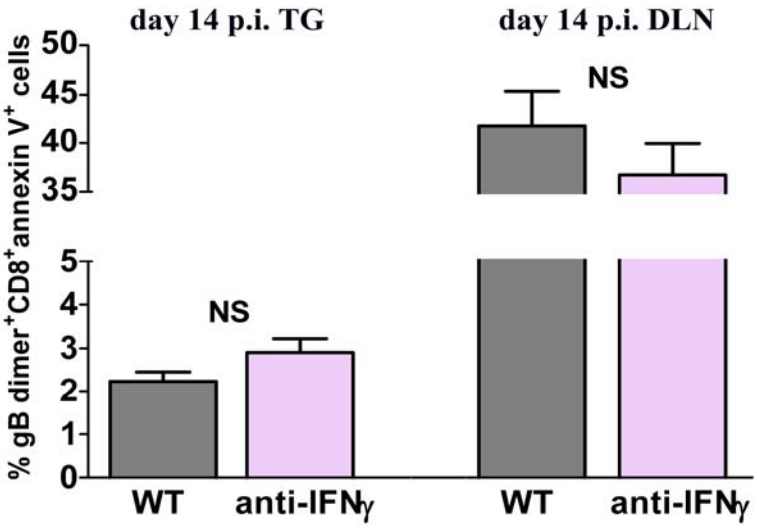

Figure 26: IFN-γ does not affect the death rate of antigen-specific $CD8_{eff}$ cells during early contraction phase.

Mice received an i.p. injection of anti-IFN-γ mAb (1mg/mouse, n = 8) at day 10 and 12 p.i. or were left untreated (n = 7). At day 14 p.i. the TGs and DLNs were removed; stained and analyzed by FCM. Data are represented as the means ± SEM of the percentage of $gB_{498-505}$-specific $CD8^+$ T cells positive annexin V per TG or DLN. NS = not significant.

To our surprise, at day 14 p.i. only ~2% of gB-specific $CD8_{eff}$ cells in the TGs of HSV-1 infected animals stained positive for annexin V, while at the same time 42% of these cells were apoptotic in the DLNs. The low percentage of apoptotic cells in the TG could be a consequence of their rapid removal by phagocytosis, or alternatively, gB-specific $CD8_{eff}$ cells could leave TG

and undergo apoptosis somewhere else. These possibilities are further addressed in Discussion, section 5.2.2.

4.2.8. gB-specific $CD8_{eff}$ cell response is not influenced by the deprivation of IFN-γ late in contraction phase

Mice received i.p. injections of anti-IFN-γ mAb at day 16 and 20 p.i. or were left untreated.

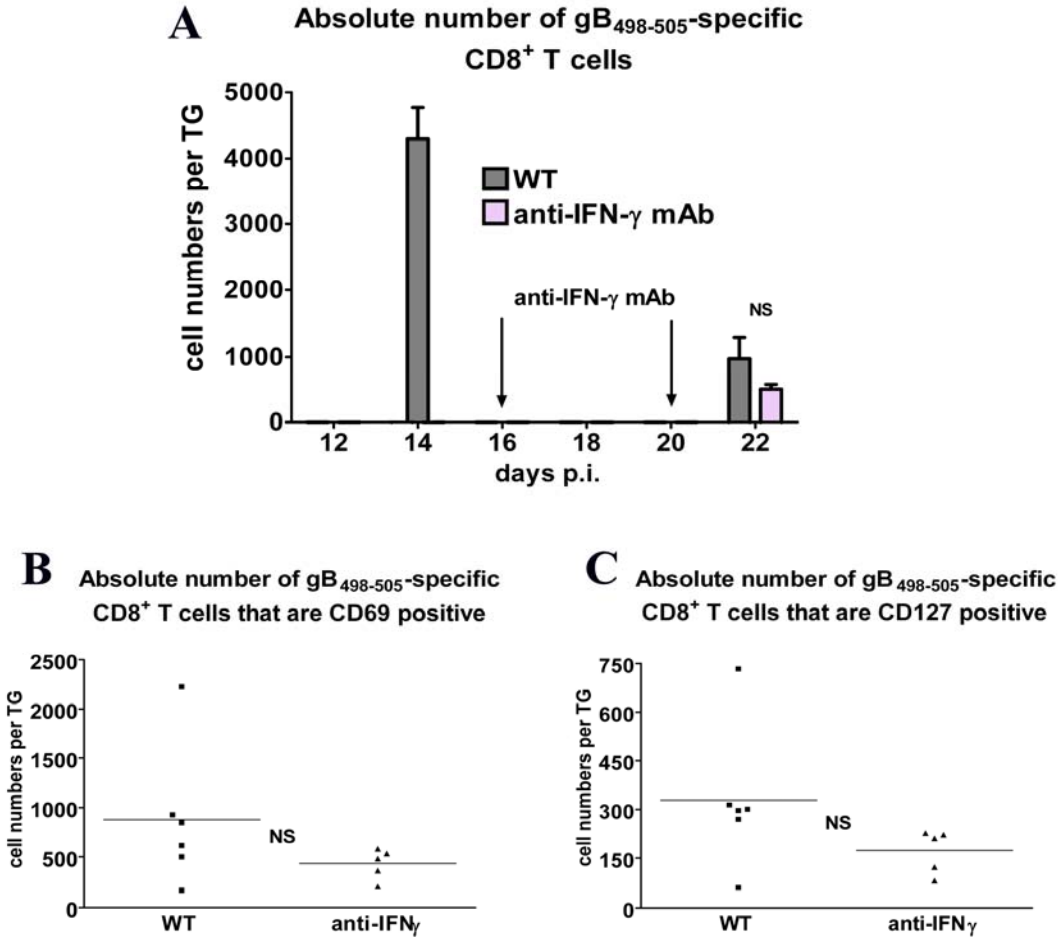

Figure 27: gB-specific $CD8_{eff}$ cell response is not influenced by the deprivation of IFN-γ late in the contraction phase.

Mice received i.p. injections of anti-IFN-γ mAb (1mg/mouse, n = 5) 16 and 20 days p.i. or were left untreated (n = 6). At 22 days p.i. the TGs were removed, stained and analyzed by FCM. Cell numbers in the TG are represented as the absolute numbers of $CD8^+$ T cells that are $gB_{498-505}$-specific at day 14 and 22 p.i. (A), and the absolute number of $gB_{498-505}$-specific $CD8^+$ T cells that are either CD69 (B) or CD127 positive (C) at day 22 p.i.. Results are shown as the means ± SEM of the absolute numbers of cells per TG. NS = not significant.

The analysis of TGs at 22 days p.i. showed that the deprivation of IFN-γ at late times during contraction did not affect the numbers of antigen-specific $CD8_{eff}$ cells (Figure 27). Thus, IFN-γ seems to be dispensable at this stage of the gB-specific $CD8^+$ T cell response.

4.2.9. The deprivation of IFN-γ early during infection does not influence the establishment or maintenance of gB-specific $CD8_{mem}$ cells

We have shown previously that an early deprivation of IFN-γ resulted in the reduced expansion of $CD8_{mp}$ (see Figure 20C) and wanted to investigate if the diminished expansion of these cells influences the establishment and maintenance of $CD8_{mem}$ population present in the TGs during homeostasis. Mice were treated with anti-IFN-γ mAb at day 6 p.i. and their TGs were analyzed 34 days later. The decrease in numbers of memory precursors early did not influence the absolute numbers or proportion of these cells within the population of HSV-1-specific $CD8^+$ T cells during homeostasis nor did it influence the establishment or maintenance of gB-specific $CD8_{mem}$ population (Figure 28). We are currently investigating if the $CD8_{mem}$ population elicited during the early deprivation of IFN-γ shows decreased or impaired functionality.

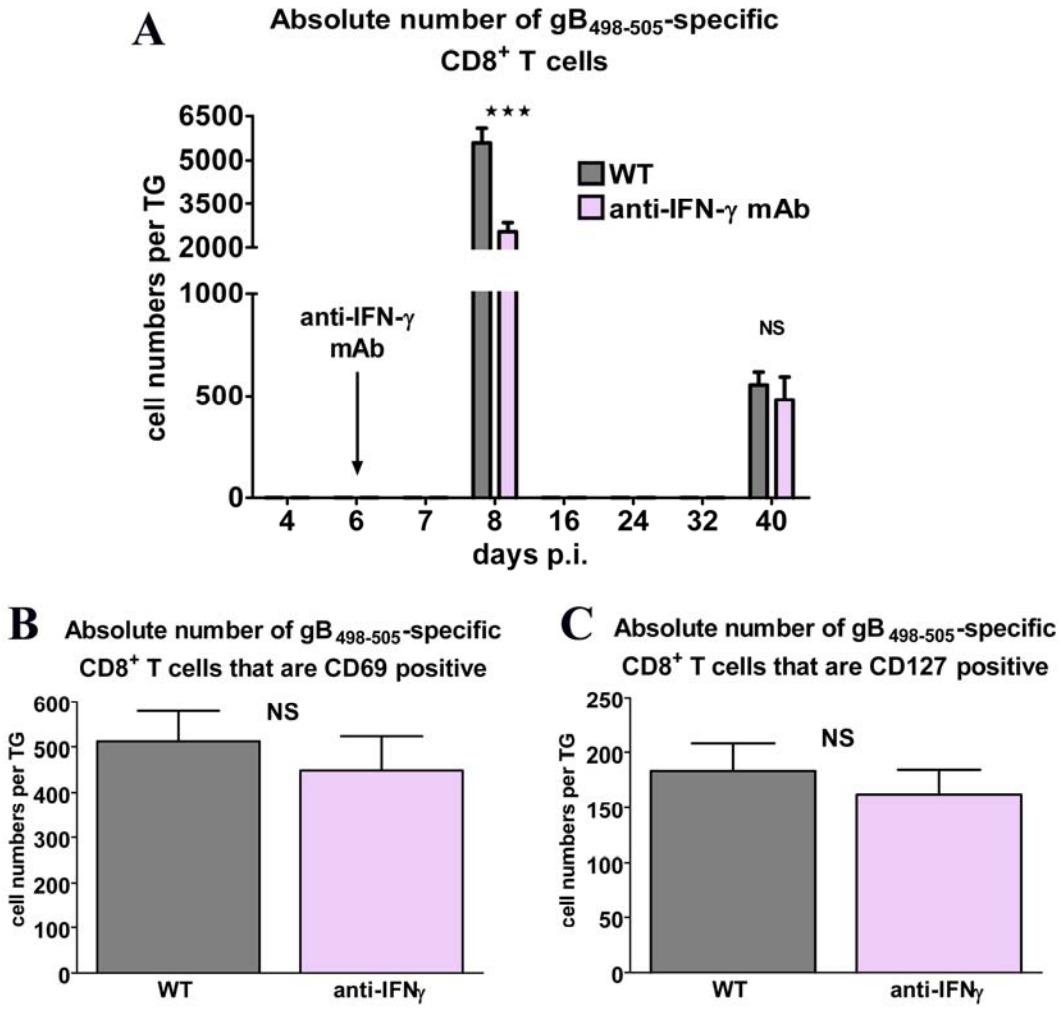

Figure 28: Neutralization of IFN-γ early during expansion phase does not affect the establishment and maintenance of gB-specific $CD8_{mem}$ cells.

Mice received an i.p. injection of anti-IFN-γ mAb (1mg/mouse, n = 14) at 6 days p.i. or were left untreated (n = 18). At day 40 p.i., the TGs were removed, stained and analyzed by FCM. Cell numbers in the TG are represented as the absolute numbers of $CD8^+$ T cells that are $gB\text{-}_{498\text{-}505}$-specific at day 8 and 40 p.i. (A), and the absolute number of $gB_{498\text{-}505}$-specific $CD8^+$ T cells that are either CD69 (B) or CD127 positive (C) at day 40 p.i.. Results are shown as the means ± SEM of the absolute numbers of cells per TG. ***, $P < 0.001$; NS = not significant.

4.2.10. IFN-γ does not influence the homeostasis of gB-specific $CD8_{mem}$ cells

HSV-1-specific $CD8_{mem}$ cells appear to play an important role in regulating HSV-1 latency, thus it was important to investigate if IFN-γ neutralization during the homeostasis phase will affect the size of memory pool. Mice received i.p. injections of anti-IFNγ mAb (1mg/mouse) at 30, 34 and 38 days p.i. Two days later, the TGs were removed and analyzed. The

neutralization of IFN-γ late in infection did not influence the homeostasis of gB-specific $CD8_{mem}$ cells as judged by the comparison of absolute numbers of these cells in untreated and treated animals (Figure 29).

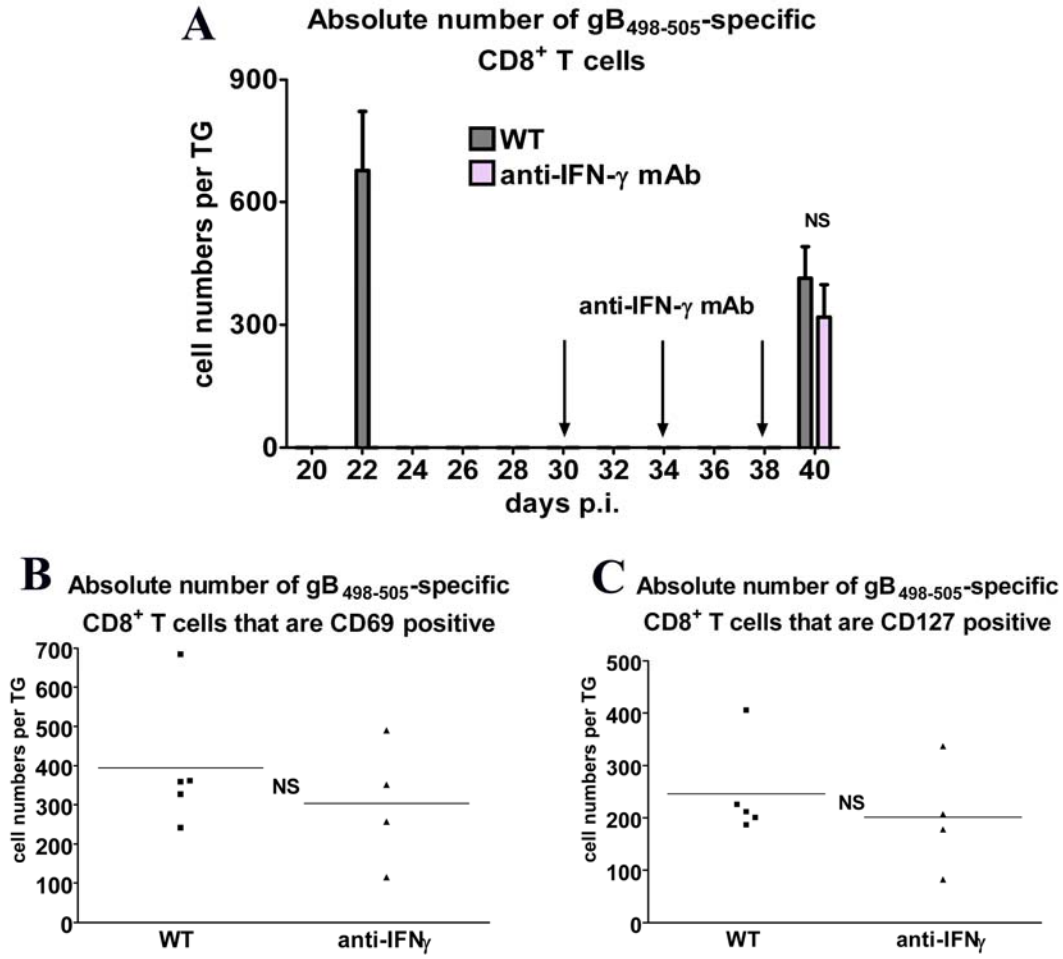

Figure 29: IFN-γ does not influence the homeostasis of gB-specific $CD8_{mem}$ cells.

Mice received i.p. injections of anti-IFN-γ mAb (1mg/mouse, n = 4) at 30, 34 and 38 days p.i. or were left untreated (n = 5). At day 40 p.i. the TGs from both sides were removed, stained and analyzed by FCM. Cell numbers in the TG are represented as the absolute numbers of $CD8^+$ T cells that are $gB_{498-505}$-specific at day 22 and 40 p.i. (A), and the absolute number of $gB_{498-505}$-specific $CD8^+$ T cells that are either CD69 (B) or CD127 positive (C) at day 40 p.i.. Results are shown as the means ± SEM of the absolute numbers of cells per TG. NS = not significant.

In summary, IFN-γ seems to be dispensable for the regulation of antigen-specific $CD8^+$ T cell response at later stages of HSV-1 infection (late contraction and homeostasis of $CD8_{mem}$

population). This could be possibly explained by the differential expression of IFN-γR on $CD8^+$ T cells during different stages of response or by the fact that at later times during infection other cytokines present in the TG could compensate for the lack of IFN-γ.

4.2.11. Neutralization of IFN-γ does not affect the viral replication or cause HSV-1 reactivation from latency

In the experiments in which IFN-γ was neutralized during initial expansion (see Figure 20), early (see Figure 24) and late contraction (see Figure 27) of gB-specific $CD8_{eff}$ cell response, as well as, in the experiment in which IFN-γ neutralization early did not influence the establishment or maintenance of gB-specific $CD8_{mem}$ population (see Figure 28), HSV-1 copy number per infected TG was determined by real-time PCR (Figure 30). Briefly, after removal of both TGs from the same animal, and preparation of a single-cell suspension, one TG equivalent was stained with appropriate antibodies and subjected to FCM. The remaining TG equivalent was used for DNA isolation and determination of a viral genome copy number. As shown in Figure 30, the neutralization of IFN-γ during initial expansion of $CD8_{eff}$ population did not result in an altered viral replication in the TG nor did IFN-γ neutralization during early contraction phase result in the reactivation of latent virus. In both instances, the IFN-γ deprivation reduced, but did not completely eliminate the gB-specific $CD8_{eff}$ population. Apparently, the remaining population was still able to control the virus. Since IFN-γ deprivation at later stages of contraction did not affect $CD8_{eff}$ population, the observation of similar HSV-1 copy numbers between treated and untreated groups was expected. Transient neutralization of IFN-γ at early times (6 days p.i.) did not influence the establishment or maintenance of $CD8_{mem}$ cells and as

expected, we did not observe an increase in HSV-1 copy number suggesting that the latent virus did not reactivate.

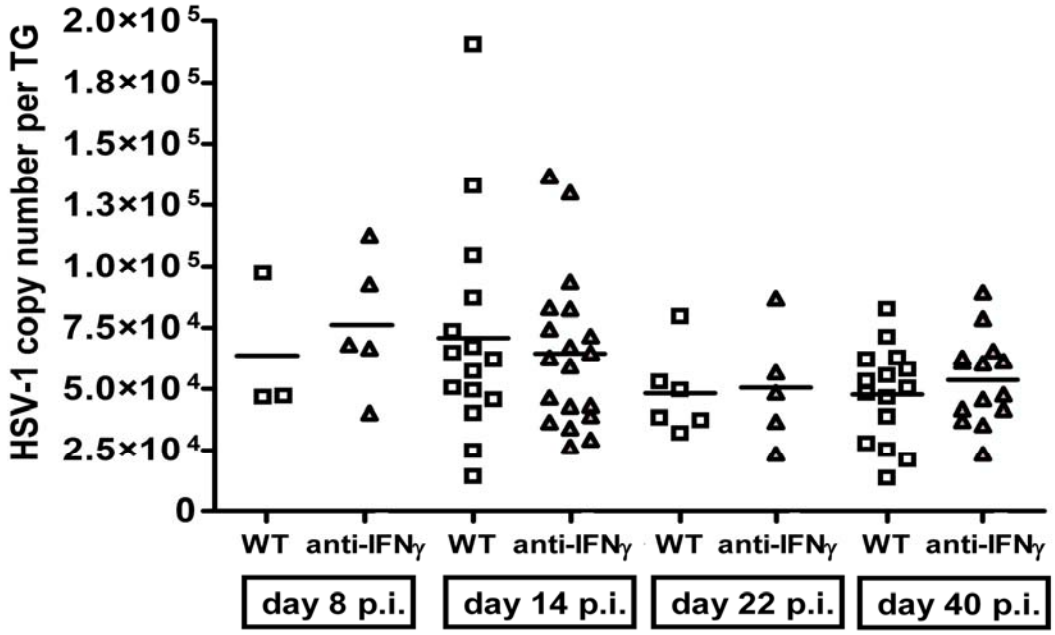

Figure 30: HSV-1 copy number per TG at different times p.i. in untreated and anti-IFN-γ mAb treated mice.

HSV-1 copy number per infected TG was determined by real-time PCR using gH primer-probe set. Mice were sacrificed at indicated times p.i. and treatments were done as follows; for day 8 p.i. time point, mice were left untreated (WT) or received a single injection of anti-IFN-γ mAb on day 6 p.i.; for day 14 p.i. time point, mice were left untreated (WT) or received anti-IFN-γ mAb injections on day 10 and 12 p.i.; for day 22 p.i. time point, mice were left untreated (WT) or received anti-IFN-γ mAb injections on day 16 and 20 p.i.; and for day 40 p.i. time point, mice were left untreated (WT) or received a single injection of anti-IFN-γ mAb on day 6 p.i. After the removal of both TGs from the same animal, and preparation of single-cell suspension, one TG equivalent was used for DNA isolation and subsequent determination of a viral genome copy number.

5. Discussion

5.1. IFN-γ inhibits HSV-1 reactivation from latency.

5.1.1. HSV-1 latency; a dynamic interaction?

The convergence of several recent findings has lead us to hypothesize that HSV-1 latency is not necessarily characterized by a silent viral genome and a passive host immune system, but rather involves a more dynamic interaction in which viral genes are persistently expressed in some latently infected neurons. Reactivation leading to virion formation might be blocked in such neurons through the activity of a population of T lymphocytes that is maintained in latently infected ganglia [9;45;75;77;82]. Although this paradigm remains to be definitively established *in vivo*, our recent findings clearly demonstrate that $CD8^+$ T cells are capable of blocking HSV-1 reactivation from latency in *ex vivo* TG cultures [67;81;82]. Several investigators have demonstrated that $CD8^+$ T cells and IFN-γ are constantly present in latently infected TG [45;74-80;82;85]. The present studies were undertaken to address the following two questions: (i) can IFN-γ block HSV-1 reactivation in some or all latently infected neurons, and if so (ii) at what stage in the viral life cycle does IFN-γ interfere with reactivation?

5.1.2. Differential susceptibility of infected neurons to IFN-γ protection

We and others [158] have observed that two to six neurons typically show full viral reactivation with virion formation in cultures comprised of the cells from a single latently

infected TG, and we have shown that $CD8^+$ T cells can block the reactivation process in these neurons. When the cells obtained from a single TG were divided into 10 cultures, up to 35% of the cultures showed HSV-1 reactivation from latency. The frequency of reactivation was reduced by approximately 50% when cultures were exposed to IFN-γ (see Figure 11). It appears, therefore, that half of the neurons that reactivate HSV-1 in *ex vivo* TG cultures are sensitive to IFN-γ protection. When WT $CD8^+$ T cells were added to undepleted D34 HSV-1 RE infected TG cultures, none of the cultures exhibited reactivation. Addition of anti-IFN-γ mAb caused reactivation in about half of reactivation-competent cultures (our unpublished data). This selective sensitivity to IFN-γ might be related to the observed heterogeneity of neurons that harbor latent HSV-1 [43] and the differential expression of IFN-γ receptors on neuronal subtypes ([159]; unpublished data). Preliminary studies in our lab showed that some of HSV-1 infected neurons express IFN-γR, while others do not. Since HSV-1 specific $CD8^+$ T cells can completely block HSV-1 reactivation in these cultures, our findings suggest that $CD8^+$ T cells utilize a different effector mechanism to protect the neurons that are refractory to IFN-γ protection.

5.1.3. Does IFN-γ affect viral gene expression during HSV-1 reactivation?

It is important to distinguish the capacity of $CD8^+$ T cells to inhibit the HSV-1 reactivation process from their capacity to respond to virus when reactivation is complete. To intervene in the reactivation process, $CD8^+$ T cells would need to detect viral proteins in latently infected neurons and produce effector molecules that are capable of inhibiting the reactivation process prior to virion formation. Since IFN-γ appears to be one of the effector molecules used by $CD8^+$ T cells to block HSV-1 reactivation from latency in sensory neurons, it was of interest to determine what step in the reactivation process is blocked by IFN-γ. To address this issue, we

created recombinant viruses that express EGFP driven by the promoters for the α gene, encoding ICP0, and the γ2 gene, encoding gC. By monitoring *ex vivo* cultures of TG that were latently infected with these recombinant viruses, we could directly observe the effect of IFN-γ on the expression of these two promoters during the process of reactivation from latency in neurons.

5.1.4. IFN-γ inhibits several necessary steps in the reactivation process

5.1.4.1. IFN-γ inhibits expression from ICP0 promoter during reactivation from latency

Our findings clearly establish that IFN-γ can inhibit expression of the ICP0 promoter during HSV-1 reactivation from latency in neurons (see Figure 12), although it is not clear if this reflects a direct effect on promoter activity or an indirect effect through impairment of an upstream event. Protein complexes that activate α gene promoters during lytic infection are composed of viral tegument and host proteins [21], of which the VP16-Oct-1-HCF complex acting through the TAATGARAT motifs is best characterized. The activation of α gene promoters during reactivation from latency occurs in the absence of VP16, most likely through the action of neuron-specific transcription factors that may substitute for VP16 during HSV-1 reactivation. Using transgenic mice in which α promoters were fused to β-galactosidase, Mitchell and colleagues [68] demonstrated that neuronal transcription factors activate the HSV-1 ICP0, ICP4, and ICP27 promoters *in vivo* in the absence of viral proteins. Moreover, ICP0 promoter activity was significantly increased by both UV irradiation and hyperthermia (stimuli that cause the reactivation of latent virus), while ICP4, ICP27, TK and gC reporter transgenes were not activated by these stimuli [69;70]. IFN-γ regulates the expression of over 200 cellular genes, including many encoding transcription factors [111]. It is reasonable to propose that IFN-γ

might inhibit reactivation in part by reducing the expression of host transcription factors that regulate the production of requisite viral proteins such as ICP0.

5.1.4.2. IFN-γ inhibits ICP0 and gC promoter expression to a similar extent during reactivation from latency

We show a comparable reduction by IFN-γ of ICP0 and gC promoter activity during reactivation (see Figure 12 and 14A). ICP0 is not required for HSV-1 γ2 gene expression in nonneuronal cells following infection at a high MOI [160]. However, ICP0 is needed for an efficient infection and γ2 gene expression at low multiplicities of infection, possibly through the manipulation of an interferon response [30]. While ICP0 is a promiscuous transactivator, its role in regulating γ2 gene expression during HSV-1 reactivation from latency in neurons is not clear. The fact that IFN-γ comparably inhibited ICP0 and gC promoter expression during HSV-1 reactivation from latency in neurons is consistent with the possibility that ICP0 is required for gC expression during reactivation, although future confirmation is required. This could be addressed by using double recombinant virus in which EGFP is under the control of ICP0 promoter, while some other fluorescent protein (i.e., red fluorescent protein [RFP]) is expressed from gC promoter. Using this virus we would be able to determine if expression from gC promoter is always accompanied by expression from ICP0 promoter or if gC promoter activity can be observed in the absence of detectable ICP0 promoter expression.

5.1.4.3. IFN-γ inhibits a very late event in viral reactivation

We provide additional evidence that IFN-γ blocks full reactivation in neurons that express EGFP from the ICP0 promoter, and perhaps more importantly, in neurons that express

the gC promoter as well as transcripts for another γ2 gene, encoding gH (see Figures 13, 14B and 16). To our knowledge, this is the first demonstration that HSV-1 γ2 genes can be expressed for extended periods (up to 9 days) in neurons without virion formation. These observations suggest an additional IFN-γ-mediated block of a very late event in viral reactivation following true late gene expression, such as viral protein trafficking to sites of assembly.

5.1.5. Could IFN-γ globally reduce viral gene transcription?

Although our data suggest that IFN-γ can inhibit several necessary steps in the reactivation process (i.e., ICP0 and gC expression and a step after gC expression), other possibilities must be considered. For instance, IFN-γ might globally reduce viral gene transcription while permitting low-level stochastic expression of a limited array of viral genes that does not result in virion formation. In this scenario, neurons that express gC might not express all other members of the γ gene family that are required for virion formation. For example, Everett et al. recently demonstrated stochastic viral gene expression in restrictive nonneuronal cells during a nonproductive infection [161].

5.1.6. ICP0 over-expression abrogates IFN-γ protective effects

Emerging evidence from past years suggests a fine interplay between interferon-induced host response and ICP0 interactions. We demonstrated that IFN-γ can inhibit HSV-1 reactivation by inhibiting ICP0 promoter expression, but we also showed that ICP0 over-expression from the replication-deficient adenovirus vector completely abrogated inhibitory effects of IFN-γ (see Figures 11 and 17). This is not surprising, considering the known role of ICP0 as a potent activator of viral gene expression and its role in the inhibition of IFN-γ regulated antiviral gene

expression [30]. By varying the concentration of DOX that is added to the cultures, the levels of ICP0 delivered from Ad.TRE-ICP0 to cultures could be regulated. It will be important to determine if in the presence of very small amounts of ICP0 all or a portion of the IFN-γ protective effects could be restored.

In summary, the cross-regulation between IFN-γ and ICP0 seems to influence the balance between HSV-1 latent and lytic infection. Together these findings suggest a model in which the presence of IFN-γ early in the reactivation process might block the functions of ICP0 that are required for HSV-1 reactivation from latency. A delay in the presence of IFN-γ would allow ICP0 protein to accumulate in the latently infected neurons, enhancing expression of viral lytic cycle genes, inhibiting IFN-γ function, and leading to reactivation from latency.

5.1.7. Closing remarks

Another interesting and consistent observation from these studies is EGFP filling of nerve axons just prior to the spread of virus to surrounding fibroblasts (see Figure 10C). Although the explanation for this phenomenon is not clear, it might relate to the observation that the anterograde transport of pseudorabies virus [162] and possibly HSV-1 [163] involves transport of the viral nucleocapsid and glycoproteins by means of distinct cellular transport mechanisms. The late step in HSV-1 reactivation that is blocked by IFN-γ could involve the inhibition of one of these cellular transport mechanisms that is also necessary for the anterograde transport of EGFP down nerve axons. Although EGFP is thought to diffuse freely through the cytoplasm, it is clearly excluded from the axons of latently infected neurons until shortly before virion formation. The relationship between anterograde transport of EGFP and viral proteins in latently infected neurons is being investigated.

It is noteworthy that a small number of cultures that were not treated with IFN-γ also showed stable expression from the ICP0 or gC promoter without reactivation. Moreover, the vast majority of neurons that harbor latent virus do not express EGFP from viral promoters or reactivate in the absence of $CD8^+$ T or $CD45^+$ cells in *ex vivo* cultures. It is clear from these observations that without assistance from the immune system, most latently infected neurons are capable of regulating virion formation even while allowing a limited expression of lytic genes. Our findings demonstrate that at any given time, only two to six neurons per latently infected TG require immune intervention to prevent HSV-1 reactivation from latency in *ex vivo* cultures. Nonetheless, this small number of neurons might be of considerable importance in recurrent disease, since the *in vivo* induction of reactivation results in virus replication in a similar number of neurons [56;57;77;158]. Since stress and stress hormones that are associated with HSV-1 reactivation from latency are known to inhibit T-cell function [164], it is reasonable to propose that recurrent herpetic disease results from a simultaneous failure of neurons and host immunity to control HSV-1 gene expression.

The recurrent nature of herpetic disease in humans results from the reactivation of latent virus in sensory neurons and its shedding at the surface. The recurrent shedding of HSV-1 in the cornea leads to progressive scarring and loss of vision. In immunosuppressed patients, the reactivation of latent HSV-1 can lead to lethal encephalitis. Therefore, understanding HSV-1 gene expression during latency and the factors that regulate it is of considerable clinical importance. Our data suggest that IFN-γ might prove to be a useful prophylactic agent to prevent recurrent herpetic disease.

5.2. IFN-γ regulates the magnitude of the antigen-specific $CD8^+$ T cell response during HSV-1 infection

All the studies published to date support the notion that IFN-γ regulates the magnitude of antigen-specific $CD8^+$ T cell response in lymphoid tissues. The importance of this cytokine in the regulation of adaptive immune response is further supported by the notion that IFN-γ effects were observed in different infection models [149;151;153]. Since in some studies IFN-γ was shown to have suppressive and in others simulative effects on the magnitude of $CD8^+$ T cell response, the exact nature of the contribution of IFN-γ to the three different phases of the $CD8^+$ T cells response remains controversial. The reasons for the discrepancies between results obtained in published studies are unknown but may relate to differences between the models used, such as pathogen virulence, the rapidity of pathogen clearance, site (tissue) of infection, and/or type of infection.

5.2.1. The role of IFN-γ in the expansion of antigen-specific $CD8_{eff}$ cells

The requirement for cytokines in initial expansion of $CD8^+$ T cells in lymphoid organs is unclear, but the growth factors IL-2 and IL-15 appear to be dispensable [165;166]. Recent evidence implicated IFN-γ in the initial expansion of effector cells, and in the establishment of immunodominance [127;153]. $CD8^+$ T cells specific for immunodominant epitopes on LCMV exhibited more rapid IFN-γ production during the expansion phase in the spleen. Moreover, after the dual adoptive transfer of IFN-γR^+ and IFN-γR^- cells into a LCMV infected host, reduced expansion of the latter cells was observed in the spleen. In the present study IFN-γ did not affect the initial expansion of HSV-1 gB-specific cells in the DLNs 8 days after HSV-1 corneal infection (see Figure 21). We hypothesize that the discrepancy observed between our results and

those of the above-mentioned study could be a consequence of a different virus and route of infection, or the fact that LCMV replicates in the spleen, whereas HSV-1 does not replicate in lymphoid organs [41;167]. It is also possible that the amount of anti-IFN-γ mAb used (1 mg/mouse), failed to completely neutralize IFN-γ present in the DLNs. Alternatively, other cytokines present in the DLNs could compensate during $CD8^+$ T cell expansion in the absence of IFN-γ.

The effector cells that are generated within lymphoid organs appear to undergo a second level of expansion when they enter infected tissue. The mechanism(s) regulating this initial expansion of $CD8^+$ T cells in non-lymphoid tissues is poorly understood although evidence suggests a role for IL-2 [165]. The differential requirement for IL-2 in the expansion of $CD8_{eff}$ cells in the lymphoid and non-lymphoid tissues implies microenvironmental influences that might involve differences in APCs and cytokine milieu, as well as, the differential contribution of infiltration, proliferation, and cell death. The involvement of IFN-γ in the initial expansion of $CD8^+$ T cells in non-lymphoid tissues, especially in latently infected nervous tissue, has not been previously addressed. It is important to understand how expansion of $CD8_{eff}$ cells is regulated in the TG since this can influence the formation of memory cells and subsequently determine the outcome of HSV-1 latent infection.

Here, we demonstrate that IFN-γ affects the abundance of antigen-specific $CD8_{eff}$ cells in the infected TGs during the expansion phase by directly affecting their proliferation in this organ (see Figures 20 and 22). We used two approaches (BrdU incorporation during a 12-hour pulse, and Ki67 staining) to assess the effect of IFN-γ neutralization on the proliferation of HSV-1-specific $CD8_{eff}$ cells in the TG (see Figures 22 and 25). There are advantages and disadvantages

to each approach. The incorporation of BrdU into cellular DNA identifies those cells that divided during the 12 hour pulse, whereas Ki-67 staining provides only a snapshot of the cells that were proliferating at the time of tissue excision. Thus, the BrdU positive cells could have divided in another organ (i.e., the DLN) and then traveled to the TG, whereas Ki-67 staining provides definitive proof that the positive cells are dividing in the TG.

The Ki-67 staining demonstrated that at any given time during the expansion phase (see Figure 22B) of HSV-1-specific $CD8_{eff}$ cells in the TG a substantial proportion (21%) of $CD8_{eff}$ cells is cycling, and that cell cycling is dramatically reduced in the anti-IFN-γ-treated mice. The observation that IFN-γ stimulates the proliferation of $CD8_{eff}$ cells is contrary to a widely accepted role of IFN-γ as an inhibitor of cell growth and proliferation [168], but in accordance with rare reports in which IFN-γ was shown to stimulate rather then suppress the growth of certain cells [169;170]. Furthermore, it was shown that IFN-γ injected *in vivo* stimulates the proliferation of $CD44^{hi}CD8^{+}$ T cells, but fails to exhibit similar effects on these cells *in vitro* [171]. It is possible that observed *in vivo* proliferative actions of IFN-γ are the consequence of indirect effects of this cytokine on production/expression of some other cytokine/growth factor. It would be interesting to see if IFN-γ stimulates the proliferation of HSV-1-specific $CD8_{eff}$ cells from day 8 infected TGs *in vitro*.

That only 21% of cells proliferate in the TG at the peak of response is not surprising, considering the possibility that not all of the gB-specific cells are synchronized. The expansion likely reflects a combination of infiltration from the blood and cell division within the TG. We presumably detected only a subpopulation of cells that proliferated recently. The fact that IFN-γ neutralization significantly reduced the number of Ki-67 positive cells, but not the number of BrdU positive cells in the TG (see Figure 22), suggests that most or all of the BrdU positive cells

acquired BrdU through division outside of the TG. Given the fact that gB-specific $CD8^+$ T cells must undergo cell division in the DLNs before entering the TG [41], and our observation that IFN-γ neutralization does not influence the division of gB-specific $CD8^+$ T cells in the DLNs, it is likely that the BrdU positive cells represent cells that divided in the DLNs and recently infiltrated TGs but have not yet begun to divide in this tissue.

In summary, it seems that following interaction with antigen-bearing APCs in DLNs and initial IFN-γ-independent expansion, $CD8^+$ T cells migrate to TG where the requirement for IFN-γ gains prominence. Alternatively, the difference in observed IFN-γ effects in the DLNs and TG could be a consequence of: i) partial neutralization of IFN-γ in the DLNs; ii) the presence of other compensating cytokines in the DLNs, but not in the TG or iii) differential expression of IFN-γR on $CD8^+$ T cells in these tissues.

5.2.2. The role of IFN-γ in contraction of antigen-specific $CD8_{eff}$ cells

The initial expansion of antigen-specific $CD8_{eff}$ cells is followed by a contraction phase in which most (~90%) of the effector cells are lost. Studies by Hardy and colleagues [149;151] suggested a role for IFN-γ in accelerating the contraction phase of the $CD8^+$ T cell response. However, our data advocate the opposite role for IFN-γ of delaying $CD8^+$ T cell contraction (see Figure 24) and suggest that the mechanism(s) governing contraction of $CD8_{eff}$ population in non-lymphoid tissues might be quite different than those in lymphoid tissues. This could be a consequence of direct vs. indirect IFN-γ effects in lymphoid and non-lymphoid tissues or alternatively, this could relate to the differential expression of IFN-γR on $CD8^+$ T cells in these tissues. Furthermore, we have shown that neutralization of IFN-γ does not influence the later stages of contraction of antigen-specific $CD8_{eff}$ cells in the TG. We are not sure if this means that

different mechanisms govern early and late stages of contraction, or that the expression of IFN-γR on $CD8_{eff}$ cells in the TG is downregulated at later times during HSV-1 infection.

Based on observed accelerated contraction in the absence of IFN-γ (see Figure 24) we were expecting to see a higher rate of apoptosis in anti-IFN-γ-treated animals, but annexin V staining demonstrated nearly identical death rates of antigen-specific $CD8_{eff}$ cells between untreated and treated groups (see Figure 26). Moreover, only 2% of gB-specific $CD8_{eff}$ cells were apoptotic in day 14 WT TG, although the number of these cells significantly decreased between day 8 and day 14 p.i. (1.37 fold difference). The detection of only a very small population of apoptotic cells could result from the rapid removal of dying cells by phagocytosis. Nonetheless, other possibilities should also be addressed. It has been proposed that the contraction of $CD8^+$ T cells can result from a combination of apoptosis and emigration [117;118]. In the emigration scenario, $CD8^+$ T cells could leave the TG and undergo apoptosis somewhere else, i.e. the liver [172;173]. Previous studies demonstrated preferential retention of activated $CD8^+$ T by the liver. The monitoring of $CD8^+$ T cell viability showed that some of the cells initiated apoptotic processes before arrival, but in the majority of them apoptosis was induced during their retention in this organ [174]. Emigration of $CD8^+$ T cells to the liver is rendered less likely by a recent study [41] that failed to detect HSV-1-specific $CD8^+$ T cells in the liver at day 10 p.i. (contraction has already started at this time point).

The mechanism(s) of apoptosis during contraction is controversial, but two pathways (AICD and ACAD) appear to control the majority of activated T cell death *in vivo* [119]. However, in some models, contraction of the $CD8^+$ effector T cell pool in the spleen was independent of caspase activation [120]. The treatment of LCMV infected mice with the pan-caspase inhibitor zVAD did not result in increased numbers of antigen-specific cells during the

contraction or memory phase; although zVAD inhibited the apoptosis (induced) of freshly isolated virus-specific cells *in vitro*, and when administrated *in vivo* was able to rescue mice from the induced lethal intrahepatic hemorrhage. Bim, a pro-apoptotic member of the Bcl-2 family, seems to be a mediator of caspase-independent T cell death. Experiments with Bim-deficient mice have shown that this protein is required for lymphocyte apoptosis induced by cytokine withdrawal [175]. Recent data indicated that Bim was crucial for the contraction of HSV-1-specific $CD8^+$ T cells [116] and we will investigate the expression this pro-apoptotic molecule in the presence and absence of IFN-γ.

5.2.3. $CD8_{mp}$ population shows a delayed expansion and contraction relative to the overall $CD8_{eff}$ population in the TG

A novel finding of these studies was that an HSV-1-specific $CD8_{mp}$ population (defined by expression of CD127) that was present as a minor subpopulation of the $CD8_{eff}$ population at 8 days p.i., exhibited a delayed expansion and contraction relative to the overall $CD8^+$ population in the TG (see Figures 18 and 19). $CD8_{mp}$ expansion was observed between 8-14 days p.i. and possibly could be explained by preferential proliferation, infiltration or survival of $CD127^+$ cells relative to $CD127^-$ cells. Alternatively, the $CD127^+$ population might differentiate from $CD127^-$ effector cells. If the latter is true, it would be interesting to see how this process is regulated and what factors are involved. A role for IFN-γ is suggested by our findings that IFN-γ neutralization dramatically reduced the expansion of $CD127^+$ cells in the TG. The contraction of $CD8_{mp}$ population occurred between 14-22 days p.i. Thus, it seems that there are two phases to overall contraction. In the first phase (8-14 days p.i.) the frequency of $CD127^+$ cells increases (from 7%-37%) and this phase is affected by IFN-γ (see Figures 19, 18 and 20). During the second phase,

the number of $CD127^+$ cells declines in conjunction with the overall population so the percentage does not change much. That phase does not seem to be influenced by IFN-γ (see Figures 18, 19 and 27).

IFN-γ neutralization dramatically reduced the $CD8_{mp}$ expansion (see Figure 20C), though ultimately the absolute numbers or proportion of $CD127^+$ $CD8_{mem}$ cells during homeostasis phase in the TG was not affected (see Figure 28). The significance of this delayed expansion and contraction of the $CD8_{mp}$ cells during the contraction phase of the $CD8_{eff}$ is not clear. We have noted in untreated mice that $CD8_{mem}$ present in the TG > 30 days p.i. have a higher average functional avidity (i.e., have a lower epitope density threshold for IFN-γ production or lytic granule exocytosis) than the $CD8_{eff}$ present in the TG at 8 days p.i.. We have also noted that the average functional avidity of the $CD8_{mem}$ present > 30 days p.i. is similar to that of the $CD8_{mp}$ present at 14 days p.i.. We are currently determining if the disruption of the expansion and contraction of $CD8_{mp}$ through IFN-γ neutralization will influence the shift to a lower functional avidity in the $CD8_{mem}$ population that ultimately develops. If so, this will suggest that important events occur during the contraction phase of the $CD8^+$ T cell response that influence the generation of a functionally optimized $CD8_{mem}$ population, and defining these events will be an important goal of future research in our laboratory. Since HSV-1-specific $CD8_{mem}$ appear to play an important role in regulating HSV-1 latency, optimizing this population could have important implications for controlling recurrent herpetic disease.

5.2.4. IFN-γ seems to be dispensable at later stages of HSV-1 infection.

We have shown that IFN-γ plays an important role in the regulation of $CD8^+$ T cell response at earlier stages of HSV-1 infection (expansion and early contraction). In contrast, IFN-

γ neutralization did not affect the homeostasis/memory phase as no change in the absolute numbers or percentage of HSV-1-specific $CD8^+$ T cells was observed when IFN-γ was neutralized between 30 and 38 days p.i. (see Figure 29). The apparent lack of the effect of IFN-γ on the $CD8_{mem}$ population suggests that this cytokine may be dispensable during homeostasis, and/or that other cytokines present could compensate for the lack of IFN-γ. It is also possible that early deprivation of IFN-γ did not affect the homeostasis of $CD8_{mem}$ population due to the inability of this cytokine to affect the gB-specific $CD8^+$ T cell response in the DLNs. By this scenario, at early times during infection, gB-specific $CD8^+$ T continually emigrate from the DLNs and infiltrate TG. We do not know if gB-specific cells are being replenished from the DLNs, but it was shown that in order to enter the TG, gB-specific $CD8^+$ T cells need to upregulate CD43 [41] and the CD43 upregulation requires stimulation. The observation of stable levels of $CD8_{mem}$ cells in the absence of IFN-γ is in agreement with previously published studies [151].

5.2.5. Closing remarks.

In summary, the studies detailed herein show that the biological effects of IFN-γ change over the course of an ongoing immune response. Early during HSV-1 infection IFN-γ strongly stimulates the development of antigen-specific $CD8^+$ T cell response, but at later stages IFN-γ seems to be dispensable. Although it is not clear if the observed IFN-γ effects are the consequence of direct or indirect actions of IFN-γ on $CD8^+$ T cells, the simplest explanation of our observations would be that $CD8^+$ T cells express IFN-γR at earlier, but not later stages of HSV-1 infection. It is also possible that early during response the presence of IFN-γ is critical in

development of $CD8^+$ T cell response, while at later stages other cytokines present could compensate for IFN-γ.

We can further expand our observations by suggesting that the regulation of $CD8^+$ T cell response and mechanisms involved might be different in lymphoid vs. non-lymphoid tissues due to microenvironmental influences, such as differences in APCs presence, cytokine milieu, as well as, due to the differential contribution of infiltration, proliferation, and cell death in these tissues.

Although our previous studies demonstrated an important role for IFN-γ in maintaining the virus in a latent state, in our current studies we did not see an effect of transient neutralization of IFN-γ on the viral loads or on reactivation of latent virus. There are a number of possible explanations for these conflicting results. First, neurons may only need IFN-γ to maintain viral latency following a strong reactivation signal such as axotomy. Second, the duration of anti-IFN-γ treatment in our studies was too short to affect reactivation *in vivo*. Third, we might not achieve a sufficiently high titer of anti-IFN-γ antibody to completely neutralize IFN-γ in the TG, particularly given our previous findings that HSV-1-specific $CD8^+$ T cells form an apparent immunologic synapse with neurons in latently infected TG. IFN-γ that is released into these tight junctions between $CD8^+$ T cells an neurons might be particularly difficult to neutralize.

6. Summary

The studies detailed in the first part of this thesis provide several important observations about IFN-γ control of HSV-1 reactivation from latency. We showed that IFN-γ inhibits HSV-1 reactivation in part by blocking ICP0 expression; and in part, by blocking a very late event in reactivation. It appears that only a subpopulation of latently infected neurons is protected by IFN-γ, but these neurons might be of considerable importance in recurrent disease. Our findings demonstrate for the first time that in the presence of IFN-γ neurons can express for extended periods both immediate early and late viral genes while maintaining latency. Why IFN-γ can block HSV-1 reactivation from latency in some neurons and not in others, and whether or not $CD8^+$ T cell effector mechanisms are differentially regulated while controlling HSV-1 reactivation in neurons are issues that are currently under investigation in our laboratory.

The studies detailed in the second part of this thesis provide compelling evidence that IFN-γ regulates the magnitude of antigen-specific $CD8^+$ T cell response in non-lymphoid tissue where virus establishes latency. We examined the contributions of this cytokine to the three phases of $CD8^+$ T cell response. Although not required for optimal expansion of HSV-1 specific $CD8^+$ T cells in the DLN, IFN-γ was necessary for the optimal expansion of $CD8_{eff}$ cells in the TG. Apparently, IFN-γ exerts a stimulatory effect on the proliferation of $CD8_{eff}$ cells in the TG. We also demonstrated that neutralization of IFN-γ accelerated the contraction phase, but did not affect the homeostasis of $CD8_{mem}$ population retained in latently infected TG. The mechanism(s) underlying the IFN-γ actions during the contraction phase are currently under investigation.

Furthermore, we will investigate the contribution of IFN-γ to the functional characteristics of the HSV-1 specific $CD8^+$ T cells memory population that is maintained in the latently infected TG. We anticipate that our work will continue to advance the understanding of the regulation of the antigen-specific $CD8^+$ T cell response in relevant non-lymphoid tissues.

APPENDIX A

Publications:

1. Khanna KM, Lepisto AJ, Decman V, Hendricks RL: **Immune control of herpes simplex virus during latency.** *Curr. Opin. Immunol.* 2004, **16**:463-469

2. Freeman ML, Decman V, Hendricks RL: **Neurons and host immunity conspire to maintain herpes simplex virus in a latent state.** SGM symposium, **64**:203-213

3. Decman V, Kinchington PR, Harvey SAK, Hendricks RL: **Gamma interferon can block herpes simplex virus type 1 reactivation from latency, even in the presence of late gene expression.** *J Virol.* 2005, **79**:10339-47

4. Decman V**,** Freeman ML, Kinchington PR, and Hendricks RL (2005) **Immune control of HSV-1 latency.** *Viral Immunol.* 2005, *In press.*

5. Prabhakaran K, Sheridan BS, Kinchington PR, Khanna KM, Decman V, Lathrop K, Hendricks RL: **Sensory neurons regulate the effector functions of activated effector memory CD8$^+$ T cells (T_{AEM}) during HSV-1 latency.** 2005, *In revision.*

BIBLIOGRAPHY

1. Nahmias AJ, Lee FK, Beckman-Nahmias S: **Sero-epidemiological and -sociological patterns of herpes simplex virus infection in the world**. *Scand.J.Infect.Dis.Suppl* 1990, **69:**19-36.

2. Smith JS, Robinson NJ: **Age-specific prevalence of infection with herpes simplex virus types 2 and 1: a global review**. *J.Infect.Dis.* 2002, **186 Suppl 1:**S3-28.

3. Siegel D, Golden E, Washington AE, Morse SA, Fullilove MT, Catania JA, Marin B, Hulley SB: **Prevalence and correlates of herpes simplex infections. The population-based AIDS in Multiethnic Neighborhoods Study**. *JAMA* 1992, **268:**1702-1708.

4. Schillinger JA, Xu F, Sternberg MR, Armstrong GL, Lee FK, Nahmias AJ, McQuillan GM, Louis ME, Markowitz LE: **National seroprevalence and trends in herpes simplex virus type 1 in the United States, 1976-1994**. *Sex Transm.Dis.* 2004, **31:**753-760.

5. Remeijer L, Osterhaus A, Verjans G: **Human herpes simplex virus keratitis: the pathogenesis revisited**. *Ocul.Immunol.Inflamm.* 2004, **12:**255-285.

6. Whitley RJ.: **Herpes simplex viruses.** In *Fields virology, 3rd ed.* Edited by Fields BN et al. Philadelphia: Lippincott-Raven; 1996:2297-2342.

7. Umene K, Sakaoka H: **Evolution of herpes simplex virus type 1 under herpesviral evolutionary processes**. *Arch.Virol.* 1999, **144:**637-656.

8. Roizman B, Sears AE: **An inquiry into the mechanisms of herpes simplex virus latency**. *Annu.Rev.Microbiol.* 1987, **41:**543-571.

9. Theil D, Derfuss T, Paripovic I, Herberger S, Meinl E, Schueler O, Strupp M, Arbusow V, Brandt T: **Latent herpesvirus infection in human trigeminal ganglia causes chronic immune response**. *Am.J.Pathol.* 2003, **163:**2179-2184.

10. Wade JC, Newton B, McLaren C, Flournoy N, Keeney RE, Meyers JD: **Intravenous acyclovir to treat mucocutaneous herpes simplex virus infection after marrow transplantation: a double-blind trial**. *Ann.Intern.Med.* 1982, **96:**265-269.

11. Whitley RJ, Levin M, Barton N, Hershey BJ, Davis G, Keeney RE, Whelchel J, Diethelm AG, Kartus P, Soong SJ: **Infections caused by herpes simplex virus in the immunocompromised host: natural history and topical acyclovir therapy**. *J.Infect.Dis.* 1984, **150:**323-329.

12. Lafferty WE, Coombs RW, Benedetti J, Critchlow C, Corey L: **Recurrences after oral and genital herpes simplex virus infection. Influence of site of infection and viral type**. *N.Engl.J.Med.* 1987, **316:**1444-1449.

13. Ichihashi M, Nagai H, Matsunaga K: **Sunlight is an important causative factor of recurrent herpes simplex**. *Cutis* 2004, **74:**14-18.

14. Hendricks RL: **Immunopathogenesis of viral ocular infections**. *Chem.Immunol.* 1999, **73:**120-136.

15. Liesegang TJ: **Herpes simplex virus epidemiology and ocular importance**. *Cornea* 2001, **20:**1-13.

16. Lowhagen GB, Tunback P, Andersson K, Bergstrom T, Johannisson G: **First episodes of genital herpes in a Swedish STD population: a study of epidemiology and transmission by the use of herpes simplex virus (HSV) typing and specific serology**. *Sex Transm.Infect.* 2000, **76:**179-182.

17. Lafferty WE: **The changing epidemiology of HSV-1 and HSV-2 and implications for serological testing**. *Herpes.* 2002, **9:**51-55.

18. Roberts CM, Pfister JR, Spear SJ: **Increasing proportion of herpes simplex virus type 1 as a cause of genital herpes infection in college students**. *Sex Transm.Dis.* 2003, **30:**797-800.

19. Looker KJ, Garnett GP: **A systematic review of the epidemiology and interaction of herpes simplex virus types 1 and 2**. *Sex Transm.Infect.* 2005, **81:**103-107.

20. Roizman B, Knipe DM: **Herpes simplex viruses and their replication**. In *Fields Virology*. Edited by Fields BN et all. Philadelphia: Lippincott-Raven; 2001:2399-2459.

21. Weir JP: **Regulation of herpes simplex virus gene expression**. *Gene* 2001, **271:**117-130.

22. Rajcani J, Andrea V, Ingeborg R: **Peculiarities of herpes simplex virus (HSV) transcription: an overview**. *Virus Genes* 2004, **28:**293-310.

23. Spear PG: **Herpes simplex virus: receptors and ligands for cell entry**. *Cell Microbiol.* 2004, **6:**401-410.

24. Garner JA: **Herpes simplex virion entry into and intracellular transport within mammalian cells**. *Adv.Drug Deliv.Rev.* 2003, **55:**1497-1513.

25. Honess RW, Roizman B: **Regulation of herpesvirus macromolecular synthesis. I. Cascade regulation of the synthesis of three groups of viral proteins**. *J.Virol.* 1974, **14:**8-19.

26. Honess RW, Roizman B: **Regulation of herpesvirus macromolecular synthesis: sequential transition of polypeptide synthesis requires functional viral polypeptides**. *Proc.Natl.Acad.Sci.USA* 1975, **72:**1276-1280.

27. Goldsmith K, Chen W, Johnson DC, Hendricks RL: **Infected cell protein (ICP)47 enhances herpes simplex virus neurovirulence by blocking the $CD8^+$ T cell response**. *J.Exp.Med.* 1998, **187:**341-348.

28. Mossman KL, Saffran HA, Smiley JR: **Herpes simplex virus ICP0 mutants are hypersensitive to interferon**. *J.Virol.* 2000, **74:**2052-2056.

29. Mossman KL, Macgregor PF, Rozmus JJ, Goryachev AB, Edwards AM, Smiley JR: **Herpes simplex virus triggers and then disarms a host antiviral response**. *J.Virol.* 2001, **75:**750-758.

30. Eidson KM, Hobbs WE, Manning BJ, Carlson P, DeLuca NA: **Expression of herpes simplex virus ICP0 inhibits the induction of interferon-stimulated genes by viral infection**. *J.Virol.* 2002, **76:**2180-2191.

31. Mossman KL, Smiley JR: **Herpes Simplex Virus ICP0 and ICP34.5 Counteract Distinct Interferon- Induced Barriers to Virus Replication**. *J Virol* 2002, **76:**1995-1998.

32. Conley AJ, Knipe DM, Jones PC, Roizman B: **Molecular genetics of herpes simplex virus. VII. Characterization of a temperature-sensitive mutant produced by in vitro mutagenesis and defective in DNA synthesis and accumulation of gamma polypeptides**. *J.Virol.* 1981, **37:**191-206.

33. O'hare P, Goding CR: **Herpes simplex virus regulatory elements and the immunoglobulin octamer domain bind a common factor and are both targets for virion transactivation**. *Cell* 1988, **52:**435-445.

34. Goding CR, O'hare P: **Herpes simplex virus Vmw65-octamer binding protein interaction: a paradigm for combinatorial control of transcription**. *Virology* 1989, **173:**363-367.

35. O'hare P, Goding CR, Haigh A: **Direct combinatorial interaction between a herpes simplex virus regulatory protein and a cellular octamer-binding factor mediates specific induction of virus immediate-early gene expression**. *EMBO J.* 1988, **7:**4231-4238.

36. Preston CM: **Repression of viral transcription during herpes simplex virus latency**. *J.Gen.Virol.* 2000, **81:**1-19.

37. Fraser NW, Valyi-Nagy T: **Viral, neuronal and immune factors which may influence herpes simplex virus (HSV) latency and reactivation**. *Microb.Pathog.* 1993, **15:**83-91.

38. Brissette-Storkus CS, Reynolds SA, Lepisto AJ, Hendricks RL: **Identification of a novel macrophage population in the normal mouse corneal stroma**. *Investigative Ophthalmology & Visual Science* 2002, **43:**2264-2271.

39. Tumpey TM, Chen SH, Oakes JE, Lausch RN: **Neutrophil-mediated suppression of virus replication after herpes simplex virus type 1 infection of the murine cornea**. *J.Virol.* 1996, **70:**898-904.

40. Shimeld C, Efstathiou S, Hill T: **Tracking the spread of a lacZ-tagged herpes simplex virus type 1 between the eye and the nervous system of the mouse: comparison of primary and recurrent infection**. *J.Virol.* 2001, **75:**5252-5262.

41. Lang A, Nikolich-Zugich J: **Development and migration of protective CD8+ T cells into the nervous system following ocular herpes simplex virus-1 infection**. *J.Immunol.* 2005, **174:**2919-2925.

42. Margolis TP, Dawson CR, LaVail JH: **Herpes simplex viral infection of the mouse trigeminal ganglion: Immunohistochemical analysis of cell populations**. *Invest.Ophthalmol.Vis.Sci.* 1992, **33:**259-267.

43. Yang L, Voytek CC, Margolis TP: **Immunohistochemical analysis of primary sensory neurons latently infected with herpes simplex virus type 1**. *J.Virol.* 2000, **74:**209-217.

44. Kodukula P, Liu T, van Rooijen N, Jager MJ, Hendricks RL: **Macrophage control of Herpes simplex virus type 1 replication in the peripheral nervous system**. *J.Immunol.* 1999, **162:**2895-2905.

45. Liu T, Tang Q, Hendricks RL: **Inflammatory infiltration of the trigeminal ganglion after herpes simplex virus type 1 corneal infection**. *J.Virol.* 1996, **70:**264-271.

46. Sciammas R, Kodukula P, Tang Q, Hendricks RL, Bluestone JA: **T cell receptor-γ/δ cells protect mice from herpes simplex virus type 1-induced lethal encephalitis**. *J.Exp.Med.* 1997, **185:**1969-1975.

47. Pereira RA, Scalzo A, Simmons A: **Cutting edge: a NK complex-linked locus governs acute versus latent herpes simplex virus infection of neurons**. *J.Immunol.* 2001, **166:**5869-5873.

48. Grubor-Bauk B, Simmons A, Mayrhofer G, Speck PG: **Impaired clearance of herpes simplex virus type 1 from mice lacking CD1d or NKT cells expressing the semivariant V alpha 14-J alpha 281 TCR**. *J.Immunol.* 2003, **170:**1430-1434.

49. Metcalf JF, Hamilton DS, Reichert RW: **Herpetic keratitis in athymic (nude) mice**. *Infect.Immun.* 1979, **26:**1164-1171.

50. Gesser RM, Valyi-Nagy T, Fraser NW: **Restricted herpes simplex virus type 1 gene expression within sensory neurons in the absence of functional B and T lymphocytes**. *Virology* 1994, **200:**791-795.

51. Ellison AR, Yang L, Voytek C, Margolis TP: **Establishment of latent herpes simplex virus type 1 infection in resistant, sensitive, and immunodeficient mouse strains**. *Virology* 2000, **268:**17-28.

52. Simmons A, Tscharke DC: **Anti-CD8 impairs clearance of herpes simplex virus from the nervous system: Implications for the fate of virally infected neurons**. *J.Exp.Med.* 1992, **175:**1337-1344.

53. Minagawa H, Yanagi Y: **Latent herpes simplex virus-1 infection in SCID mice transferred with immune CD4+T cells: a new model for latency**. *Arch.Virol* 2000, **145:**2259-2272.

54. Ohara PT, Tauscher AN, LaVail JH: **Two paths for dissemination of Herpes simplex virus from infected trigeminal ganglion to the murine cornea**. *Brain Res.* 2001, **899:**260-263.

55. Ohara PT, Chin MS, LaVail JH: **The spread of herpes simplex virus type 1 from trigeminal neurons to the murine cornea: an immunoelectron microscopy study**. *J.Virol.* 2000, **74:**4776-4786.

56. Sawtell NM, Thompson RL: **Rapid in vivo reactivation of herpes simplex virus in latently infected murine ganglionic neurons after transient hyperthermia**. *J.Virol.* 1992, **66:**2150-2156.

57. Shimeld C, Easty DL, Hill TJ: **Reactivation of herpes simplex virus type 1 in the mouse trigeminal ganglion: an in vivo study of virus antigen and cytokines**. *J Virol* 1999, **73:**1767-1773.

58. Padgett DA, Sheridan JF, Dorne J, Berntson GG, Candelora J, Glaser R: **Social stress and the reactivation of latent herpes simplex virus type 1**. *Proc.Natl.Acad.Sci.U.S.A* 1998, **95:**7231-7235.

59. Feldman LT, Ellison AR, Voytek CC, Yang L, Krause P, Margolis TP: **Spontaneous molecular reactivation of herpes simplex virus type 1 latency in mice**. *Proc.Natl.Acad.Sci.U.S.A* 2002, **99:**978-983.

60. Ahn K, Meyer TH, Uebel S, Sempé P, Djaballah H, Yang Y, Peterson PA, Früh K, Tampé R: **Molecular mechanism and species specificity of TAP inhibition by herpes simplex virus protein ICP47**. *EMBO J.* 1996, **15:**3247-3255.

61. Tomazin R, Hill AB, Jugovic P, York I, van Endert P, Ploegh HL, Andrews DW, Johnson DC: **Stable binding of the herpes simplex virus ICP47 protein to the peptide binding site of TAP**. *EMBO J.* 1996, **15:**3256-3266.

62. Kennedy PG: **Key issues in varicella-zoster virus latency**. *J.Neurovirol.* 2002, **8 Suppl 2:**80-84.

63. Rowe M, Rowe DT, Gregory CD, Young LS, Farrell PJ, Rupani H, Rickinson AB: **Differences in B cell growth phenotype reflect novel patterns of Epstein-Barr virus latent gene expression in Burkitt's lymphoma cells**. *EMBO J.* 1987, **6:**2743-2751.

64. Stevens JG, Wagner EK, Devi-Rao GB, Cook ML, Feldman LT: **RNA complementary to a herpesvirus alpha gene mRNA is prominent in latently infected neurons**. *Science* 1987, **235:**1056-1059.

65. Krause PR, Croen KD, Straus SE, Ostrove JM: **Detection and preliminary characterization of herpes simplex virus type 1 transcripts in latently infected human trigeminal ganglia**. *J.Virol.* 1988, **62:**4819-4823.

66. Kramer MF, Coen DM: **Quantification of transcripts from the ICP4 and thymidine kinase genes in mouse ganglia latently infected with herpes simplex virus**. *J.Virol.* 1995, **69:**1389-1399.

67. Liu T, Khanna KM, Chen X, Fink DJ, Hendricks RL: **CD8(+) T cells can block herpes simplex virus type 1 (HSV-1) reactivation from latency in sensory neurons**. *J.Exp.Med.* 2000, **191:**1459-1466.

68. Loiacono CM, Myers R, Mitchell WJ: **Neurons differentially activate the herpes simplex virus type 1 immediate-early gene ICP0 and ICP27 promoters in transgenic mice**. *J.Virol.* 2002, **76:**2449-2459.

69. Loiacono CM, Taus NS, Mitchell WJ: **The herpes simplex virus type 1 ICP0 promoter is activated by viral reactivation stimuli in trigeminal ganglia neurons of transgenic mice**. *J Neurovirol.* 2003, **9:**336-345.

70. Loiacono CM, Myers R, Mitchell WJ: **The herpes simplex virus type 1 early gene (thymidine kinase) promoter is activated in neurons of brain, but not trigeminal ganglia, of transgenic mice in the absence of viral proteins**. *J.Neurovirol.* 2004, **10:**116-122.

71. Tal-Singer R, Lasner TM, Podrzucki W, Skokotas A, Leary JJ, Berger SL, Fraser NW: **Gene expression during reactivation of herpes simplex virus type 1 from latency in the peripheral nervous system is different from that during lytic infection of tissue cultures**. *J.Virol.* 1997, **71:**5268-5276.

72. Kosz-Vnenchak M, Jacobson J, Coen DM, Knipe DM: **Evidence for a novel regulatory pathway for herpes simplex virus gene expression in trigeminal ganglion neurons**. *J.Virol.* 1993, **67:**5383-5393.

73. Rezuchova I, Kudelova M, Durmanova V, Vojvodova A, Kosovsky J, Rajcani J: **Transcription at early stages of herpes simplex virus 1 infection and during reactivation**. *Intervirology* 2003, **46:**25-34.

74. Cantin EM, Hinton DR, Chen J, Openshaw H: **Gamma interferon expression during acute and latent nervous system infection by herpes simplex virus type 1**. *J.Virol.* 1995, **69:**4898-4905.

75. Shimeld C, Whiteland JL, Nicholls SM, Grinfeld E, Easty DL, Gao H, Hill TJ: **Immune cell infiltration and persistence in the mouse trigeminal ganglion after infection of the cornea with herpes simplex virus type 1**. *J.Neuroimmunol.* 1995, **61:**7-16.

76. Halford WP, Gebhardt BM, Carr DJJ: **Persistent cytokine expression in trigeminal ganglion latently infected with herpes simplex virus type 1**. *J.Immunol.* 1996, **157:**3542-3549.

77. Shimeld C, Whiteland JL, Williams NA, Easty D, Hill TJ: **Reactivation of herpes simplex virus type 1 in the mouse trigeminal ganglion: an in vivo study of virus antigen and immune cell infiltration**. *J.Gen.Virol.* 1996, **77:**2583-2590.

78. Halford WP, Gebhardt BM, Carr DJ: **Acyclovir blocks cytokine gene expression in trigeminal ganglia latently infected with herpes simplex virus type 1**. *Virology* 1997, **238:**53-63.

79. Cantin E, Tanamachi B, Openshaw H: **Role for gamma interferon in control of herpes simplex virus type 1 reactivation**. *J.Virol.* 1999, **73:**3418-3423.

80. Chen SH, Garber DA, Schaffer PA, Knipe DM, Coen DM: **Persistent elevated expression of cytokine transcripts in ganglia latently infected with herpes simplex virus in the absence of ganglionic replication or reactivation**. *Virology* 2000, **278:**207-216.

81. Liu T, Khanna KM, Carriere BN, Hendricks RL: **Gamma interferon can prevent herpes simplex virus type 1 reactivation from latency in sensory neurons**. *J.Virol.* 2001, **75:**11178-11184.

82. Khanna KM, Bonneau RH, Kinchington PR, Hendricks RL: **Herpes simplex virus-specific memory CD8+ T cells are selectively activated and retained in latently infected sensory ganglia**. *Immunity.* 2003, **18:**593-603.

83. Shimeld C, Whiteland JL, Williams NA, Easty DL, Hill TJ: **Cytokine production in the nervous system of mice during acute and latent infection with herpes simplex virus type 1**. *J Gen Virol* 1997, **78 (Pt 12):**3317-3325.

84. Cook WJ, Kramer MF, Walker RM, Burwell TJ, Holman HA, Coen DM, Knipe DM: **Persistent expression of chemokine and chemokine receptor RNAs at primary and latent sites of herpes simplex virus 1 infection**. *Virol.J.* 2004, **1:**5.

85. Carr DJ, Noisakran S, Halford WP, Lukacs N, Asensio V, Campbell IL: **Cytokine and chemokine production in HSV-1 latently infected trigeminal ganglion cell cultures: effects of hyperthermic stress**. *J.Neuroimmunol.* 1998, **85:**111-121.

86. Cantin E, Tanamachi B, Openshaw H, Mann J, Clarke K: **Gamma interferon (IFN-gamma) receptor null-mutant mice are more susceptible to herpes simplex virus type 1 infection than IFN-gamma ligand null-mutant mice**. *J.Virol.* 1999, **73:**5196-5200.

87. Han X, Lundberg P, Tanamachi B, Openshaw H, Longmate J, Cantin E: **Gender influences herpes simplex virus type 1 infection in normal and gamma interferon-mutant mice**. *J.Virol.* 2001, **75:**3048-3052.

88. Lekstrom-Himes JA, LeBlanc RA, Pesnicak L, Godleski M, Straus SE: **Gamma interferon impedes the establishment of herpes simplex virus type 1 latent infection but has no impact on its maintenance or reactivation in mice**. *J.Virol.* 2000, **74:**6680-6683.

89. Minami M, Kita M, Yan XQ, Yamamoto T, Iida T, Sekikawa K, Iwakura Y, Imanishi J: **Role of IFN-gamma and tumor necrosis factor-alpha in herpes simplex virus type 1 infection**. *J.Interferon Cytokine Res.* 2002, **22:**671-676.

90. Sainz B, Jr., Halford WP: **Alpha/Beta interferon and gamma interferon synergize to inhibit the replication of herpes simplex virus type 1**. *J.Virol.* 2002, **76:**11541-11550.

91. Hagglund R, Roizman B: **Role of ICP0 in the strategy of conquest of the host cell by herpes simplex virus 1**. *J.Virol.* 2004, **78:**2169-2178.

92. Halford WP, Schaffer PA: **ICP0 is required for efficient reactivation of herpes simplex virus type1 from neuronal latency**. *J.Virol.* 2001, **75:**3240-3249.

93. Halford WP, Kemp CD, Isler JA, Davido DJ, Schaffer PA: **ICP0, ICP4, or VP16 expressed from adenovirus vectors induces reactivation of latent herpes simplex virus type 1 in primary cultures of latently infected trigeminal ganglion cells**. *J Virol* 2001, **75:**6143-6153.

94. Jackson SA, DeLuca NA: **Relationship of herpes simplex virus genome configuration to productive and persistent infections**. *Proc.Natl.Acad.Sci.U.S.A* 2003, **100:**7871-7876.

95. Jordan R, Schaffer PA: **Activation of gene expression by herpes simplex virus type 1 ICP0 occurs at the level of mRNA synthesis**. *J.Virol.* 1997, **71:**6850-6862.

96. Pickart CM: **Mechanisms underlying ubiquitination**. *Annu.Rev.Biochem.* 2001, **70:**503-533.

97. Van Sant C, Hagglund R, Lopez P, Roizman B: **The infected cell protein 0 of herpes simplex virus 1 dynamically interacts with proteasomes, binds and activates the cdc34 E2 ubiquitin-conjugating enzyme, and possesses in vitro E3 ubiquitin ligase activity**. *Proc.Natl.Acad.Sci.U.S.A* 2001, **98:**8815-8820.

98. Gu H, Roizman B: **The degradation of promyelocytic leukemia and Sp100 proteins by herpes simplex virus 1 is mediated by the ubiquitin-conjugating enzyme UbcH5a**. *Proc.Natl.Acad.Sci.U.S.A* 2003, **100:**8963-8968.

99. Lopez P, Jacob RJ, Roizman B: **Overexpression of promyelocytic leukemia protein precludes the dispersal of ND10 structures and has no effect on accumulation of infectious herpes simplex virus 1 or its proteins**. *J.Virol.* 2002, **76:**9355-9367.

100. Chee AV, Lopez P, Pandolfi PP, Roizman B: **Promyelocytic leukemia protein mediates interferon-based anti-herpes simplex virus 1 effects**. *J Virol* 2003, **77:**7101-7105.

101. Lin R, Noyce RS, Collins SE, Everett RD, Mossman KL: **The herpes simplex virus ICP0 RING finger domain inhibits IRF3- and IRF7-mediated activation of interferon-stimulated genes**. *J Virol* 2004, **78:**1675-1684.

102. Harle P, Sainz B, Jr., Carr DJ, Halford WP: **The Immediate-Early Protein, ICP0, Is Essential for the Resistance of Herpes Simplex Virus to Interferon-alpha/beta**. *Virology* 2002, **293:**295-304.

103. Taylor JL, Little SD, O'Brien WJ: **The comparative anti-herpes simplex virus effects of human interferons**. *J Interferon Cytokine Res.* 1998, **18:**159-165.

104. Chelbi-Alix MK, Pelicano L, Quignon F, Koken MH, Venturini L, Stadler M, Pavlovic J, Degos L, de The H: **Induction of the PML protein by interferons in normal and APL cells**. *Leukemia* 1995, **9:**2027-2033.

105. Mandal M, Bandyopadhyay D, Goepfert TM, Kumar R: **Interferon-induces expression of cyclin-dependent kinase-inhibitors p21WAF1 and p27Kip1 that prevent activation of cyclin-dependent kinase by CDK-activating kinase (CAK)**. *Oncogene* 1998, **16:**217-225.

106. Schang LM, Rosenberg A, Schaffer PA: **Transcription of herpes simplex virus immediate-early and early genes is inhibited by roscovitine, an inhibitor specific for cellular cyclin-dependent kinases**. *J.Virol.* 1999, **73:**2161-2172.

107. Schang LM, Phillips J, Schaffer PA: **Requirement for cellular cyclin-dependent kinases in herpes simplex virus replication and transcription**. *J Virol* 1998, **72:**5626-5637.

108. Schang LM, Bantly A, Schaffer PA: **Explant-Induced Reactivation of Herpes Simplex Virus Occurs in Neurons Expressing Nuclear cdk2 and cdk4**. *J.Virol.* 2002, **76:**7724-7735.

109. Davido DJ, Leib DA, Schaffer PA: **The cyclin-dependent kinase inhibitor roscovitine inhibits the transactivating activity and alters the posttranslational modification of herpes simplex virus type 1 ICP0**. *J.Virol.* 2002, **76:**1077-1088.

110. Davido DJ, Von Zagorski WF, Maul GG, Schaffer PA: **The differential requirement for cyclin-dependent kinase activities distinguishes two functions of herpes simplex virus type 1 ICP0**. *J Virol* 2003, **77:**12603-12616.

111. Boehm U, Klamp T, Groot M, Howard JC: **Cellular responses to interferon-gamma**. *Annu.Rev.Immunol.* 1997, **15:**749-795.

112. Kaech SM, Hemby S, Kersh E, Ahmed R: **Molecular and functional profiling of memory CD8 T cell differentiation**. *Cell* 2003, **111:**837-851.

113. Slifka MK, Whitton JL: **Activated and memory CD8$^+$ T cells can be distinguished by their cytokine profiles and phenotypic markers**. *J.Immunol.* 2000, **164:**208-216.

114. Slifka MK, Whitton JL: **Functional avidity maturation of CD8(+) T cells without selection of higher affinity TCR**. *Nat.Immunol.* 2001, **2:**711-717.

115. Kaech SM, Wherry EJ, Ahmed R: **Effector and memory T-cell differentiation: implications for vaccine development**. *Nat.Rev.Immunol.* 2002, **2:**251-262.

116. Pellegrini M, Belz G, Bouillet P, Strasser A: **Shutdown of an acute T cell immune response to viral infection is mediated by the proapoptotic Bcl-2 homology 3-only protein Bim**. *Proc.Natl.Acad.Sci.U.S.A* 2003, **100:**14175-14180.

117. Strasser A, Pellegrini M: **T-lymphocyte death during shutdown of an immune response**. *Trends Immunol.* 2004, **25:**610-615.

118. Marrack P, Kappler J: **Control of T cell viability**. *Annu.Rev.Immunol.* 2004, **22:**765-787.

119. Hildeman DA, Zhu Y, Mitchell TC, Kappler J, Marrack P: **Molecular mechanisms of activated T cell death in vivo**. *Curr.Opin.Immunol.* 2002, **14:**354-359.

120. Nussbaum AK, Whitton JL: **The contraction phase of virus-specific CD8+ T cells is unaffected by a pan-caspase inhibitor**. *J.Immunol.* 2004, **173:**6611-6618.

121. Masopust D, Kaech SM, Wherry EJ, Ahmed R: **The role of programming in memory T-cell development**. *Curr.Opin.Immunol.* 2004, **16:**217-225.

122. Lau LL, Jamieson BD, Somasundaram T, Ahmed R: **Cytotoxic T-cell memory without antigen**. *Nature* 1994, **369:**648-652.

123. Demkowicz WE, Jr., Littaua RA, Wang J, Ennis FA: **Human cytotoxic T-cell memory: long-lived responses to vaccinia virus**. *J.Virol.* 1996, **70:**2627-2631.

124. Gourley TS, Wherry EJ, Masopust D, Ahmed R: **Generation and maintenance of immunological memory**. *Semin.Immunol.* 2004, **16:**323-333.

125. Kaech SM, Tan JT, Wherry EJ, Konieczny BT, Surh CD, Ahmed R: **Selective expression of the interleukin 7 receptor identifies effector CD8 T cells that give rise to long-lived memory cells**. *Nat.Immunol.* 2003, **4:**1191-1198.

126. Yewdell JW, Bennink JR: **Immunodominance in major histocompatibility complex class I-restricted T lymphocyte responses**. *Annu.Rev.Immunol.* 1999, **17:**51-88.

127. Liu F, Whitton JL, Slifka MK: **The rapidity with which virus-specific CD8+ T cells initiate IFN-gamma synthesis increases markedly over the course of infection and correlates with immunodominance**. *J.Immunol.* 2004, **173:**456-462.

128. Yamagami S, Dana MR, Tsuru T: **Draining lymph nodes play an essential role in alloimmunity generated in response to high-risk corneal transplantation**. *Cornea* 2002, **21:**405-409.

129. Schroder K, Hertzog PJ, Ravasi T, Hume DA: **Interferon-gamma: an overview of signals, mechanisms and functions**. *J.Leukoc.Biol.* 2004, **75:**163-189.

130. Slifka MK, Rodriguez F, Whitton JL: **Rapid on/off cycling of cytokine production by virus-specific CD8+ T cells**. *Nature* 1999, **401:**76-79.

131. Ealick SE, Cook WJ, Vijay-Kumar S, Carson M, Nagabhushan TL, Trotta PP, Bugg CE: **Three-dimensional structure of recombinant human interferon-gamma**. *Science* 1991, **252:**698-702.

132. Walter MR, Windsor WT, Nagabhushan TL, Lundell DJ, Lunn CA, Zauodny PJ, Narula SK: **Crystal structure of a complex between interferon-gamma and its soluble high-affinity receptor**. *Nature* 1995, **376:**230-235.

133. Bach EA, Tanner JW, Marsters S, Ashkenazi A, Aguet M, Shaw AS, Schreiber RD: **Ligand-induced assembly and activation of the gamma interferon receptor in intact cells**. *Mol.Cell Biol.* 1996, **16:**3214-3221.

134. Igarashi K, Garotta G, Ozmen L, Ziemiecki A, Wilks AF, Harpur AG, Larner AC, Finbloom DS: **Interferon-gamma induces tyrosine phosphorylation of interferon-gamma receptor and regulated association of protein tyrosine kinases, Jak1 and Jak2, with its receptor**. *J.Biol.Chem.* 1994, **269:**14333-14336.

135. Greenlund AC, Morales MO, Viviano BL, Yan H, Krolewski J, Schreiber RD: **Stat recruitment by tyrosine-phosphorylated cytokine receptors: an ordered reversible affinity-driven process**. *Immunity.* 1995, **2:**677-687.

136. Heim MH, Kerr IM, Stark GR, Darnell JE, Jr.: **Contribution of STAT SH2 groups to specific interferon signaling by the Jak-STAT pathway**. *Science* 1995, **267:**1347-1349.

137. Briscoe J, Rogers NC, Witthuhn BA, Watling D, Harpur AG, Wilks AF, Stark GR, Ihle JN, Kerr IM: **Kinase-negative mutants of JAK1 can sustain interferon-gamma-inducible gene expression but not an antiviral state**. *EMBO J.* 1996, **15:**799-809.

138. Ramana CV, Chatterjee-Kishore M, Nguyen H, Stark GR: **Complex roles of Stat1 in regulating gene expression**. *Oncogene* 2000, **19:**2619-2627.

139. Kerr IM, Stark GR: **The control of interferon-inducible gene expression**. *FEBS Lett.* 1991, **285:**194-198.

140. Alcami A, Koszinowski UH: **Viral mechanisms of immune evasion**. *Immunol.Today* 2000, **21:**447-455.

141. Chee AV, Roizman B: **Herpes simplex virus 1 gene products occlude the interferon signaling pathway at multiple sites**. *J.Virol.* 2004, **78:**4185-4196.

142. Fruh K, Yang Y: **Antigen presentation by MHC class I and its regulation by interferon gamma**. *Curr.Opin.Immunol.* 1999, **11:**76-81.

143. Jouanguy E, Doffinger R, Dupuis S, Pallier A, Altare F, Casanova JL: **IL-12 and IFN-gamma in host defense against mycobacteria and salmonella in mice and men**. *Curr.Opin.Immunol.* 1999, **11:**346-351.

144. Pearl JE, Saunders B, Ehlers S, Orme IM, Cooper AM: **Inflammation and lymphocyte activation during mycobacterial infection in the interferon-gamma-deficient mouse**. *Cell Immunol.* 2001, **211:**43-50.

145. Huang S, Hendricks W, Althage A, Hemmi S, Bluethmann H, Kamijo R, Vilcek J, Zinkernagel RM, Aguet M: **Immune response in mice that lack the interferon-gamma receptor**. *Science* 1993, **259:**1742-1745.

146. Van den Broek MF, Muller U, Huang S, Zinkernagel RM, Aguet M: **Immune defence in mice lacking type I and/or type II interferon receptors**. *Immunol.Rev.* 1995, **148:**5-18.

147. Van den Broek MF, Muller U, Huang S, Aguet M, Zinkernagel RM: **Antiviral defense in mice lacking both alpha/beta and gamma interferon receptors**. *J.Virol.* 1995, **69:**4792-4796.

148. Huang S, Hendriks W, Althage A, Hemmi S, Bluethmann H, Kamijo R, Vilcek J, Zinkernagel RM, Aguet M: **Immune response in mice that lack the interferon-gamma receptor**. *Science* 1993, **259:**1742-1745.

149. Badovinac VP, Tvinnereim AR, Harty JT: **Regulation of antigen-specific CD8+ T cell homeostasis by perforin and interferon-gamma**. *Science* 2000, **290:**1354-1358.

150. Rodriguez F, Harkins S, Slifka MK, Whitton JL: **Immunodominance in virus-induced CD8(+) T-cell responses is dramatically modified by DNA immunization and is regulated by gamma interferon**. *J.Virol.* 2002, **76:**4251-4259.

151. Harty JT, Badovinac VP: **Influence of effector molecules on the CD8(+) T cell response to infection**. *Curr.Opin.Immunol.* 2002, **14:**360-365.

152. Dalton DK, Haynes L, Chu CQ, Swain SL, Wittmer S: **Interferon gamma eliminates responding CD4 T cells during mycobacterial infection by inducing apoptosis of activated CD4 T cells**. *J.Exp.Med.* 2000, **192:**117-122.

153. Whitmire JK, Tan JT, Whitton JL: **Interferon-gamma acts directly on CD8+ T cells to increase their abundance during virus infection**. *J.Exp.Med.* 2005, **201:**1053-1059.

154. Thompson RL, Shieh MT, Sawtell NM: **Analysis of herpes simplex virus ICP0 promoter function in sensory neurons during acute infection, establishment of latency, and reactivation in vivo**. *J.Virol.* 2003, **77:**12319-12330.

155. Sawtell NM: **Comprehensive quantification of herpes simplex virus latency at the single-cell level**. *J.Virol.* 1997, **71:**5423-5431.

156. Anglen CS, Truckenmiller ME, Schell TD, Bonneau RH: **The dual role of CD8+ T lymphocytes in the development of stress-induced herpes simplex encephalitis**. *J Neuroimmunol.* 2003, **140:**13-27.

157. Brown DC, Gatter KC: **Ki67 protein: the immaculate deception?** *Histopathology* 2002, **40:**2-11.

158. Sawtell NM, Thompson RL: **Comparison of herpes simplex virus reactivation in ganglia in vivo and in explants demonstrates quantitative and qualitative differences**. *J.Virol.* 2004, **78:**7784-7794.

159. Vikman K, Robertson B, Grant G, Liljeborg A, Kristensson K: **Interferon-gamma receptors are expressed at synapses in the rat superficial dorsal horn and lateral spinal nucleus**. *J.Neurocytol.* 1998, **27:**749-759.

160. Cai W, Schaffer PA: **Herpes simplex virus type 1 ICP0 regulates expression of immediate-early, early, and late genes in productively infected cells**. *J.Virol.* 1992, **66:**2904-2915.

161. Everett RD, Boutell C, Orr A: **Phenotype of a herpes simplex virus type 1 mutant that fails to express immediate-early regulatory protein ICP0**. *J.Virol.* 2004, **78:**1763-1774.

162. Tomishima MJ, Enquist LW: **In vivo egress of an alphaherpesvirus from axons**. *J.Virol.* 2002, **76:**8310-8317.

163. Miranda-Saksena M, Armati P, Boadle RA, Holland DJ, Cunningham AL: **Anterograde transport of herpes simplex virus type 1 in cultured, dissociated human and rat dorsal root ganglion neurons**. *J.Virol.* 2000, **74:**1827-1839.

164. Bonneau RH: **Stress-induced effects on integral immune components involved in herpes simplex virus (HSV)-specific memory cytotoxic T lymphocyte activation**. *Brain Behav.Immun.* 1996, **10:**139-163.

165. D'Souza WN, Schluns KS, Masopust D, Lefrancois L: **Essential role for IL-2 in the regulation of antiviral extralymphoid CD8 T cell responses**. *J.Immunol.* 2002, **168:**5566-5572.

166. Schluns KS, Lefrancois L: **Cytokine control of memory T-cell development and survival**. *Nat.Rev.Immunol.* 2003, **3:**269-279.

167. Mueller SN, Jones CM, Smith CM, Heath WR, Carbone FR: **Rapid cytotoxic T lymphocyte activation occurs in the draining lymph nodes after cutaneous herpes simplex virus infection as a result of early antigen presentation and not the presence of virus**. *J.Exp.Med.* 2002, **195:**651-656.

168. Ramana CV, Grammatikakis N, Chernov M, Nguyen H, Goh KC, Williams BR, Stark GR: **Regulation of c-myc expression by IFN-gamma through Stat1-dependent and -independent pathways**. *EMBO J.* 2000, **19:**263-272.

169. Caux C, Moreau I, Saeland S, Banchereau J: **Interferon-gamma enhances factor-dependent myeloid proliferation of human CD34+ hematopoietic progenitor cells**. *Blood* 1992, **79:**2628-2635.

170. Shiohara M, Koike K, Nakahata T: **Synergism of interferon-gamma and stem cell factor on the development of murine hematopoietic progenitors in serum-free culture**. *Blood* 1993, **81:**1435-1441.

171. Tough DF, Zhang X, Sprent J: **An IFN-gamma-dependent pathway controls stimulation of memory phenotype CD8+ T cell turnover in vivo by IL-12, IL-18, and IFN-gamma**. *J.Immunol.* 2001, **166:**6007-6011.

172. Mehal WZ, Juedes AE, Crispe IN: **Selective retention of activated CD8+ T cells by the normal liver**. *J.Immunol.* 1999, **163:**3202-3210.

173. Crispe IN, Dao T, Klugewitz K, Mehal WZ, Metz DP: **The liver as a site of T-cell apoptosis: graveyard, or killing field?** *Immunol.Rev.* 2000, **174:**47-62.

174. Park S, Murray D, John B, Crispe IN: **Biology and significance of T-cell apoptosis in the liver**. *Immunol.Cell Biol.* 2002, **80:**74-83.

175. Strasser A, Pellegrini M: **T-lymphocyte death during shutdown of an immune response**. *Trends Immunol.* 2004, **25:**610-615.